Document Type	Design Description
Document Number	ESS-0432365
Date	Apr 17, 2020
Revision	1 (8)
State	Preliminary
Confidentiality Level	Internal
Page	1 (79)

BEER - Radiation Safety Analysis

	Name	Role/Title
Owner	Premysl Beran	BEER Lead Scientist (ESS, NPI)
Authors	Jan Saroun[a], Radim Svejda[b], Martin Vankat[c], Michal Kaspar[c], Jaroslav Soltes[c], Martin Schulc[c], Evzen Losa[c]	[a]Nuclear Physics Institute [b]NUVIA [c]UJV Rez
Reviewer	Peter Sångberg Günter Muhrer	Systems Engineer Group Leader for ESS Spallation Physics
Notified	Sigrid Kozielski Andrew Jackson	Group Leader Radiation Protection Head of Neutron Instruments Division
Approver	Gabor Laszlo	NSS Lead Instrument Engineer

CONTENT

CONTENT 2
LIST OF FIGURES 4
LIST OF TABLES 7
1. SCOPE 8
2. ISSUING ORGANISATION 8
3. CONTEXT 8
4. INTRODUCTION 8
4.1. Task description 8
4.2. Shielding design requirements 9
4.2.1. Supervised areas: 9
4.2.2. Unrestricted controlled areas: 9
4.3. Definition of H1 and H2 scenarios 10
4.4. Simulation tool description 10
5. INPUTS AND MODELS FOR SIMULATIONS 13
5.1. Calculation inputs 13
5.1.1. Shutter pit 13
5.1.2. Chopper pit 15
5.1.3. Neutron guide 16
5.1.3.1. Fast neutrons – simulation of neutron transport through the bunker 16
5.1.3.2. Simulation of neutron guide shielding tunnel 19
5.1.4. Instrument cave 21
5.2. Summary of input fluxes and doses 26
5.3. Models and materials 27
5.3.1. Models description 27
5.3.1.1. Shutter and shutter pit 27
5.3.1.2. Chopper pit 29
5.3.1.3. Neutron guide 30
5.3.1.4. Guide tunnel 31
5.3.1.5. Instrument cave 32
5.3.2. Materials 35
6. RESULTS OF SIMULATIONS 38

6.1. Full beam in the Shutter pit 38
6.1.1. Activation of the shutter 38
6.1.2. Closed shutter – H1.1 43
6.1.3. Opened shutter – H1.2 48
6.1.4. Behind shutter put when the shutter is open – H1.3 49
6.2. Full beam within the chopper pit – H1.5 51
6.3. Neutron Guide 55
6.3.1. Thermal neutron shielding – H1.4 55
6.3.2. Focusing guide and slits system – H1.6 56
6.4. Instrument cave 58
6.4.1. AFM beam scattered from the sample location – H2.1 59
6.4.2. Nickel sample in AFM beam – H2.2 62
6.4.3. Nickel Sample in MWB beam – H2.5 65
6.4.4. Cadmium plate in MWB beam – H2.6 68
6.4.5. Full beam hitting the beam-stop – H2.7 71
6.4.6. General cave shielding summary 74
6.4.7. B_4C layer activation 76
6.5. Conclusions 77
7. GLOSSARY 78
8. REFERENCES 79
DOCUMENT REVISION HISTORY 79

LIST OF FIGURES

Figure 1: BEER beamline schematic layout 9

Figure 2: Fast neutron spectrum at the entrance to the shutter pit (input) and leaking through the shutter. 14

Figure 3: MCNP bunker model with the BEER facility guide 17

Figure 4: Fast neutron spectrum at the bunker exit. 17

Figure 5: Neutron spectra over beam area (2 cm × 8 cm), area of 25 cm ×25 cm, and 200 cm × 200 cm at the inner face of the bunker wall. 18

Figure 6: Neutron and photon doses over the beam area at the inner entrance to the bunker wall. The guide dimensions are 2×8 cm^2. 18

Figure 7: Neutron and photon doses over 200x200 cm^2 at the inner entrance to the bunker wall, for geometry details, see Figure 3. 19

Figure 8: Thermal neutrons losses in the neutron guides in D03 and E02 halls, simulated by McStas ver. 2.6. 20

Figure 9: Photon spectrum generated through neutron capture on the NiTi layer of the neutron guide. 20

Figure 10: Thermal neutron spectrum at the sample location for AFB (denoted as H1 in the chart) and MWB (denoted as H2 in the chart). 24

Figure 11 - Prompt-γ emission from a series of examined samples after being hit by the H1 beam in the sample position. 26

Figure 12: Final shutter design. 28

Figure 13: Shutter pit design in y-z (side view) and x-z (top view) cuts. 29

Figure 14: Chopper pit geometry. 30

Figure 15: Neutron guide cross-section. 30

Figure 16: Shutter pit exit. 31

Figure 17: Thermal neutron guide shielding cross-section. 32

Figure 18: BEER instrument cave layout drawing. Green lines indicate the shielding wall. 33

Figure 19: BEER instrument cave MCNP model description. 34

Figure 20: BEER beam-stop model description. 35

Figure 21: Photon spectrum behind the shutter pit wall. 44

Figure 22: Neutron spectrum behind the shutter pit wall. 44

Figure 23: Neutron doses rates in and around the shutter. 45

Figure 24: Photon doses rates in and around the shutter. 46

Figure 25: Neutron dose rates in the shutter pit in the closed state. 47

Figure 26: Photon dose rates in the shutter pit in the closed state. 48

Figure 27: Fast neutron dose rates in the shutter pit in the opened state. 49

Figure 28: Fast neutron doses behind the bunker wall on the first 8 meters. 50

Figure 29: Fast neutron and photon doses behind the shutter pit on the first 3 meters 51

Figure 30: Neutron dose rates in the chopper pit in the case where all the neutrons are isotopically scattered. 52

Figure 31: Photon dose rates in the chopper pit in the case where all the neutrons are isotopically scattered. 53

Figure 32: Neutron doses in the chopper pit in the case where all the neutrons absorbed by a B_4C plate. 54

Figure 33: Photon doses in the chopper pit in the case where all the neutrons absorbed by a B_4C plate. 55

Figure 34: γ dose rates generated by thermal neutron interactions with the supermirror coating. Dose rates map around the wide section of the neutron guide shielding. 56

Figure 35: Neutron dose rates in the final 3 m of the guide tunnel around the B_4C slits before cave entering. 57

Figure 36: γ dose rates in the final 3 m of the guide tunnel around the B_4C slits before cave entering. 58

Figure 37: Instrument cave model with the identification of the planar sections where the dose rates are shown. 59

Figure 38: Spatial neutron dose rate distribution in the instrument cave for the H2.1 scenario– isotropically scattering sample. 60

Figure 39: Spatial γ dose rate distribution in the instrument cave for the H2.1 scenario – isotropically scattering sample. 61

Figure 40: Spatial neutron dose rate distribution in the instrument cave for the nickel sample placed in the AFM beam – H2.2. 63

Figure 41: Spatial γ dose rate distribution in the instrument cave for the nickel sample placed in the AFM beam – H2.2 64

Figure 42: Spatial neutron dose rate distribution in the instrument cave for the nickel sample placed in the MWB beam – H2.5 66

Figure 43: Spatial γ dose rate distribution in the instrument cave for the nickel sample placed in the MWB beam – H2.5. 67

Figure 44: Spatial neutron dose rate distribution in the instrument cave for the cadmium plate in the MWB scenario – H2.6. 69

Figure 45: Spatial γ dose rate distribution in the instrument cave for the cadmium plate in the MWB scenario – H2.6. 70

Figure 46: Neutron dose rate profiles at the entry point of the beam-stop.....72

Figure 47: Spatial neutron dose rate distribution in the instrument cave for MWB beam hitting the beam-stop.....73

Figure 48: Spatial γ dose rate distribution in the instrument cave for MWB beam hitting the beam stop. 74

Figure 49: Dose rate hotspot identification for detailed calculations. 75

LIST OF TABLES

Table 1: Summary of H1&H2 events with the corresponding reference to the appropriate chapter. 10

Table 2: Flux to dose rate conversion factors – neutrons. 11

Table 3 : Flux to dose rate conversion factors – photons. 12

Table 4: Input fast neutron spectrum (calculation input) at the central position, averaged over beam area. 14

Table 5: Input thermal neutron spectrum (calculation input) 15

Table 6: Photon spectrum generated through neutron capture on the NiTi layer of the neutron guide on the surface (calculation input). 20

Table 7: Input thermal neutron spectrum for both used scenarios averaged over beam area 22

Table 8 - Prompt-γ emission from a series of examined samples after being hit by the WMB beam at the sample position. 25

Table 9: Source parameters and intensities in the model 26

Table 10: Densities of materials used in the model 35

Table 11: Composition of the ESS concrete 35

Table 12: Composition of heavy concrete 36

Table 13: Composition of iron 36

Table 14: Composition of PE (5% weight of boron) 36

Table 15: Composition of B_4C 37

Table 16: Composition of copper 37

Table 17: Composition of light water 37

Table 18: Composition of MirroBor™ 37

Table 19: Composition of borosilicate glass 37

Table 20: Calculated activities in the shutter copper for 1-year activation and several defined cooling times. 38

Table 21: Calculated activities in the shutter lead for 1-year activation and several defined cooling times. 40

Table 22: Calculated sums of γ and neutron dose rates in the defined hotspot points. 76

Table 23: ICRP-61 yearly intake limits. 77

Table 24: Radiological simulations summary 78

Table 25: Area-averaged dose rates 78

1. SCOPE

The aim of this technical report is to provide information on the status of the radiological shielding calculation carried out during the final design stage of the components for the BEER instrument at ESS. The main focus is to provide a final design of shielding requirements for the neutron guide, shutter pit, chopper pit and instrument cave of the facility.

Note: The BEER team joined the ESS common shielding project, which means that the calculations of the neutron guide shielding tunnel and both pits will be re-done. The simulation results of those parts presented here were part of the detail design contract, which was terminated, so they should be taken as preliminary ones.

2. ISSUING ORGANISATION

Nuclear Physics Institute (NPI) and NUVIA

3. CONTEXT

The BEER instrument is the engineering instrument dedicated to the in-situ and in-operando studies in the field of material science under real conditions. The novel technique of the pulse modulation will allow the fast strain scanning of even real shape engineering samples.

4. INTRODUCTION

4.1. Task description

The aim of this technical report is to provide information on the status of the radiological shielding calculation carried out during the final design stage of the components for the BEER instrument. The main focus is to provide shielding requirements for the final design of neutron guide shielding, safety shutter, shutter pit, chopper pit and the experimental cave of the instrument (see Figure 1). The main interest is focused on the following components:

- Bunker in regards to dose rates in the beam cross-section and on the inner and outer bunker wall, an evaluation of the fast neutron input spectrum to the shutter pit.
- Neutron guide shielding, in regards to shielding tunnel wall design, material composition, thickness estimation.
- Shutter and its shielding pit, in regards of shutter dimensions, material composition, shutter thickness estimation, walls thickness and material composition all in opened and closed state.
- Chopper pit, in regards of wall thickness and composition in the case of all neutrons scattered or absorbed in the chopper disc.
- Instrument cave, in regards to wall design, material composition, wall thickness estimation and beam-stop design, considering normal operation (H1) and likely or severe accident (H2) scenarios.

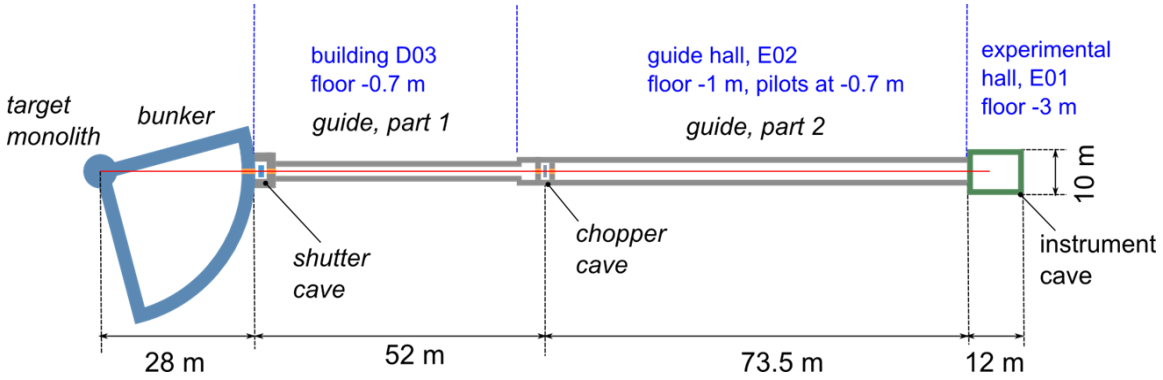

Figure 1: BEER beamline schematic layout

4.2. Shielding design requirements

The instrument shielding shell be designed in accordance with the ESS guidelines for designing instrument shielding for radiation safety [1][2], as appropriate for ESS implementation of radiation safety rules in supervised and controlled areas [3][4]. As for the shielding design, only external radiation is considered as the risk factor during ESS operation. Following rules are thus applied specifically for the BEER:

4.2.1. Supervised areas:

- All freely accessible areas up to the outer face of biological shielding, including safety shutter pit and neutron guide shielding tunnel (buildings D03 and E02) and experimental cave in the building E01.
- Space inside the experimental cave when the safety shutter is closed.

Requirements:

1. Long-term whole-body dose for normal operations (H1) shall be less than 3 µSv/h.
2. Temporary hotspots shall not exceed 3 µSv integrated dose over any one-hour period. The dose to a worker in a controlled area from accident (H2) event shall not exceed 1 mSv.

4.2.2. Unrestricted controlled areas:

- Space inside the neutron guide shielding tunnel when the safety shutter is closed.
- Space inside the safety shutter pit when the ESS source is switched off.

Requirements:

3. Whole-body dose shall be limited for normal operations (H1) to less than 25 µSv/h.
4. Temporary hotspots shall not exceed 25 µSv integrated doses over any one-hour period.
5. The dose to a worker in a controlled area from accident (H2) event shall not exceed 10 mSv.

The shielding design shall provide passive protection for all normal operation (H1) events at 5 MW. And in the case of an accident (H2) provide sufficient biological shielding to fulfil the above-mentioned requirement number 2 or 5, depending on the defined area.

4.3. Definition of H1 and H2 scenarios

The definition of normal operation (H1) and accident (H2) scenarios is made in separate document *BEER - H1 and H2 scenarios for radiation shielding* [5].

Table 1 summarises the defined events from [5] and the corresponding chapter within this document which provide simulation results. The scenarios marked with green colour are shielded passively with proposed shielding design. The red coloured once (they are all severe accident scenarios) exceed the dose rates of the surveyed area, and they will need extra handling.

Table 1: Summary of H1&H2 events with the corresponding reference to the appropriate chapter.

Event	Notes	Event	Notes
H1.1	Chapter 6.1.2	H2.1	Chapter 6.4.1
H1.2	Chapter 6.1.3	H2.2	Chapter 6.4.2
H1.3	Chapter 6.1.4	H2.3	It is superseded by H2.7.
H1.4	Chapter 6.3.1	H2.4	Handled as H2.2 and H2.7
H1.5	Chapter 6.2	H2.5	Chapter 6.4.3
H1.6	Chapter 6.3.2	H2.6	Chapter 6.4.4
H1.7	It is superseded by H1.9.	H2.7	Chapter 6.4.5
H1.8	It is superseded by H2.1.		
H1.9	It is superseded by H2.2.		
H1.10	It is superseded by H2.3.		

4.4. Simulation tool description

All performed simulations covered in this report were carried out using the Monte Carlo particle transport code MCNP 6.1 [7] and the standard ENDF/B-VII.1 [8] nuclear data library provided with the code from RSICC distribution. The calculations were carried out using either the source term provided by ESS for the W01 beam or the ray-tracing simulations of thermal neutron beam (programs SIMRES and McStas), which provided input files containing neutron energy spectra and where applicable also spatial and angular distributions. If not stated otherwise, all calculations assumed neutron beam produced at 5 MW with all choppers stopped in the open position. The main quantities used in the calculations are neutron/photon fluxes in particle/cm^2/s calculated over unit volume cells using MCNP's f4 tallies for scoring. The particle fluxes are converted into equivalent dose rate values through the so-called flux to dose conversion factors defined in the ICRP-116 standards for both neutrons and photons (Table 2 and Table 3) which correspond to the ESS shielding guidelines [3].

The doses values were calculated using both FMESH and TMESH mesh tally, and f4 tally as a mesh tally results check since MCNP6.1 does not carry out statistical consistency checks in the case of the mesh tally calculations. The mesh grid was always chosen in such a way to achieve a

reasonable statistic in a reasonable time. In the case of thermal neutrons calculations, MCPL (Monte Carlo Particle List) [9] files from the previously realized ray-tracing simulations were provided. Each MCPL file contains thermal neutron energy spectrum and angular distributions at several points of the neutron guide. These data were implemented into the MCNP6 model by converting them into the surface source read files (SSR) via the MCPL routine. No variance reduction techniques were used for the transport and deep penetration calculations.

Table 2: Flux to dose rate conversion factors – neutrons.

E [MeV]	($\mu Sv.h^{-1}$) / (particle $cm^{-2}s^{-1}$)	E [MeV]	($\mu Sv.h^{-1}$) / (particle $cm^{-2}s^{-1}$)
1.00E-09	1.11E-02	3.00E+00	1.65E+00
1.00E-08	1.28E-02	4.00E+00	1.74E+00
2.50E-08	1.44E-02	5.00E+00	1.78E+00
1.00E-07	1.87E-02	6.00E+00	1.79E+00
2.00E-07	2.11E-02	7.00E+00	1.80E+00
5.00E-07	2.37E-02	8.00E+00	1.80E+00
1.00E-06	2.53E-02	9.00E+00	1.80E+00
2.00E-06	2.66E-02	1.00E+01	1.80E+00
5.00E-06	2.78E-02	1.20E+01	1.80E+00
1.00E-05	2.82E-02	1.40E+01	1.78E+00
2.00E-05	2.82E-02	1.50E+01	1.77E+00
5.00E-05	2.82E-02	1.60E+01	1.76E+00
1.00E-04	2.80E-02	1.80E+01	1.74E+00
2.00E-04	2.78E-02	2.00E+01	1.72E+00
5.00E-04	2.71E-02	2.10E+01	1.71E+00
1.00E-03	2.71E-02	3.00E+01	1.63E+00
2.00E-03	2.74E-02	5.00E+01	1.56E+00
5.00E-03	2.87E-02	7.50E+01	1.58E+00
1.00E-02	3.28E-02	1.00E+02	1.60E+00
2.00E-02	4.39E-02	1.30E+02	1.61E+00
3.00E-02	5.65E-02	1.50E+02	1.61E+00
5.00E-02	8.28E-02	1.80E+02	1.61E+00
7.00E-02	1.10E-01	2.00E+02	1.61E+00
1.00E-01	1.51E-01	3.00E+02	1.67E+00
1.50E-01	2.18E-01	4.00E+02	1.79E+00
2.00E-01	2.84E-01	5.00E+02	1.92E+00
3.00E-01	4.10E-01	6.00E+02	2.05E+00
5.00E-01	6.37E-01	7.00E+02	2.16E+00
7.00E-01	8.35E-01	8.00E+02	2.24E+00

E [MeV]	(µSv.h^{-1}) / (particle cm^{-2}s^{-1})	E [MeV]	(µSv.h^{-1}) / (particle cm^{-2}s^{-1})
9.00E-01	1.00E+00	9.00E+02	2.30E+00
1.00E+00	1.08E+00	1.00E+03	2.35E+00
1.20E+00	1.19E+00	2.00E+03	2.76E+00
1.50E+00	1.31E+00	5.00E+03	3.64E+00
2.00E+00	1.47E+00	1.00E+04	4.75E+00

Table 3 : Flux to dose rate conversion factors – photons.

E [MeV]	(µSv.h^{-1}) / (particle cm^{-2}s^{-1})	E [MeV]	(µSv.h^{-1}) / (particle cm^{-2}s^{-1})
1.00E-02	2.47E-04	6.13E+00	5.47E-02
1.50E-02	5.62E-04	8.00E+00	6.70E-02
2.00E-02	8.10E-04	1.00E+01	7.92E-02
3.00E-02	1.13E-03	1.50E+01	1.09E-01
4.00E-02	1.26E-03	2.00E+01	1.38E-01
5.00E-02	1.33E-03	3.00E+01	1.85E-01
6.00E-02	1.40E-03	4.00E+01	2.23E-01
7.00E-02	1.49E-03	5.00E+01	2.60E-01
8.00E-02	1.60E-03	6.00E+01	2.95E-01
1.00E-01	1.87E-03	8.00E+01	3.52E-01
1.50E-01	2.69E-03	1.00E+02	3.96E-01
2.00E-01	3.60E-03	1.50E+02	4.68E-01
3.00E-01	5.44E-03	2.00E+02	5.15E-01
4.00E-01	7.20E-03	3.00E+02	5.80E-01
5.00E-01	8.89E-03	4.00E+02	6.19E-01
5.11E-01	9.07E-03	5.00E+02	6.48E-01
6.00E-01	1.05E-02	6.00E+02	6.70E-01
6.62E-01	1.14E-02	8.00E+02	7.02E-01
8.00E-01	1.34E-02	1.00E+03	7.24E-01
1.00E+00	1.62E-02	1.50E+03	7.63E-01
1.12E+00	1.76E-02	2.00E+03	7.92E-01
1.33E+00	2.01E-02	3.00E+03	8.35E-01
1.50E+00	2.20E-02	4.00E+03	8.75E-01
2.00E+00	2.69E-02	5.00E+03	9.04E-01
3.00E+00	3.51E-02	6.00E+03	9.29E-01
4.00E+00	4.21E-02	8.00E+03	9.65E-01

E [MeV]	(µSv.h^{-1}) / (particle cm^{-2}s^{-1})	E [MeV]	(µSv.h^{-1}) / (particle cm^{-2}s^{-1})
5.00E+00	4.82E-02	1.00E+04	9.94E-01
6.00E+00	5.40E-02		

5. INPUTS AND MODELS FOR SIMULATIONS

This part of the report deals with the realized simulations of the radiation shielding components design starting from the provided inputs, model geometry, materials descriptions and computational results.

5.1. Calculation inputs

Details on significant components in terms of the simulation (material composition, basic design, etc.) were provided. A simplified MCNP model of the ESS bunker [10] developed by the ESS Neutron Optics and Shielding Group was also provided.

5.1.1. Shutter pit

The shutter pit is adjacent to the bunker wall; thus, there is a significant contribution of the fast neutrons in addition to the thermal ones. Dimensions of the pit and used materials are described in chapter 5.3.1.1. The shielding around the shutter must provide sufficient biological shielding for both opened and closed state. The limiting factors are dose rates outside the pit and guide tunnel shielding following the shutter pit (maximum 3 µSv/h), and also behind the pit wall inside the guide tunnel when the shutter is closed (maximum 25 µSv/h). The spectra of fast neutrons in different parts of the shutter are shown in Figure 2. The input spectrum is also tabulated in Table 4. The spectrum was calculated at the exit from the bunker wall (at the centre of the shutter cross-section, on the front face) averaged over the beam area, the divergence of the beam was also taken into account in the subsequent calculations.

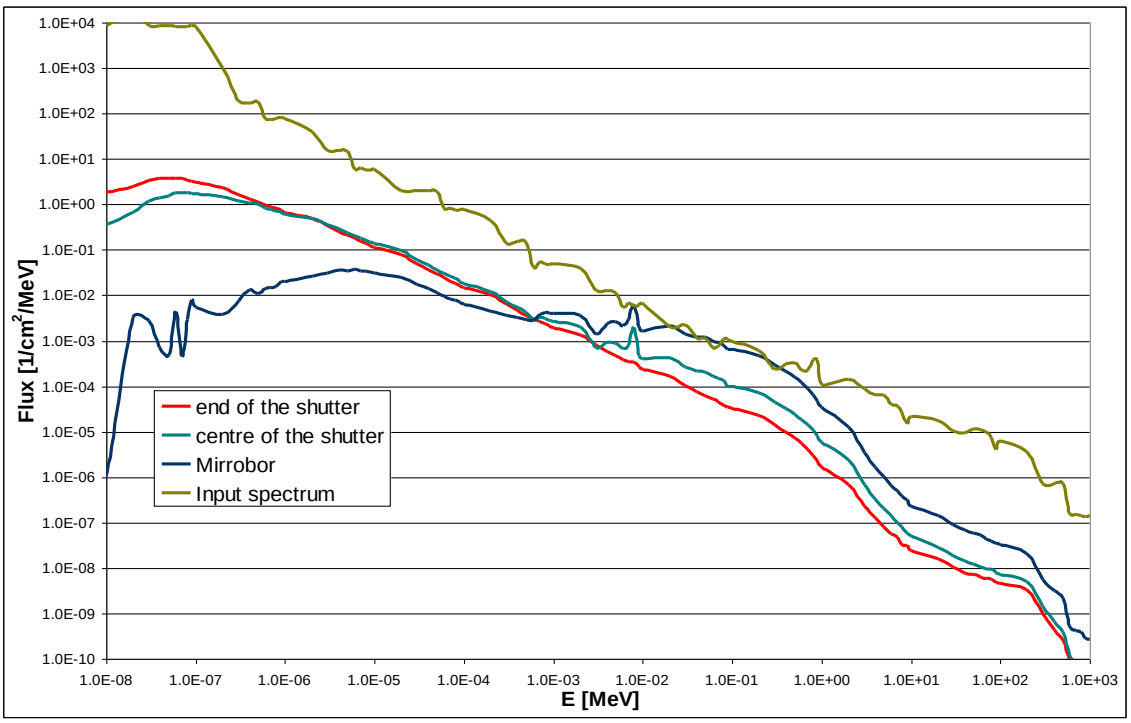

Figure 2: Fast neutron spectrum at the entrance to the shutter pit (input) and leaking through the shutter.

Table 4: Input fast neutron spectrum (calculation input) at the central position, averaged over beam area.

E [MeV]	Φ [cm^{-2} s^{-1}]	E [MeV]	Φ [cm^{-2} s^{-1}]
1.00E-10	0.0	5.00E-01	1.78E+03
1.00E-08	2.36E+03	7.00E-01	1.30E+03
2.00E-08	4.48E+03	9.00E-01	2.19E+03
1.00E-07	1.88E+04	1.00E+00	3.26E+02
2.00E-07	2.95E+03	2.00E+00	3.91E+03
5.00E-07	1.45E+03	3.00E+00	2.55E+03
1.00E-06	1.09E+03	4.00E+00	1.85E+03
2.00E-06	1.08E+03	5.00E+00	1.76E+03
5.00E-06	1.28E+03	6.00E+00	1.10E+03
1.00E-05	8.63E+02	7.00E+00	1.06E+03
2.00E-05	5.89E+02	8.00E+00	7.56E+02
5.00E-05	1.67E+03	9.00E+00	4.03E+02
1.00E-04	1.14E+03	1.00E+01	6.16E+02
2.00E-04	1.25E+03	1.50E+01	2.46E+03
5.00E-04	1.25E+03	2.00E+01	2.48E+03
1.00E-03	6.73E+02	3.00E+01	2.93E+03
2.00E-03	1.17E+03	4.00E+01	2.63E+03
5.00E-03	1.04E+03	5.00E+01	3.25E+03
1.00E-02	8.28E+02	6.00E+01	3.09E+03
2.00E-02	5.89E+02	7.00E+01	2.68E+03
3.00E-02	6.54E+02	8.00E+01	1.92E+03
5.00E-02	6.95E+02	9.00E+01	1.12E+03
7.00E-02	4.03E+02	1.00E+02	1.71E+03
1.00E-01	8.82E+02	2.00E+02	9.92E+03
2.00E-01	1.69E+03	5.00E+02	6.19E+03
3.00E-01	6.95E+02	1.00E+03	2.11E+03
		Total	**1.12E+05**

5.1.2. Chopper pit

The chopper pit is situated at the distance of 80 m from the source. No significant flux of fast neutrons is expected at such distance and is neglected in simulations. Chopper discs in the closed position will absorb practically all neutrons with thermal energies. An input MCPL file covering the area of 5×10 cm^2 (exceeding the actual guide cross-section of 4×8 cm^2) with an integrated intensity of 5.8E+10 n/s corresponding to the maximum flux at 5 MW was generated by ray-tracing simulation. Thermal neutron spectrum is similar to one shown in Figure 10 (at the sample position), but with different neutron fluxes which are listed in Table 5. Two scenarios with two limiting factors for shielding were assumed:

a) all thermal neutrons scattered on the chopper disc,

b) all thermal neutrons converted to γ on the chopper disc, modelled as boron layer, γ arises from ^{10}B capture.

Table 5: Input thermal neutron spectrum (calculation input)

E [MeV]	Φ [cm^{-2} s^{-1}]	E [MeV]	Φ [cm^{-2} s^{-1}]	E [MeV]	Φ [cm^{-2} s^{-1}]	E [MeV]	Φ [cm^{-2} s^{-1}]
1.10E-09	1.85E+06	2.09E-09	5.90E+06	4.53E-09	1.83E+07	1.62E-08	1.91E+07
1.23E-09	2.48E+06	2.16E-09	5.96E+06	4.75E-09	2.02E+07	1.77E-08	1.88E+07
1.26E-09	1.87E+06	2.23E-09	6.03E+06	4.99E-09	2.15E+07	1.95E-08	1.88E+07
1.29E-09	2.55E+06	2.31E-09	6.74E+06	5.24E-09	2.23E+07	2.15E-08	2.02E+07
1.33E-09	2.58E+06	2.39E-09	7.64E+06	5.52E-09	2.40E+07	2.39E-08	2.25E+07
1.36E-09	1.94E+06	2.47E-09	6.90E+06	5.82E-09	2.55E+07	2.67E-08	2.47E+07
1.40E-09	2.59E+06	2.56E-09	8.33E+06	6.14E-09	2.71E+07	3.00E-08	2.74E+07
1.44E-09	3.30E+06	2.66E-09	8.34E+06	6.49E-09	2.89E+07	3.40E-08	2.97E+07
1.47E-09	2.64E+06	2.75E-09	8.60E+06	6.87E-09	3.08E+07	3.89E-08	2.97E+07
1.51E-09	3.39E+06	2.86E-09	1.01E+07	7.29E-09	3.30E+07	4.49E-08	2.81E+07
1.56E-09	2.71E+06	2.97E-09	1.01E+07	7.74E-09	3.45E+07	5.24E-08	2.33E+07
1.60E-09	3.44E+06	3.08E-09	1.09E+07	8.24E-09	3.79E+07	6.19E-08	1.61E+07
1.65E-09	4.14E+06	3.21E-09	1.16E+07	8.79E-09	3.63E+07	7.42E-08	8.36E+06
1.69E-09	3.51E+06	3.34E-09	1.16E+07	9.40E-09	3.93E+07	9.06E-08	2.97E+06
1.74E-09	4.22E+06	3.48E-09	1.32E+07	1.01E-08	4.47E+07	1.13E-07	7.91E+05
1.80E-09	4.28E+06	3.63E-09	1.38E+07	1.08E-08	3.77E+07	1.45E-07	2.62E+05
1.85E-09	4.32E+06	3.78E-09	1.44E+07	1.16E-08	3.48E+07	1.94E-07	8.03E+04
1.91E-09	4.36E+06	3.95E-09	1.60E+07	1.26E-08	2.96E+07	2.70E-07	0.00E+00
1.97E-09	5.09E+06	4.13E-09	1.65E+07	1.36E-08	2.39E+07	4.04E-07	0.00E+00
2.03E-09	5.12E+06	4.32E-09	1.80E+07	1.48E-08	2.18E+07	6.68E-07	0.00E+00
						total	**1.16E+09**

5.1.3. Neutron guide

5.1.3.1. Fast neutrons – simulation of neutron transport through the bunker

In the shielding design of the neutron guide, the problem is similar as in the case of the cave with one additional aspect. At the point of the bunker exit, a non-negligible presence of fast and high-energy neutrons remaining from the bunker section of the facility is present. These affect the design of the shutter pit and possibly the first meters of the neutron guide.

For the needs of the determination of the fast neutron spectrum at the point of the bunker exit, a simplified MCNP bunker model developed by ESS [10] was used in the form available in 4/2017, while the source was extracted from the ESS-0416080. The model was adapted to the needs of the BEER facility, namely the original NMX monolith insert and guide configuration was replaced by the proposed configuration for BEER, as shown in Figure 3. The source term was defined at 2 m from the moderator and rescaled to the flux provided by ESS for the W02 beam port.

The neutron guide model was represented by a 10 mm thick Cu covered with 10 mm B_4C. The Cu thickness was increased to 40 mm at the places indicated in Figure 3. Starting at 10 m from the source, the guide was curved to *R*=2000 m, closing the direct line of sight at the exit from the bunker (if considering an isotropic source at the guide entry at 10 m). Based on this model, a source term was simulated at the exit from the bunker, containing the fast neutron spectrum (above 0.1 MeV) and angular distribution at the bunker exit over an area of the beam, 2×8 cm^2 with an integral intensity of 1.1E+5 n/s and a spectrum shown in Figure 4. This was recorded as an SSR (Surface Source Read) file and used for later guide shielding calculations. The total fast neutron dose (energies from 0.1 MeV to 1 GeV) on the bunker exit over the beam area was estimated using average cell flux f4 tally as 17 mSv/h. This dose was calculated in MCNP. This is a dose which has to be shielded in the shutter pit.

The simulation also yielded dose rates at the inner bunker wall. Figure 5 shows the neutron spectra of the different areas on the inner bunker wall. Normalization corresponds to the total number of neutrons per second, and the value was in this case taken as 5.38E+14. Figure 6 and Figure 7 show the dose map over the inner bunker wall in different meshes.

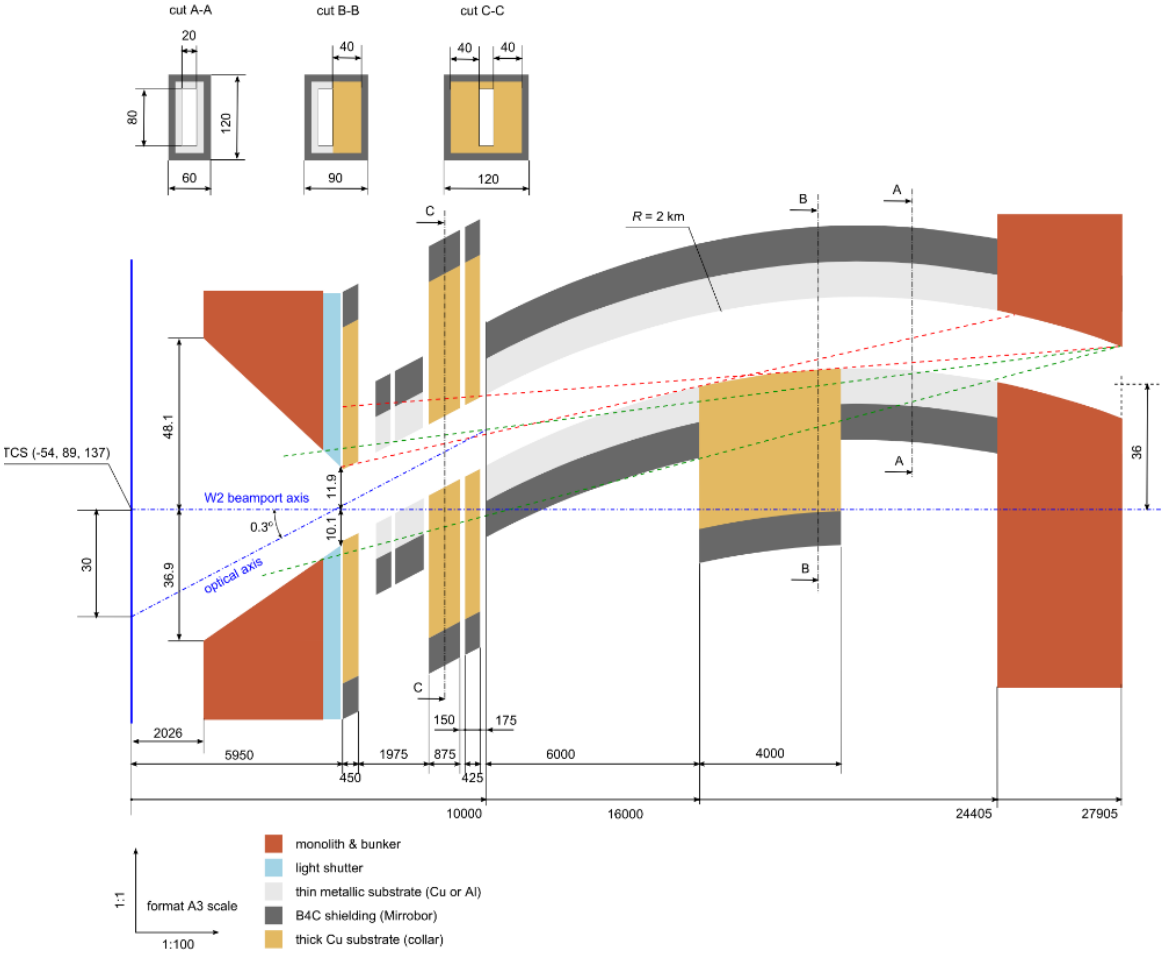

Figure 3: MCNP bunker model with the BEER facility guide

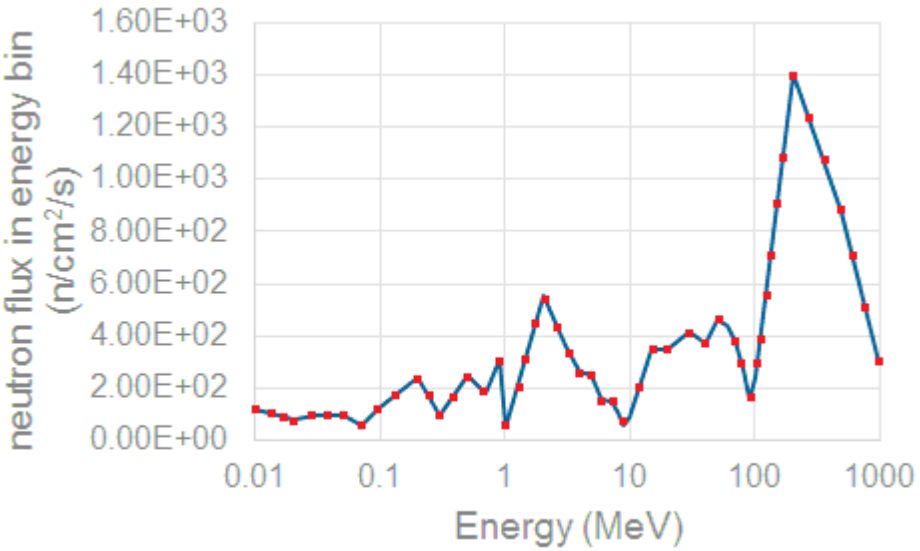

Figure 4: Fast neutron spectrum at the bunker exit.

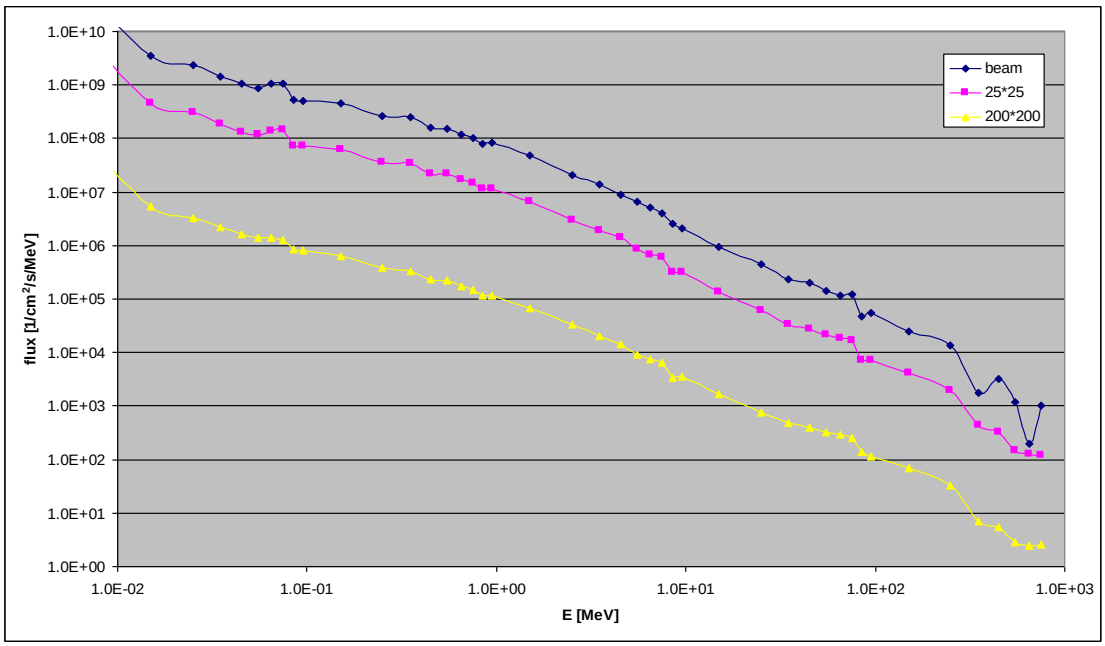

Figure 5: Neutron spectra over beam area (2 cm × 8 cm), area of 25 cm ×25 cm, and 200 cm × 200 cm at the inner face of the bunker wall.

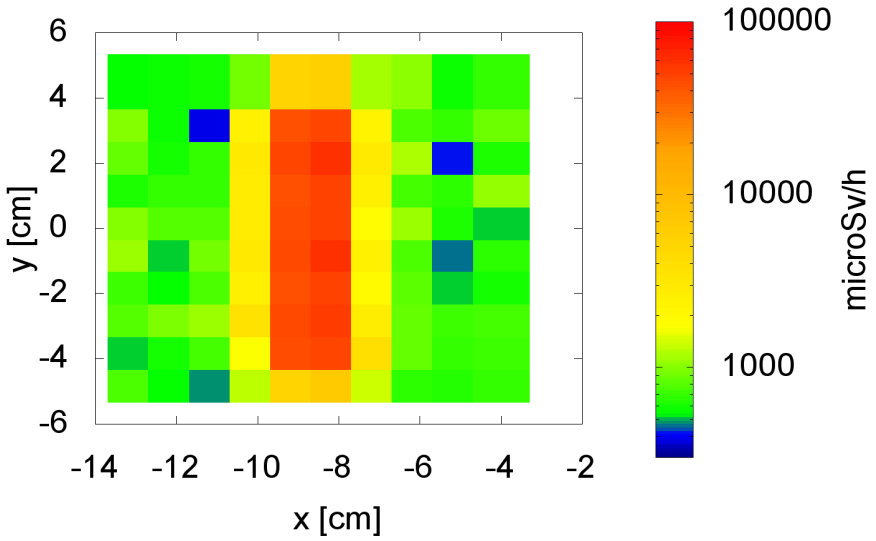

Figure 6: Neutron and photon doses over the beam area at the inner entrance to the bunker wall. The guide dimensions are 2×8 cm².

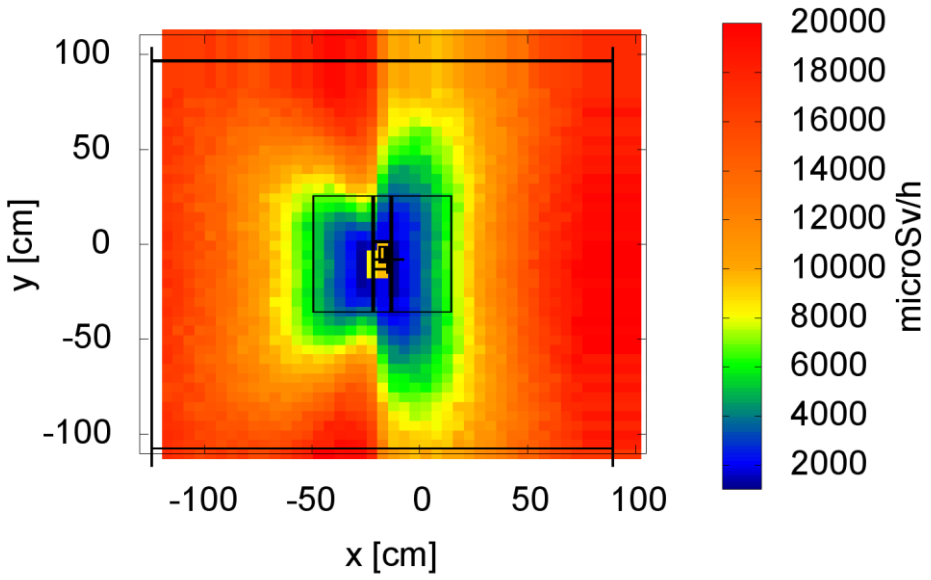

Figure 7: Neutron and photon doses over 200x200 cm^2 at the inner entrance to the bunker wall, for geometry details, see Figure 3.

5.1.3.2. Simulation of neutron guide shielding tunnel

For the neutron guide shielding design far from the bunker, the main source of radiation is the conversion of thermal neutrons to prompt gamma in the NiTi multilayer coating, where the absorption on nickel nuclei makes the dominant contribution to the dose rates behind the guide shielding. Thermal neutrons losses in the neutron guides in D03 and E02 halls, simulated by McStas ver. 2.6 are shown in Figure 8. A conservative model setting without accounting for surface roughness has been used. The results thus provide an upper estimate for neutron capture rates [11]. For this conservative estimate, a linear photon source along a 10 m long segment of the guide was considered. The spectrum of the photon source was equal to the prompt gamma emission from nickel as the capture on nickel is dominant, and the energy spectrum is harder compared to titanium. The model gamma spectrum was determined by modelling of a point neutron source with the energy spectrum equal the thermal spectrum in the neutron guide, surrounded by a thin spherical nickel layer, which resulted in 1.45 photons emitted per one neutron capture on nickel. As seen from the capture rates shown in Figure 8 over the whole distance of the neutron guide behind the shutter pit towards the entry to the instrumental cave, the capture rate is below 3E+7 n/s/m for the whole length between 35 and 150 m. This corresponds to the production of 4.35E+7 p/s/m photons. Over the guide profile of 2 × 8 cm^2 and its surface area of 2000 cm2 per 1 m of distance, this photon production implies an average flux of 2.18E+4 p/cm2/s with the spectra shown in Figure 9 and Table 6.

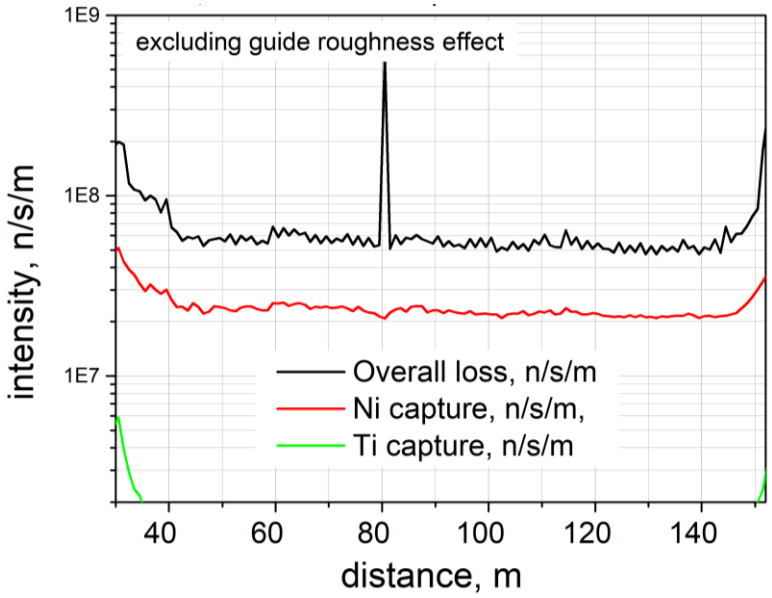

Figure 8: Thermal neutrons losses in the neutron guides in D03 and E02 halls, simulated by McStas ver. 2.6.

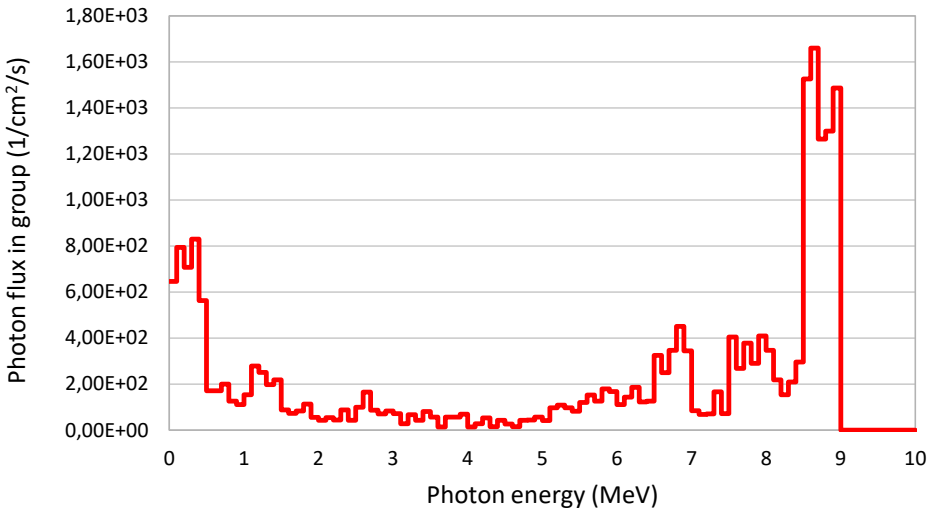

Figure 9: Photon spectrum generated through neutron capture on the NiTi layer of the neutron guide.

Table 6: Photon spectrum generated through neutron capture on the NiTi layer of the neutron guide on the surface (calculation input).

E [MeV]	Φ [cm^{-2} s^{-1}]	E [MeV]	Φ [cm^{-2} s^{-1}]	E [MeV]	Φ [cm^{-2} s^{-1}]
1.00E-01	6.46E+02	3.50E+00	8.04E+01	6.90E+00	4.51E+02
2.00E-01	7.94E+02	3.60E+00	5.58E+01	7.00E+00	3.44E+02
3.00E-01	7.07E+02	3.70E+00	1.29E+01	7.10E+00	8.38E+01
4.00E-01	8.30E+02	3.80E+00	5.68E+01	7.20E+00	6.76E+01
5.00E-01	5.62E+02	3.90E+00	5.59E+01	7.30E+00	7.02E+01

E [MeV]	Φ [cm^{-2} s^{-1}]	E [MeV]	Φ [cm^{-2} s^{-1}]	E [MeV]	Φ [cm^{-2} s^{-1}]
6.00E-01	1.71E+02	4.00E+00	6.93E+01	7.40E+00	1.66E+02
7.00E-01	1.71E+02	4.10E+00	1.39E+01	7.50E+00	7.11E+01
8.00E-01	2.00E+02	4.20E+00	2.76E+01	7.60E+00	4.04E+02
9.00E-01	1.26E+02	4.30E+00	5.29E+01	7.70E+00	2.67E+02
1.00E+00	1.11E+02	4.40E+00	1.49E+01	7.80E+00	3.78E+02
1.10E+00	1.53E+02	4.50E+00	4.26E+01	7.90E+00	2.90E+02
1.20E+00	2.78E+02	4.60E+00	2.66E+01	8.00E+00	4.09E+02
1.30E+00	2.50E+02	4.70E+00	1.45E+01	8.10E+00	3.46E+02
1.40E+00	1.97E+02	4.80E+00	4.28E+01	8.20E+00	2.18E+02
1.50E+00	2.18E+02	4.90E+00	4.37E+01	8.30E+00	1.53E+02
1.60E+00	8.74E+01	5.00E+00	5.67E+01	8.40E+00	2.09E+02
1.70E+00	7.23E+01	5.10E+00	4.17E+01	8.50E+00	2.96E+02
1.80E+00	8.27E+01	5.20E+00	9.68E+01	8.60E+00	1.53E+03
1.90E+00	1.13E+02	5.30E+00	1.08E+02	8.70E+00	1.66E+03
2.00E+00	5.55E+01	5.40E+00	9.66E+01	8.80E+00	1.26E+03
2.10E+00	4.24E+01	5.50E+00	8.15E+01	8.90E+00	1.30E+03
2.20E+00	5.37E+01	5.60E+00	1.19E+02	9.00E+00	1.49E+03
2.30E+00	4.31E+01	5.70E+00	1.52E+02	9.10E+00	0.00E+00
2.40E+00	8.73E+01	5.80E+00	1.25E+02	9.20E+00	0.00E+00
2.50E+00	4.20E+01	5.90E+00	1.78E+02	9.30E+00	0.00E+00
2.60E+00	9.92E+01	6.00E+00	1.68E+02	9.40E+00	0.00E+00
2.70E+00	1.65E+02	6.10E+00	1.10E+02	9.50E+00	0.00E+00
2.80E+00	8.57E+01	6.20E+00	1.43E+02	9.60E+00	0.00E+00
2.90E+00	7.05E+01	6.30E+00	1.86E+02	9.70E+00	0.00E+00
3.00E+00	8.32E+01	6.40E+00	1.22E+02	9.80E+00	0.00E+00
3.10E+00	7.14E+01	6.50E+00	1.26E+02	9.90E+00	0.00E+00
3.20E+00	2.77E+01	6.60E+00	3.25E+02	1.00E+01	0.00E+00
3.30E+00	6.70E+01	6.70E+00	2.49E+02		
3.40E+00	4.18E+01	6.80E+00	3.46E+02	**Total**	**2.18E+04**

5.1.4. Instrument cave

The design of the instrument cave shielding was realized considering some postulated irradiation scenarios at the sample location, where samples are studied while irradiated by an intense

focused thermal neutron beam. During the irradiation, neutrons can be scattered by the sample in any direction or be absorbed emitting thus secondary prompt-γ radiation. These two factors (primary neutrons and secondary prompt-γ photons) are limiting factors to be considered while designing the cave walls. Additional sources of radiation can be considered as radiation decay of the activated sample or neutron interactions with neutron optics. These, however, do not represent major contribution to the overall γ radiation considered for the worst case H1 scenario, thus, they are not the limiting sources.

As the input for the calculation, two MCPL files coming from the ray-tracing simulation of the whole BEER instrument representing the thermal neutron beam parameters at the sample location were implemented into the models. They are described in more details in *BEER - H1 and H2 scenarios for radiation shielding* [5] and *Optics Report for the BEER Instrument* [6]:

1. **Accidentally full beam** (AFB[5], F1[6]): all choppers stopped except FC choppers, divergence slits open, the last slit removed, the last focusing guide GEX1 on (beam size at sample approx. 40x18 mm^2 using FWHM), wavelength band centre at 3.1 Å, proton beam at 5 MW, neutron flux in the centre: $2.94 \cdot 10^9$ $n \cdot s^{-1} \cdot cm^{-2}$, integrated intensity over the beam size and for wavelength range 0.2-8.2 Å: $2.26 \cdot 10^{10}$ $n \cdot s^{-1}$.
2. **Maximum white beam** (MWB[5], F0[6]): maximum physically possible beam intensity that can be delivered to the sample: like AFB, but all choppers including FC are parked open. Neutron flux in the centre: $5.3 \cdot 10^9$ $n \cdot s^{-1} \cdot cm^{-2}$, integrated intensity for wavelength range 0.2-8.2 Å: $4.07 \cdot 10^{10}$ $n \cdot s^{-1}$.

Figure 10 shows the neutron spectrum at the sample location. The maxima in the figure at 67.6 meV and 10.1 meV correspond to the maxima of the bi-spectral ESS source. The spectrum of both **AFB** and **MWB** is listed in the Table 7.

Table 7: Input thermal neutron spectrum for both used scenarios averaged over beam area

E [MeV]	Φ [cm^{-2} s^{-1}]	E [MeV]	Φ [cm^{-2} s^{-1}]	E [MeV]	Φ [cm^{-2} s^{-1}]	E [MeV]	Φ [cm^{-2} s^{-1}]
AFB							
5.00E-10	8.35E+07	7.50E-09	1.17E+09	1.45E-08	4.93E+08	2.15E-08	1.00E+08
1.00E-09	5.90E+08	8.00E-09	1.14E+09	1.50E-08	4.38E+08	2.20E-08	7.27E+07
1.50E-09	6.49E+07	8.50E-09	1.08E+09	1.55E-08	3.96E+08	2.25E-08	5.40E+07
2.00E-09	1.01E+09	9.00E-09	1.06E+09	1.60E-08	3.45E+08	2.30E-08	3.06E+07
2.50E-09	1.29E+09	9.50E-09	1.02E+09	1.65E-08	2.94E+08	2.35E-08	1.38E+07
3.00E-09	6.24E+08	1.00E-08	9.91E+08	1.70E-08	2.79E+08	2.40E-08	7.01E+06
3.50E-09	0.00E+00	1.05E-08	9.48E+08	1.75E-08	2.60E+08	2.45E-08	1.33E+06
4.00E-09	0.00E+00	1.10E-08	8.62E+08	1.80E-08	2.43E+08	2.50E-08	4.26E+05
4.50E-09	0.00E+00	1.15E-08	8.60E+08	1.85E-08	2.17E+08	2.55E-08	1.71E+05
5.00E-09	0.00E+00	1.20E-08	8.39E+08	1.90E-08	2.20E+08	2.60E-08	3.77E+04
5.50E-09	0.00E+00	1.25E-08	7.91E+08	1.95E-08	1.99E+08	2.65E-08	1.01E+04
6.00E-09	2.28E+08	1.30E-08	7.36E+08	2.00E-08	1.71E+08	2.70E-08	1.20E+03

E [MeV]	Φ [cm^{-2} s^{-1}]	E [MeV]	Φ [cm^{-2} s^{-1}]	E [MeV]	Φ [cm^{-2} s^{-1}]	E [MeV]	Φ [cm^{-2} s^{-1}]
6.50E-09	1.14E+09	1.35E-08	6.53E+08	2.05E-08	1.56E+08	2.75E-08	0.00E+00
						Total	**1.44e+09**
MWB							
5.00E-10	2.07E+08	2.55E-08	1.22E+08	5.05E-08	6.28E+07	7.55E-08	2.08E+07
1.00E-09	8.21E+08	2.60E-08	1.11E+08	5.10E-08	6.54E+07	7.60E-08	3.28E+07
1.50E-09	1.07E+09	2.65E-08	1.16E+08	5.15E-08	6.24E+07	7.65E-08	2.97E+07
2.00E-09	1.21E+09	2.70E-08	1.22E+08	5.20E-08	4.98E+07	7.70E-08	3.23E+07
2.50E-09	1.31E+09	2.75E-08	1.12E+08	5.25E-08	6.13E+07	7.75E-08	2.17E+07
3.00E-09	1.36E+09	2.80E-08	1.03E+08	5.30E-08	6.53E+07	7.80E-08	1.79E+07
3.50E-09	1.38E+09	2.85E-08	1.14E+08	5.35E-08	5.97E+07	7.85E-08	3.04E+07
4.00E-09	1.37E+09	2.90E-08	1.03E+08	5.40E-08	6.01E+07	7.90E-08	2.66E+07
4.50E-09	1.37E+09	2.95E-08	1.08E+08	5.45E-08	6.38E+07	7.95E-08	2.67E+07
5.00E-09	1.32E+09	3.00E-08	9.83E+07	5.50E-08	5.46E+07	8.00E-08	2.44E+07
5.50E-09	1.32E+09	3.05E-08	1.04E+08	5.55E-08	4.38E+07	8.05E-08	1.80E+07
6.00E-09	1.29E+09	3.10E-08	1.15E+08	5.60E-08	5.26E+07	8.10E-08	2.56E+07
6.50E-09	1.25E+09	3.15E-08	1.07E+08	5.65E-08	6.02E+07	8.15E-08	2.24E+07
7.00E-09	1.18E+09	3.20E-08	9.92E+07	5.70E-08	4.62E+07	8.20E-08	2.90E+07
7.50E-09	1.19E+09	3.25E-08	1.18E+08	5.75E-08	5.04E+07	8.25E-08	2.03E+07
8.00E-09	1.12E+09	3.30E-08	1.09E+08	5.80E-08	5.64E+07	8.30E-08	2.51E+07
8.50E-09	1.12E+09	3.35E-08	1.03E+08	5.85E-08	5.52E+07	8.35E-08	1.83E+07
9.00E-09	1.06E+09	3.40E-08	1.05E+08	5.90E-08	5.39E+07	8.40E-08	1.45E+07
9.50E-09	1.03E+09	3.45E-08	9.02E+07	5.95E-08	5.90E+07	8.45E-08	2.24E+07
1.00E-08	9.79E+08	3.50E-08	9.68E+07	6.00E-08	4.51E+07	8.50E-08	2.11E+07
1.05E-08	9.30E+08	3.55E-08	9.87E+07	6.05E-08	4.82E+07	8.55E-08	1.55E+07
1.10E-08	8.81E+08	3.60E-08	1.06E+08	6.10E-08	3.75E+07	8.60E-08	1.14E+07
1.15E-08	8.19E+08	3.65E-08	1.00E+08	6.15E-08	4.18E+07	8.65E-08	2.10E+07
1.20E-08	8.06E+08	3.70E-08	9.20E+07	6.20E-08	4.20E+07	8.70E-08	1.60E+07
1.25E-08	7.78E+08	3.75E-08	8.72E+07	6.25E-08	3.26E+07	8.75E-08	2.26E+07
1.30E-08	7.04E+08	3.80E-08	9.14E+07	6.30E-08	5.15E+07	8.80E-08	1.58E+07
1.35E-08	6.21E+08	3.85E-08	9.10E+07	6.35E-08	3.10E+07	8.85E-08	1.49E+07
1.40E-08	5.74E+08	3.90E-08	9.74E+07	6.40E-08	4.56E+07	8.90E-08	1.68E+07
1.45E-08	5.21E+08	3.95E-08	7.68E+07	6.45E-08	4.29E+07	8.95E-08	2.25E+07
1.50E-08	4.55E+08	4.00E-08	9.07E+07	6.50E-08	3.11E+07	9.00E-08	1.46E+07
1.55E-08	3.72E+08	4.05E-08	9.34E+07	6.55E-08	3.86E+07	9.05E-08	1.49E+07
1.60E-08	3.42E+08	4.10E-08	7.94E+07	6.60E-08	4.37E+07	9.10E-08	1.77E+07

E [MeV]	Φ [cm^{-2} s^{-1}]	E [MeV]	Φ [cm^{-2} s^{-1}]	E [MeV]	Φ [cm^{-2} s^{-1}]	E [MeV]	Φ [cm^{-2} s^{-1}]
1.65E-08	3.18E+08	4.15E-08	8.29E+07	6.65E-08	3.12E+07	9.15E-08	1.26E+07
1.70E-08	2.82E+08	4.20E-08	6.57E+07	6.70E-08	4.51E+07	9.20E-08	1.41E+07
1.75E-08	2.59E+08	4.25E-08	8.06E+07	6.75E-08	3.00E+07	9.25E-08	1.21E+07
1.80E-08	2.44E+08	4.30E-08	7.92E+07	6.80E-08	4.44E+07	9.30E-08	1.49E+07
1.85E-08	2.19E+08	4.35E-08	6.73E+07	6.85E-08	3.74E+07	9.35E-08	1.68E+07
1.90E-08	2.07E+08	4.40E-08	8.69E+07	6.90E-08	3.79E+07	9.40E-08	1.62E+07
1.95E-08	1.92E+08	4.45E-08	7.68E+07	6.95E-08	3.80E+07	9.45E-08	1.74E+07
2.00E-08	1.85E+08	4.50E-08	7.23E+07	7.00E-08	2.93E+07	9.50E-08	1.23E+07
2.05E-08	1.76E+08	4.55E-08	6.63E+07	7.05E-08	2.94E+07	9.55E-08	1.13E+07
2.10E-08	1.73E+08	4.60E-08	8.08E+07	7.10E-08	2.41E+07	9.60E-08	1.40E+07
2.15E-08	1.52E+08	4.65E-08	5.48E+07	7.15E-08	2.35E+07	9.65E-08	1.30E+07
2.20E-08	1.57E+08	4.70E-08	6.12E+07	7.20E-08	2.71E+07	9.70E-08	1.47E+07
2.25E-08	1.47E+08	4.75E-08	7.89E+07	7.25E-08	3.15E+07	9.75E-08	9.67E+06
2.30E-08	1.47E+08	4.80E-08	7.35E+07	7.30E-08	3.23E+07	9.80E-08	6.89E+06
2.35E-08	1.24E+08	4.85E-08	6.89E+07	7.35E-08	3.76E+07	9.85E-08	1.36E+07
2.40E-08	1.37E+08	4.90E-08	5.92E+07	7.40E-08	2.91E+07	9.90E-08	5.96E+06
2.45E-08	1.36E+08	4.95E-08	7.32E+07	7.45E-08	1.65E+07	9.95E-08	9.30E+06
2.50E-08	1.23E+08	5.00E-08	5.60E+07	7.50E-08	3.35E+07	1.00E-07	8.08E+06
						Total	**2.61E+09**

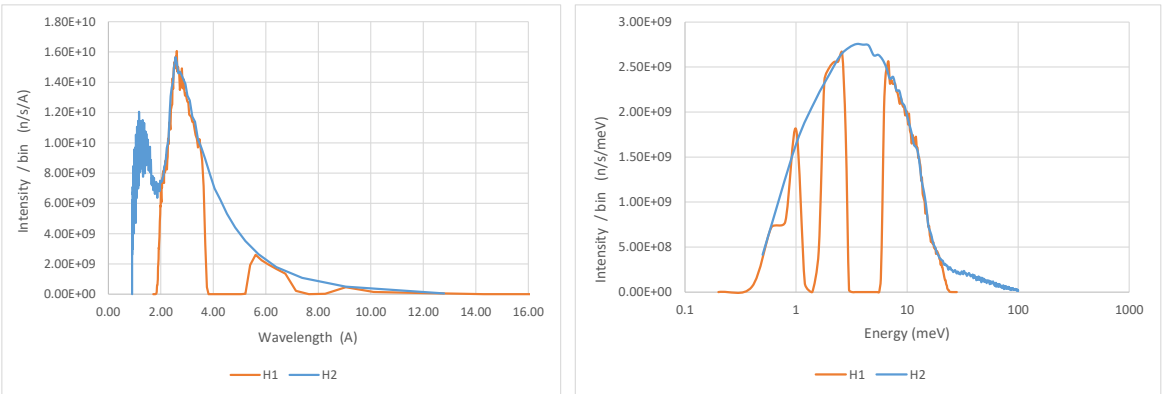

Figure 10: Thermal neutron spectrum at the sample location for AFB (denoted as H1 in the chart) and MWB (denoted as H2 in the chart).

Two worst-case samples in the term of neutron scattering (**WNS**) and production of prompt-γ (**WGE**) were defined in the *BEER - H1 and H2 scenarios for radiation shielding* [5]. Beside those samples, several other elements were checked.

In Figure 11 and Table 8 are shown spectra and listed a series of examined samples which are mainly high energy prompt-γ emitter and could be considered as samples at the BEER instrument.

The dimensions of each sample were chosen to cover the whole impacting neutron beam and minimize its self-shielding effect. Photon fluxes in 100 keV energy bins were calculated directly behind the samples as well as radiation doses behind a 100 cm modelled concrete wall placed behind the sample, in order to identify the most limiting prompt-γ emitting sample material for the BEER shielding design. Nickel and chromium were identified as the worst-case samples, due to their significant over 8 MeV γ lines present in the spectra. Scandium appears to be a worse-case emitter, by means of high energy prompt-γ. The resulting dose rate behind the modelled shielding; however, samples with high scandium content are not expected to be in the samples measured at the instrument in such quantity in comparison to nickel or chromium. Neither high content of manganese in the samples is expected compared to nickel or chromium. Nickel was chosen as a reference sample because it is highly used in common engineering samples.

Table 8 - Prompt-γ emission from a series of examined samples after being hit by the WMB beam at the sample position.

Sample	Dimensions (w×h×t) (cm^3)	Photon flux behind the sample ($n/cm^2/s$)	Photon dose rate after 100 cm of concrete (µSv/h)
Nickel	4.4×4.4×1	4.10E+08	58.9
Manganese	4.4×4.4×1	7.47E+08	57.2
Water	4.4×4.4×1	1.91E+07	12.0
Iron	4.4×4.4×1	3.21E+08	43.9
Copper	4.4×4.4×1	4.41E+08	39.3
Chromium	4.4×4.4×1	4.18E+08	56.6
Cadmium	4.4×4.4×0.1	1.04E+09	44.8
Boron carbide	4.4×4.4×1	2.86E+08	-
Aluminium	4.4×4.4×10	3.29E+07	17.8
Vanadium	4.4×4.4×1	5.07E+08	37.9
Titanium	4.4×4.4×1	5.49E+08	48.1
Gadolinium	4.4×4.4×0.1	9.27E+08	28.7
Zinc	4.4×4.4×1	8.86E+06	18.6
Cobalt	4.4×4.4×1	7.99E+08	39.0
Scandium	4.4×4.4×1	1.13E+09	65.8
Selenium	4.4×4.4×1	4.35E+06	13.2

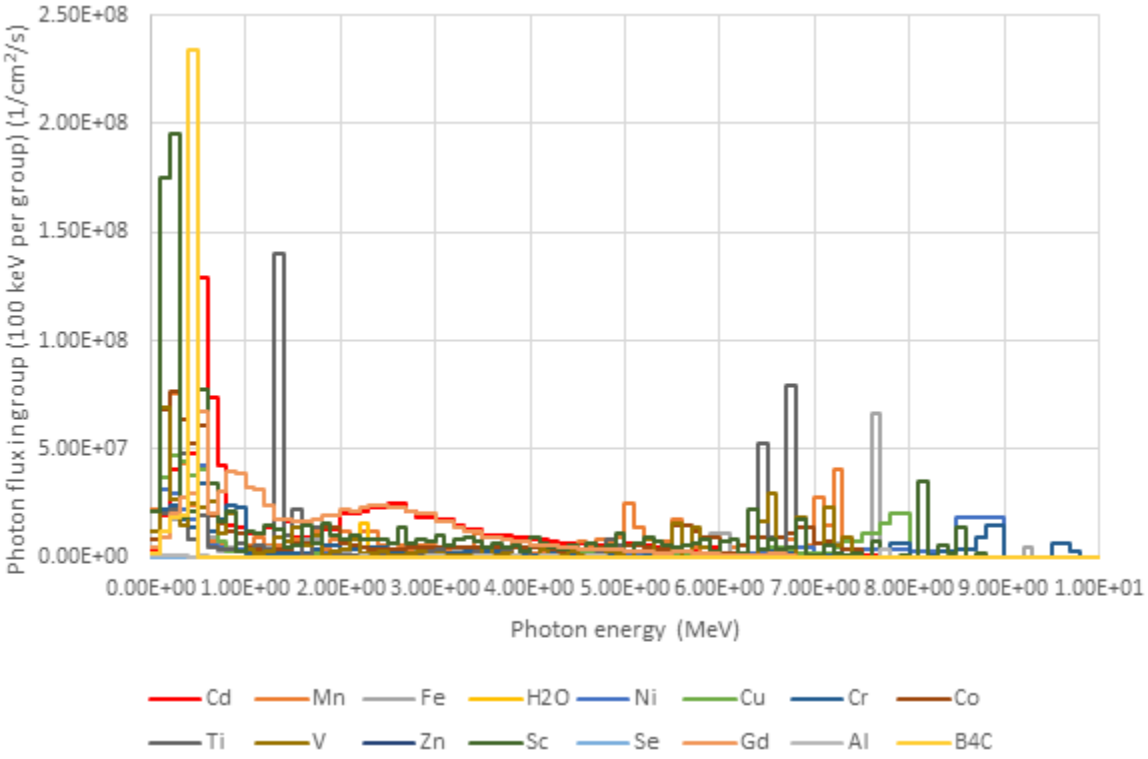

Figure 11 - Prompt-γ emission from a series of examined samples after being hit by the H1 beam in the sample position.

5.2. Summary of input fluxes and doses

The following table summarizes the source parameters used in the models.

Table 9: Source parameters and intensities in the model

Place in the model	Beam dimensions h×w [cm]	Integral intensity [n/s]
Instrument cave (AFB)	About 4x4	2.31E+10
Instrument cave (MWB)	About 4x4	4.18E+10
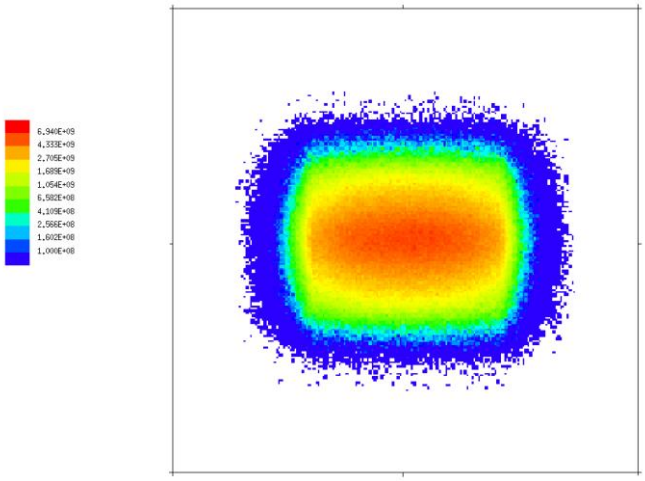		
Neutron guide	linear source	1.0E+8 n/m/s

Place in the model	Beam dimensions h×w [cm]	Integral intensity [n/s]
Shutter pit	Fast: point source derivate from the bunker model Thermal: 2×8	1.1E+5 (fast - at the exit of the beam) 6.33E+10 (thermal)
Fast		**Thermal**
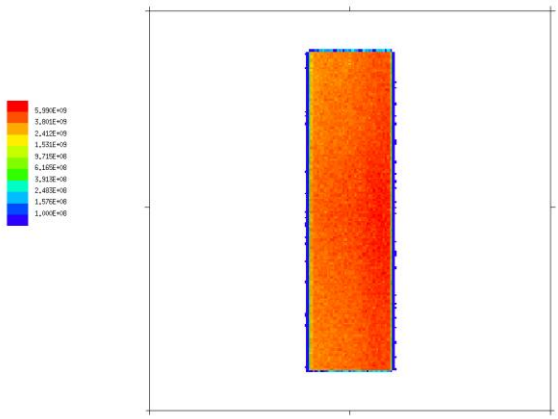		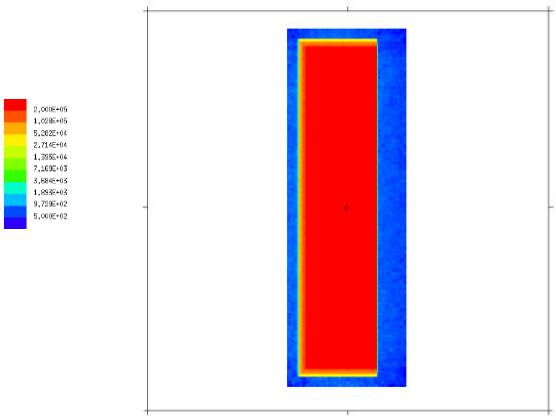
Chopper pit (full beam)	4×8	5.8E+10
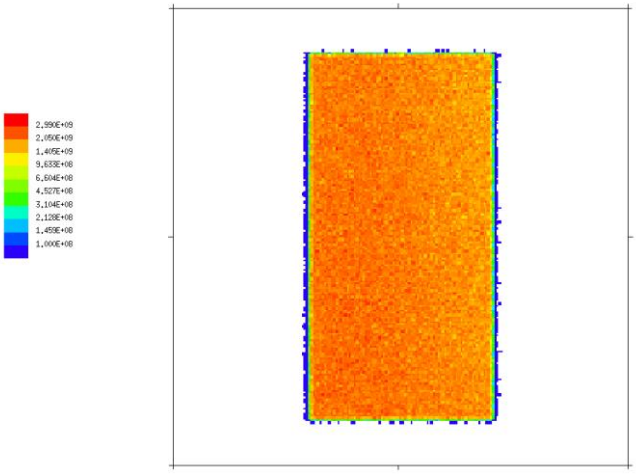		

5.3. Models and materials

The following section contains information concerning the simulation geometry models and material definitions. The void is used in all models instead of air for better statistics of the calculations.

5.3.1. Models description

5.3.1.1. Shutter and shutter pit

Beam shutter and its shielding pit are designed to suppress dose rates from fast and thermal neutrons emerging from the bunker. The shutter will be housed inside a shutter pit, which was modelled as a room with inner dimensions of 1.4×1.85×2.27 m^3 (W×H×L) attached to the bunker wall. Based on the detailed calculations, the shutter will consist of layers of Mirrobor, copper and polyethylene with 5% of boron stacked in the direction of the beam. The total length of the

shutter will be 61 cm, and perpendicular dimensions will be 50×50 cm^2. The first layer is Mirrobor which will be 1 cm thick, a second copper layer will be 50 centimetres thick, and finally, polyethylene with 5% of boron will be also 10 cm thick, see Figure 12. Total weight of the shutter shielding block will be approximately 1148 kg. The whole shutter will be coated by Mirrobor coating (approximately 5 mm thickness) to absorb thermal neutrons and thus reduce activation. The centre of the shutter block is placed at the centre of the neutron beam coming out from the bunker and 40 cm and 50 cm to the left and right from the pit walls, respectively. The shutter is closer to one of the walls since it will be mounted on a pendulum mechanism (note that actual design will consider the shorter distance to the NMX instrument, i.e. opposite to the simulation model). The wall adjacent to the NMX instrument consists of 20 cm of iron, 10 cm of polyethylene with 5% of boron and 20 cm of iron, respectively.

The shutter will be housed in a shutter pit, providing additional shielding against the scattered neutrons (Figure 13). The shutter pit consists of iron layer 20 cm thick, borated PE 10 cm (5% B) thick and standard concrete (2.35 g/cm^3) 70 cm thick. Therefore, the total thickness of the pit walls will be 100 cm. The neutron guide (inner cross-section 2 × 8 cm^2) running through the shutter pit wall was surrounded by 1 cm of Cu substrate and by 0.5 cm void gap from all sides in all calculations.

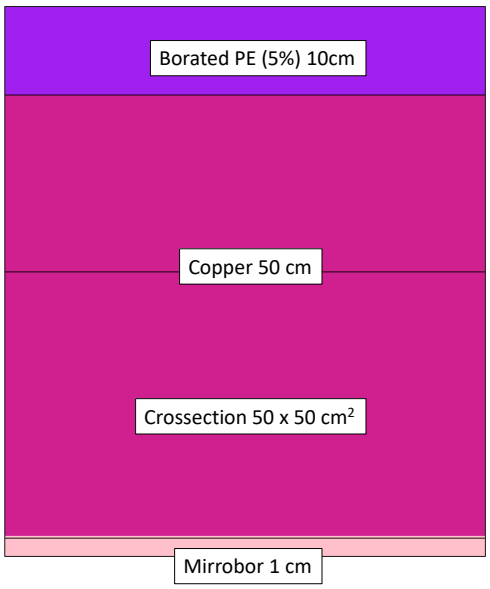

Figure 12: Final shutter design.

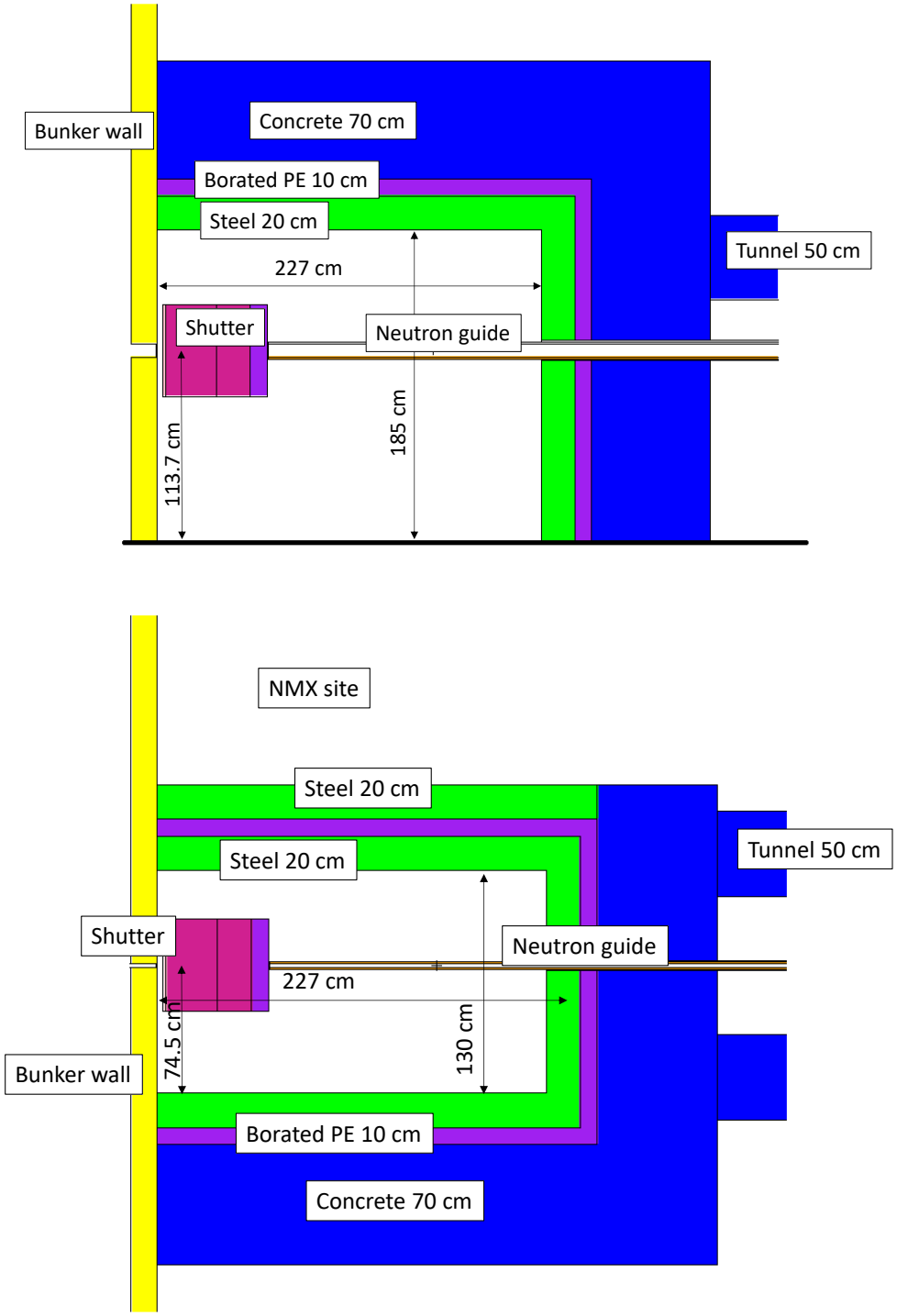

Figure 13: Shutter pit design in y-z (side view) and x-z (top view) cuts.

5.3.1.2. Chopper pit

Chopper pit has inner dimensions of 2.3 m height × 1.05 m width ×1.05 m length. A 70 cm thick concrete block with 5 millimetres of Mirrobor plates on the inner walls was designed to provide necessary shielding capabilities, for geometry, see Figure 14.

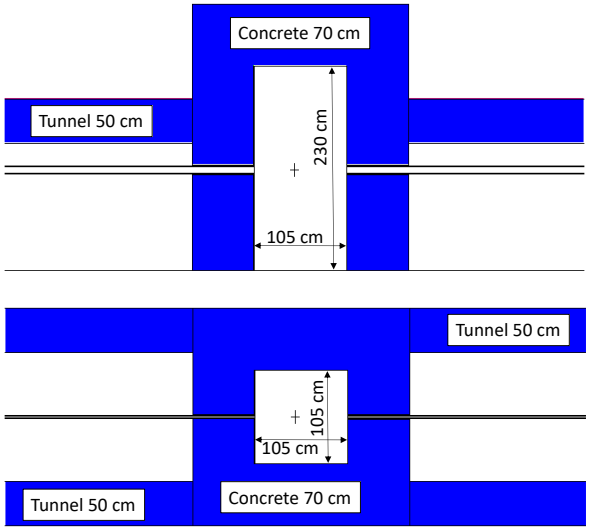

Figure 14: Chopper pit geometry.

5.3.1.3. Neutron guide

The primary function of the neutron guide is to transport thermal neutrons with a minimum of loses from the moderator to the sample position in the experimental cave. The thickness of the substrate was considered to be 10 mm in the modelled cases (Figure 15). In this case, the boron content (conservatively modelled at 4 %) in the glass has proven to be sufficient to absorb the escaped thermal neutrons.

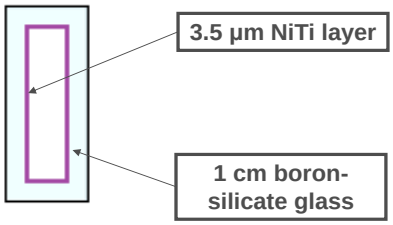

Figure 15: Neutron guide cross-section.

With regard to the possible two limiting factors, which take into the account fast neutron shielding and secondary prompt-γ emission after thermal neutron interactions, the task for the neutron guide shielding design was split into two separate problems: shielding of thermal neutrons and shielding fast neutrons possibly leaking from the shutter pit.

Upon a detailed calculation with the fast neutron source at the entry to the shutter pit and shutter opened, a 10 m long straight section of the neutron guide behind the pit wall was simulated (see Figure 16)

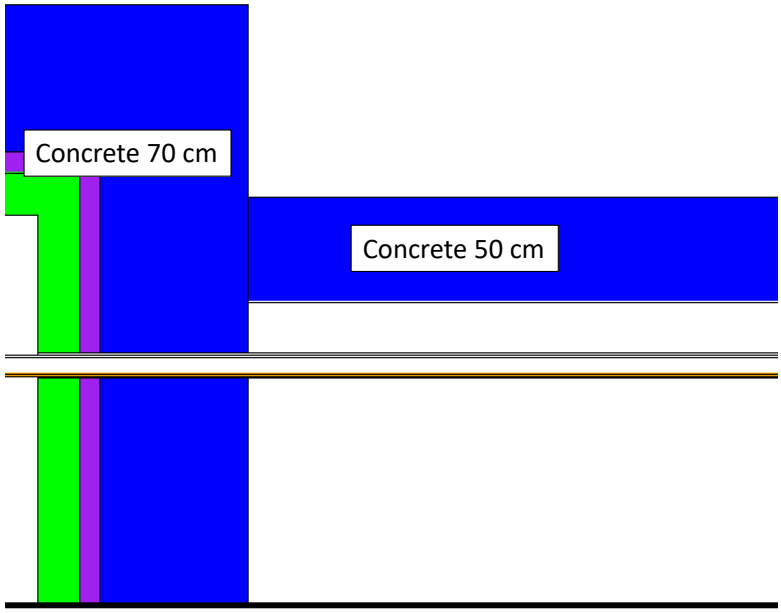

Figure 16: Shutter pit exit.

5.3.1.4. Guide tunnel

For the neutron guide shielding part, standard concrete was suggested to shield the emitted prompt-γ photons from neutron interactions with the reflective layer and boron-silicate glass substrate. The necessary thickness was estimated upon preliminary calculations to be 50 cm for both the narrow (for D03) and wide (for E02) profiles (Figure 17). In the case of a 10 mm thick borosilicate glass substrate around the guide, no other thermal neutron absorbers need to be applied as the glass provides necessary self-shielding, see section 6.3.1 for results. However, equivalent B_4C shielding still needs to be applied at the guide gaps (not considered in this simulation).

In the distance of 152 m from the target, just before entering the experimental cave, the neutron guide is interrupted by B_4C shaping slits capable of cutting the full beam and creating a possible larger source of γ radiation than the NiTi layer. For this reason, the final 3 m of the guide tunnel were simulated separately with a full thermal beam being absorbed on a B_4C disc, and the thickness of the concrete was increased to 60 cm.

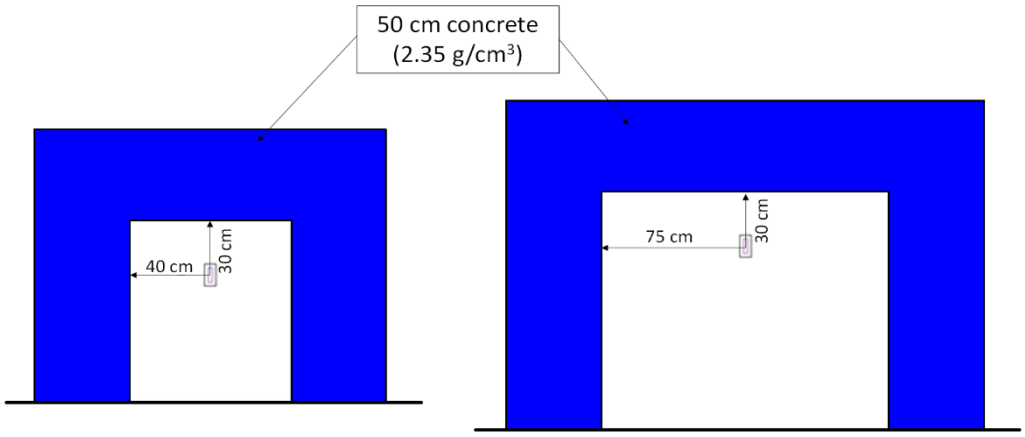

Figure 17: Thermal neutron guide shielding cross-section.

5.3.1.5. Instrument cave

According to a preliminary cave disposition layout denoted as “v7” (Figure 18) and several realized optimization simulations, an MCNP model was created for further simulations. A combination of concrete (density 2.35 g/cm^3) and heavy concrete (3.80 g/cm^3) was found to be appropriate material for the cave walls capable of sufficient attenuation of γ photons emitted mainly from the sample area. The necessary wall dimensions to reach the required dose rate limit at the outer wall surface of the cave were found to be 55 cm of heavy concrete for the side and back walls (see Figure 19) and 65 cm for the front wall and a leaning part of the sidewall. To limit the weight of the roof, a control area is expected to be established on the roof of the cave. To absorb the scattered thermal neutrons, the inner walls in the cave were covered by a 1 mm thick layer of 100 % B_4C equivalent. This can be realized as an absorber painting layer, B_4C containing material coating or by the addition of B_4C inside the walls.

Upon the layout shown in Figure 18 a 3D simulation model was created (Figure 19). Along the cave walls, the model includes two access doors, a large manipulation entry and a personal access door, cable trenches in the wall and openings for the air condition unit. The large door is going to be equipped with a heavy shielding sliding door. Steel was chosen as the optimal construction material with a necessary thickness of 20 cm and a thermal neutron absorber surface treatment. A wall chicane of a 55 cm concrete block with a height of 220 cm was designed around the standard personal access door to provide sufficient shielding.

On the back wall of the cave, a beam stop is to be equipped to attenuate the direct neutron beam. The beam stop was modelled as a 20 mm plate of B_4C housed in a lead shell. The detailed beam stop concept is shown in Figure 20.

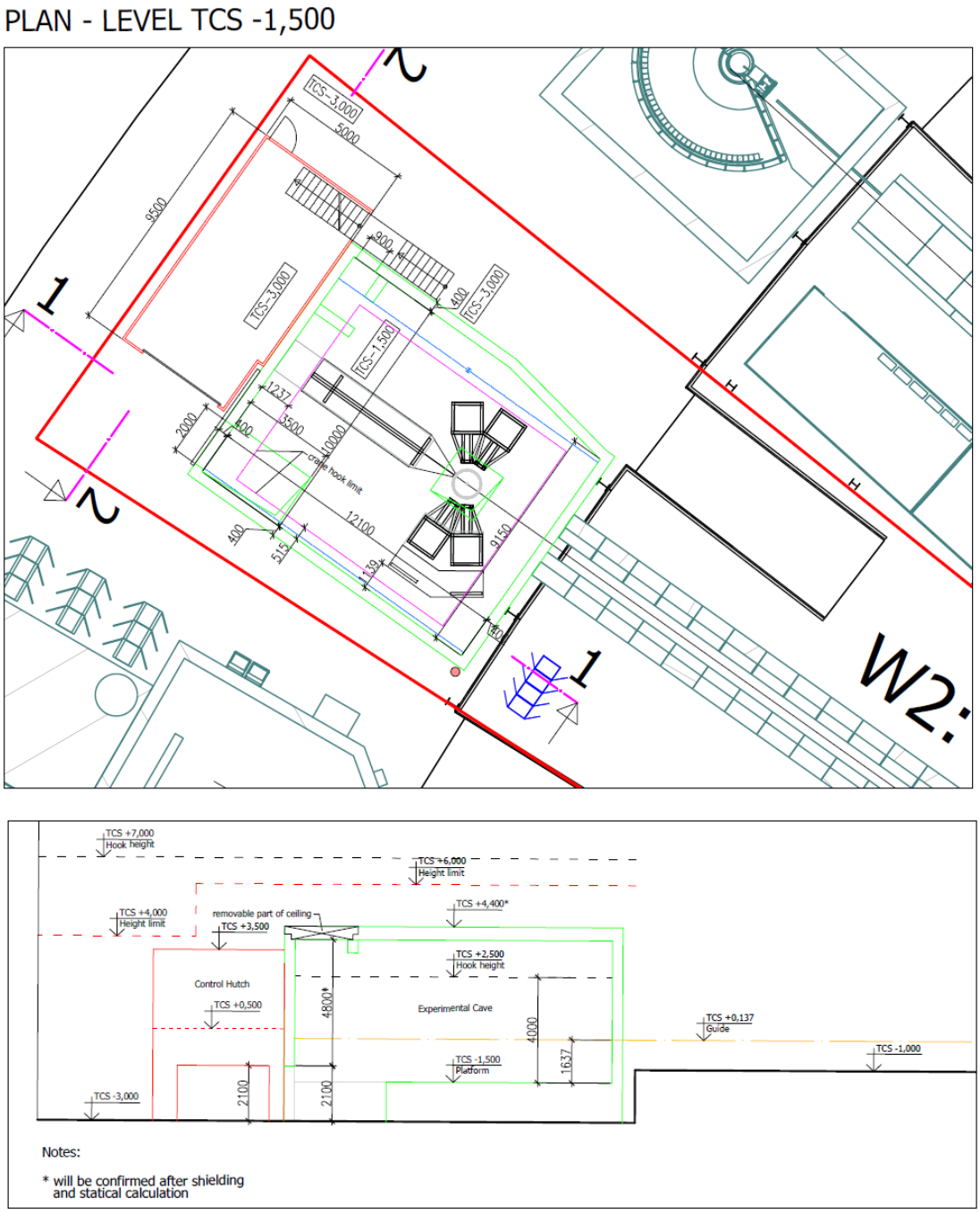

Figure 18: BEER instrument cave layout drawing. Green lines indicate the shielding wall.

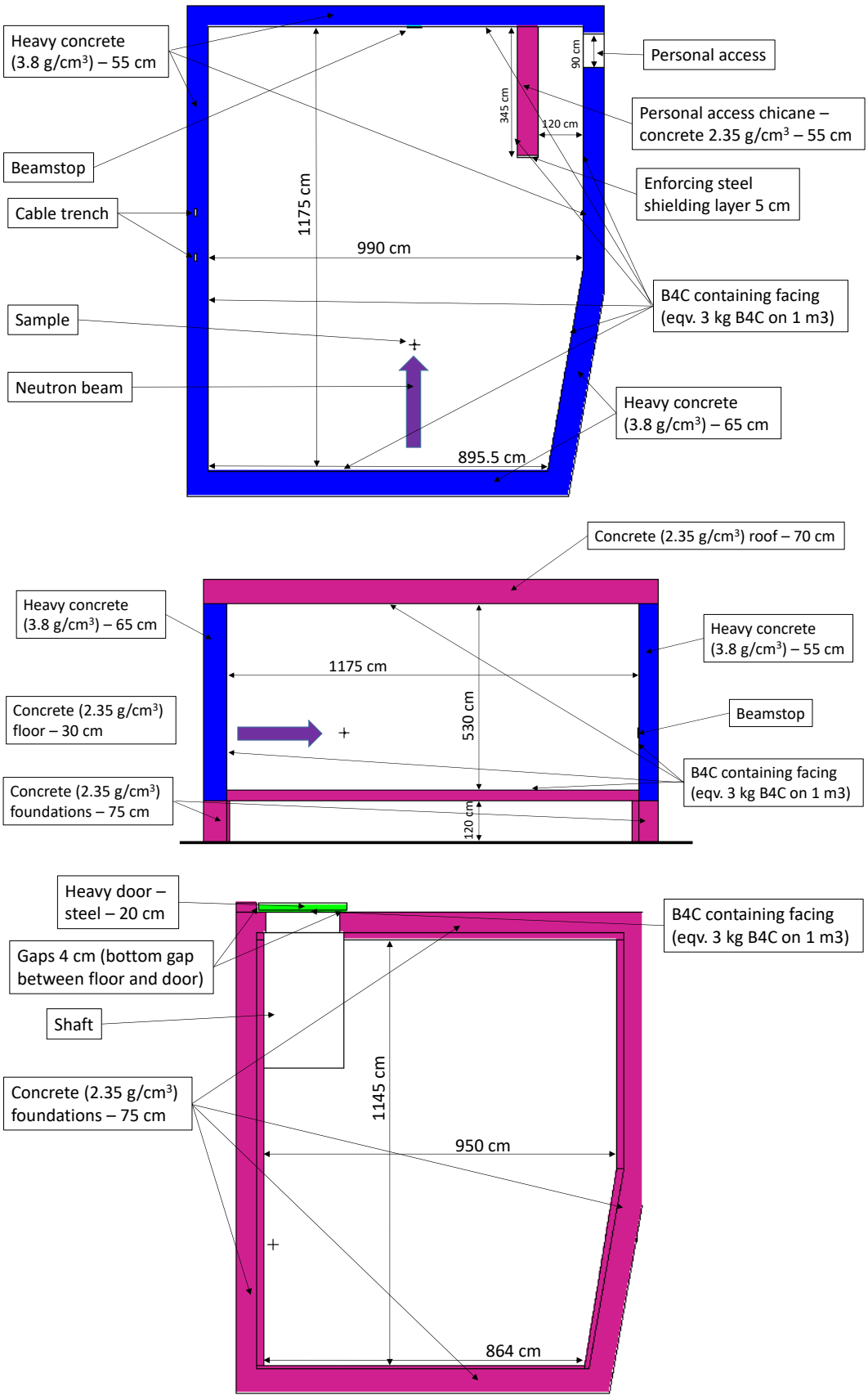

Figure 19: BEER instrument cave MCNP model description.

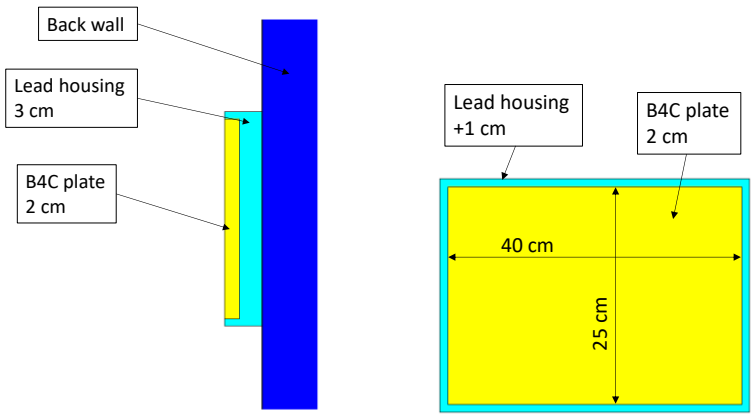

Figure 20: BEER beam-stop model description.

5.3.2. Materials

Material densities and compositions used in the models are listed in this section.

Table 10: Densities of materials used in the model

Material	Density [g/cm^3]
Concrete	2.35
Heavy concrete	3.8
Iron/Steel	7.80
PE (5% weight of boron)	1.01
B_4C	2.52
Copper	8.94
Light water	0.998
Nickel	8.90
Cadmium	8.65
MirroBor™	1.36
Borosilicate glass	2.23

Table 11: Composition of the ESS concrete

Material	Mass fraction
H-1	0.010
O-16	0.529
Na-23	0.016
Mg-natural	0.002
Al-27	0.034

Material	Mass fraction
Si-natural	0.337
K-natural	0.013
Ca-natural	0.044
Fe-natural	0.014
C-natural	0.001

Table 12: Composition of heavy concrete

Material	Mass fraction
H-1	0.0031
O-16	0.3305
Mg-natural	0.0093
Al-27	0.0234
Si-natural	0.0258
S-natural	0.0014
Ca-natural	0.0710
Ti-natural	0.0543
Va-natural	0.0031
Cr-natural	0.0017
Mn-55	0.0020
Fe-natural	0.4742

Table 13: Composition of iron

Material	Atomic fraction
Fe-54	0.0585
Fe-56	0.9175
Fe-57	0.0212
Fe-58	0.0028

Table 14: Composition of PE (5% weight of boron)

Material	Mass fraction
C-natural	0.831
H-1	0.139
B-10	0.002
B-11	0.007
O-16	0.021

Table 15: Composition of B_4C

Material	Mass fraction
B-10	0.156522
B-11	0.626088
C-natural	0.21739

Table 16: Composition of copper

Material	Mass fraction
Cu-63	0.6915
Cu-65	0.3085

Table 17: Composition of light water

Material	Atomic fraction
H-1	2
O-16	1

Table 18: Composition of MirroBor™

Material	Mass fraction
C-natural	0.31
O-16	0.05
H-1	0.01
B-10	0.13
B-11	0.50

Table 19: Composition of borosilicate glass

Material	Mass fraction
Si-natural	0.3772
O-16	0.5396
Na-23	0.0282
Al-27	0.0116
K-natural	0.0033
B-10	0.0079
B-11	0.0323

6. RESULTS OF SIMULATIONS

Calculation results obtained by means of the MCNP6 simulations are presented in the following sections. For each of the considered cases, a 2D dose rate map through the beam axis is provided, in addition to detailed calculations with better statistics realized for certain points. The coordinate system in all figures is the following: z along the beam, y vertical, x is the right-handed complement.

6.1. Full beam in the Shutter pit

Three cases were studied: dose rates for the shutter in open and closed states and activation of the shutter materials. Neutron guide in the shutter pit wall was modelled with a 0.5 cm gap around the guide at the location where the guide crosses the shutter pit wall. The simulations are dependent on the divergence of the fast neutron beam; however, the design will meet the requirements for any reasonable divergence.

6.1.1. Activation of the shutter

The activation of the shutter materials to consider is only the copper layer. Only fast neutrons were considered (over 0.1 MeV-1GeV). To investigate this, calculations in FISPACT-II 4.0 code were done for 50 cm × 50 cm × 1 cm (thickness) of Mirrobor in front of 50 cm × 50 cm × 50 cm (thickness) blocks of lead or copper for different irradiation and cooling times. The input neutron spectrum was taken from Figure 4. Tables compare a scenario of 1-year irradiation at full time at maximum power and several cooling time periods. In general, the activation rate of both materials (lead vs copper) is in the same order of magnitude, but with the increased cooling time the activity of the lead shutter drops at a faster rate due to the presence of shorter living nuclides. However, when taking the total mass of metal part of the shutter (1148 kg for Cu and 1448 kg for lead), the induced specific activities are sufficiently low for both materials. Thus, the copper is the preferred choice for the shutter material for its better fast neutron shielding properties compared to lead. Based on the results from Table 23, additional MCNP calculations were performed to estimate the surface doses. After one year of activation at full power, the dose at the surface is 5.49 µSv/h immediately after the end of the irradiation. After one hour of cooling, the surface dose corresponds to 3.17 µSv/h.

Table 20: Calculated activities in the shutter copper for 1-year activation and several defined cooling times.

Copper shutter irradiation for one year at full power							
Nuclide	Activities per the whole shutter (1148 kg, without Mirrobor part)						Half-life (s)
	Cooling time						
	0 min	1 hour	1 day	1 week	1 month	1 year	
Cu62	9.62E+06	1.35E+05	0.00E+00	0.00E+00	0.00E+00	0.00E+00	5.85E+02
Cu64	5.33E+06	5.05E+06	1.44E+06	5.56E+02	5.26E+02	0.00E+00	4.57E+04
Co58	3.17E+06	3.16E+06	3.14E+06	2.96E+06	2.96E+06	8.93E+04	6.12E+06
Cu61	2.10E+06	1.71E+06	1.43E+04	0.00E+00	0.00E+00	0.00E+00	1.20E+04
Co58m	1.76E+06	1.63E+06	2.71E+05	3.65E+00	3.38E+00	0.00E+00	3.20E+04
Co57	1.32E+06	1.32E+06	1.32E+06	1.30E+06	1.30E+06	5.21E+05	2.35E+07
Co61	1.19E+06	7.82E+05	4.99E+01	0.00E+00	0.00E+00	0.00E+00	5.94E+03
Co60m	8.20E+05	1.54E+04	0.00E+00	0.00E+00	0.00E+00	0.00E+00	6.28E+02
Cr51	5.54E+05	5.54E+05	5.40E+05	4.65E+05	4.65E+05	5.99E+01	2.39E+06
Mn54	4.73E+05	4.73E+05	4.72E+05	4.65E+05	4.65E+05	2.10E+05	2.70E+07
Co56	4.08E+05	4.08E+05	4.05E+05	3.84E+05	3.83E+05	1.55E+04	6.68E+06
Fe59	3.08E+05	3.08E+05	3.03E+05	2.76E+05	2.76E+05	1.05E+03	3.84E+06
Cu60	2.96E+05	5.13E+04	0.00E+00	0.00E+00	0.00E+00	0.00E+00	1.42E+03
Mn52	2.91E+05	2.89E+05	2.57E+05	1.22E+05	1.21E+05	0.00E+00	4.83E+05
Fe55	2.75E+05	2.75E+05	2.75E+05	2.74E+05	2.74E+05	2.14E+05	8.63E+07
Co60	2.57E+05	2.57E+05	2.57E+05	2.56E+05	2.56E+05	2.25E+05	1.66E+08
Mn56	2.41E+05	1.84E+05	3.84E+02	0.00E+00	0.00E+00	0.00E+00	9.30E+03
Co62m	2.24E+05	1.13E+04	0.00E+00	0.00E+00	0.00E+00	0.00E+00	8.35E+02
V48	1.99E+05	1.99E+05	1.91E+05	1.47E+05	1.47E+05	0.00E+00	1.38E+06
V49	1.79E+05	1.79E+05	1.79E+05	1.77E+05	1.77E+05	8.34E+04	2.85E+07
Ni65	1.52E+05	1.16E+05	2.07E+02	0.00E+00	0.00E+00	0.00E+00	9.07E+03
H3	1.52E+05	1.52E+05	1.52E+05	1.51E+05	1.51E+05	1.43E+05	3.89E+08
Co62	1.46E+05	0.00E+00	0.00E+00	0.00E+00	0.00E+00	0.00E+00	9.00E+01
Mn52m	1.15E+05	1.62E+04	3.37E+02	0.00E+00	0.00E+00	0.00E+00	1.27E+03
Mn57	9.87E+04	0.00E+00	0.00E+00	0.00E+00	0.00E+00	0.00E+00	8.54E+01
Mn51	8.60E+04	3.50E+04	0.00E+00	0.00E+00	0.00E+00	0.00E+00	2.77E+03
Cr49	8.24E+04	3.05E+04	0.00E+00	0.00E+00	0.00E+00	0.00E+00	2.51E+03
Cu66	8.14E+04	2.34E+01	0.00E+00	0.00E+00	0.00E+00	0.00E+00	3.06E+02
V47	6.74E+04	1.88E+04	0.00E+00	0.00E+00	0.00E+00	0.00E+00	1.96E+03

Copper shutter irradiation for one year at full power							
Nuclide	Activities per the whole shutter (1148 kg, without Mirrobor part)						Half-life (s)
	Cooling time						
	0 min	1 hour	1 day	1 week	1 month	1 year	
Sc44	5.14E+04	4.32E+04	1.83E+04	3.36E+03	2.82E+03	1.15E+02	1.43E+04
Fe53	5.13E+04	3.87E+02	0.00E+00	0.00E+00	0.00E+00	0.00E+00	5.11E+02
Ti45	4.38E+04	3.50E+04	1.97E+02	0.00E+00	0.00E+00	0.00E+00	1.11E+04
Co55	3.95E+04	3.80E+04	1.53E+04	5.15E+01	4.95E+01	0.00E+00	6.31E+04
Co63	3.83E+04	0.00E+00	0.00E+00	0.00E+00	0.00E+00	0.00E+00	2.74E+01
Sc43	2.69E+04	2.25E+04	3.74E+02	0.00E+00	0.00E+00	0.00E+00	1.40E+04
Sc44m	2.23E+04	2.21E+04	1.68E+04	3.06E+03	3.02E+03	0.00E+00	2.11E+05
V52	2.04E+04	0.00E+00	0.00E+00	0.00E+00	0.00E+00	0.00E+00	2.25E+02
Ni63	1.96E+04	1.95E+04	1.96E+04	1.95E+04	1.95E+04	1.94E+04	3.18E+09
Sc46	1.61E+04	1.61E+04	1.60E+04	1.52E+04	1.52E+04	7.87E+02	7.24E+06
Total	**3.05E+07**	**1.76E+07**	**9.33E+06**	**7.03E+06**	**7.02E+06**	**1.52E+06**	

Table 21: Calculated activities in the shutter lead for 1-year activation and several defined cooling times.

Lead shutter irradiation for one year at full power							
Nuclide	Activities per the whole shutter (1448 kg, without Mirrobor part)						Half-life (s)
	Cooling time						
	0 min	1 hour	1 day	1 week	1 month	1 year	
Pb203	5.57E+06	5.50E+06	4.05E+06	5.91E+05	6.99E+01	0.00E+00	1.99E+05
Pb207m	4.59E+06	0.00E+00	0.00E+00	0.00E+00	0.00E+00	0.00E+00	8.06E-01
Tl201	3.47E+06	3.44E+06	3.02E+06	7.86E+05	1.04E+03	0.00E+00	2.71E+05
Pb204m	3.28E+06	1.77E+06	1.25E+00	0.00E+00	0.00E+00	0.00E+00	4.05E+03
Pb203m	3.27E+06	0.00E+00	0.00E+00	0.00E+00	0.00E+00	0.00E+00	6.29E+00
Pb201	2.75E+06	2.56E+06	4.69E+05	1.15E+01	0.00E+00	0.00E+00	3.38E+04
Pb202m	2.44E+06	2.01E+06	2.31E+04	0.00E+00	0.00E+00	0.00E+00	1.29E+04
Tl200	2.33E+06	2.27E+06	1.77E+06	8.41E+04	0.00E+00	0.00E+00	9.40E+04
Tl199	2.28E+06	2.08E+06	2.94E+05	0.00E+00	0.00E+00	0.00E+00	2.67E+04
Pb199	1.83E+06	1.15E+06	2.93E+01	0.00E+00	0.00E+00	0.00E+00	5.40E+03
Pb200	1.72E+06	1.67E+06	7.95E+05	7.66E+03	0.00E+00	0.00E+00	7.74E+04
Pb201m	1.28E+06	0.00E+00	0.00E+00	0.00E+00	0.00E+00	0.00E+00	6.10E+01

Lead shutter irradiation for one year at full power							
Nuclide	Activities per the whole shutter (1448 kg, without Mirrobor part)						Half-life (s)
	Cooling time						
	0 min	1 hour	1 day	1 week	1 month	1 year	
Tl206	1.23E+06	6.20E+01	0.00E+00	0.00E+00	0.00E+00	0.00E+00	2.52E+02
Tl202	1.20E+06	1.20E+06	1.14E+06	8.09E+05	1.48E+05	5.33E+01	1.06E+06
Pb203n	1.08E+06	0.00E+00	0.00E+00	0.00E+00	0.00E+00	0.00E+00	4.80E-01
Hg197	1.01E+06	1.00E+06	8.40E+05	1.88E+05	8.35E+01	0.00E+00	2.33E+05
Tl207	8.73E+05	1.43E+02	0.00E+00	0.00E+00	0.00E+00	0.00E+00	2.86E+02
Tl198	8.59E+05	7.54E+05	6.08E+04	0.00E+00	0.00E+00	0.00E+00	1.91E+04
Tl197	8.42E+05	6.60E+05	2.77E+03	0.00E+00	0.00E+00	0.00E+00	1.02E+04
Pb198	6.17E+05	4.62E+05	6.03E+02	0.00E+00	0.00E+00	0.00E+00	8.64E+03
Pb199m	5.81E+05	1.92E+04	0.00E+00	0.00E+00	0.00E+00	0.00E+00	7.32E+02
Hg195	5.67E+05	5.28E+05	1.78E+05	7.47E+03	0.00E+00	0.00E+00	3.56E+04
Tl196	5.49E+05	3.77E+05	9.45E+01	0.00E+00	0.00E+00	0.00E+00	6.62E+03
Au195	4.83E+05	4.83E+05	4.83E+05	4.73E+05	4.23E+05	1.25E+05	1.61E+07
Tl207m	4.80E+05	0.00E+00	0.00E+00	0.00E+00	0.00E+00	0.00E+00	1.33E+00
Tl195	4.60E+05	2.53E+05	0.00E+00	0.00E+00	0.00E+00	0.00E+00	4.18E+03
Pb196	4.52E+05	1.47E+05	0.00E+00	0.00E+00	0.00E+00	0.00E+00	2.22E+03
Au193	4.40E+05	4.23E+05	2.34E+05	9.43E+02	0.00E+00	0.00E+00	6.35E+04
Au192	4.03E+05	3.50E+05	5.92E+04	0.00E+00	0.00E+00	0.00E+00	1.78E+04
Hg192	3.94E+05	3.41E+05	1.30E+04	0.00E+00	0.00E+00	0.00E+00	1.75E+04
Hg193	3.67E+05	3.06E+05	6.98E+03	0.00E+00	0.00E+00	0.00E+00	1.37E+04
Pb197	3.65E+05	2.02E+03	0.00E+00	0.00E+00	0.00E+00	0.00E+00	4.80E+02
Tl206m	3.56E+05	5.59E+00	0.00E+00	0.00E+00	0.00E+00	0.00E+00	2.26E+02
Pt191	3.30E+05	3.27E+05	2.74E+05	6.20E+04	6.64E+01	0.00E+00	2.63E+05
Au191	3.29E+05	2.64E+05	2.43E+03	0.00E+00	0.00E+00	0.00E+00	1.15E+04
Pb197m	3.05E+05	1.20E+05	0.00E+00	0.00E+00	0.00E+00	0.00E+00	2.68E+03
Tl194	2.94E+05	8.32E+04	0.00E+00	0.00E+00	0.00E+00	0.00E+00	1.98E+03
Tl193	2.63E+05	3.91E+04	0.00E+00	0.00E+00	0.00E+00	0.00E+00	1.31E+03
Au190	2.55E+05	9.65E+04	0.00E+00	0.00E+00	0.00E+00	0.00E+00	2.57E+03
Tl204	2.50E+05	2.50E+05	2.50E+05	2.49E+05	2.45E+05	2.08E+05	1.20E+08
Ir189	2.45E+05	2.44E+05	2.39E+05	1.76E+05	3.63E+04	0.00E+00	1.14E+06

Lead shutter irradiation for one year at full power							
Nuclide	Activities per the whole shutter (1448 kg, without Mirrobor part)						Half-life (s)
	Cooling time						
	0 min	1 hour	1 day	1 week	1 month	1 year	
Pt189	2.45E+05	2.29E+05	5.59E+04	5.75E+00	0.00E+00	0.00E+00	3.91E+04
Hg190	2.44E+05	3.05E+04	0.00E+00	0.00E+00	0.00E+00	0.00E+00	1.20E+03
Au189	2.30E+05	5.40E+04	0.00E+00	0.00E+00	0.00E+00	0.00E+00	1.72E+03
Pb195m	2.25E+05	1.41E+04	0.00E+00	0.00E+00	0.00E+00	0.00E+00	9.00E+02
Pb194	2.15E+05	6.72E+03	0.00E+00	0.00E+00	0.00E+00	0.00E+00	7.20E+02
Hg191m	2.09E+05	9.23E+04	0.00E+00	0.00E+00	0.00E+00	0.00E+00	3.05E+03
Pt188	2.01E+05	2.00E+05	1.88E+05	1.25E+05	1.63E+04	0.00E+00	8.81E+05
Ir188	2.01E+05	1.97E+05	1.98E+05	1.48E+05	0.00E+00	0.00E+00	1.50E+05
Au188	1.98E+05	1.78E+03	0.00E+00	0.00E+00	0.00E+00	0.00E+00	5.30E+02
Ir187	1.94E+05	1.81E+05	5.20E+04	3.87E+00	0.00E+00	0.00E+00	3.78E+04
Pt187	1.94E+05	1.44E+05	1.76E+02	0.00E+00	0.00E+00	0.00E+00	8.46E+03
Au187	1.90E+05	1.34E+03	0.00E+00	0.00E+00	0.00E+00	0.00E+00	5.04E+02
Tl198m	1.77E+05	1.22E+05	2.43E+01	0.00E+00	0.00E+00	0.00E+00	6.73E+03
Hg188	1.77E+05	0.00E+00	0.00E+00	0.00E+00	0.00E+00	0.00E+00	1.95E+02
Hg195m	1.72E+05	1.69E+05	1.15E+05	1.05E+04	0.00E+00	0.00E+00	1.73E+05
Tl197m	1.66E+05	0.00E+00	0.00E+00	0.00E+00	0.00E+00	0.00E+00	5.40E-01
Hg197m	1.60E+05	1.55E+05	7.96E+04	1.22E+03	0.00E+00	0.00E+00	8.60E+04
Au187m	1.58E+05	0.00E+00	0.00E+00	0.00E+00	0.00E+00	0.00E+00	2.30E+00
Hg199m	1.51E+05	5.61E+04	0.00E+00	0.00E+00	0.00E+00	0.00E+00	2.53E+03
Tl196m	1.49E+05	9.10E+04	1.13E+00	0.00E+00	0.00E+00	0.00E+00	5.08E+03
Hg203	1.41E+05	1.41E+05	1.39E+05	1.27E+05	8.13E+04	6.18E+02	4.03E+06
Tl192	1.36E+05	1.78E+03	0.00E+00	0.00E+00	0.00E+00	0.00E+00	5.76E+02
Ir186	1.30E+05	1.24E+05	5.52E+04	1.37E+02	0.00E+00	0.00E+00	5.99E+04
Pt186	1.30E+05	9.29E+04	4.78E+01	0.00E+00	0.00E+00	0.00E+00	7.49E+03
Pb192	1.23E+05	0.00E+00	0.00E+00	0.00E+00	0.00E+00	0.00E+00	2.10E+02
Au186	1.23E+05	2.51E+03	0.00E+00	0.00E+00	0.00E+00	0.00E+00	6.42E+02
Hg189	1.21E+05	5.09E+02	0.00E+00	0.00E+00	0.00E+00	0.00E+00	4.56E+02
Hg187m	1.14E+05	0.00E+00	0.00E+00	0.00E+00	0.00E+00	0.00E+00	1.44E+02
Hg191	1.09E+05	4.60E+04	0.00E+00	0.00E+00	0.00E+00	0.00E+00	2.90E+03

Lead shutter irradiation for one year at full power							
Nuclide	Activities per the whole shutter (1448 kg, without Mirrobor part)						Half-life (s)
	Cooling time						
	0 min	1 hour	1 day	1 week	1 month	1 year	
Tl191m	1.04E+05	3.59E+01	0.00E+00	0.00E+00	0.00E+00	0.00E+00	3.13E+02
Hg189m	1.03E+05	8.61E+02	0.00E+00	0.00E+00	0.00E+00	0.00E+00	5.22E+02
Tl195m	1.02E+05	0.00E+00	0.00E+00	0.00E+00	0.00E+00	0.00E+00	3.60E+00
Hg186	8.87E+04	0.00E+00	0.00E+00	0.00E+00	0.00E+00	0.00E+00	8.28E+01
Pb193	8.77E+04	2.14E+01	0.00E+00	0.00E+00	0.00E+00	0.00E+00	3.00E+02
Pb195	8.36E+04	5.22E+03	0.00E+00	0.00E+00	0.00E+00	0.00E+00	9.00E+02
Tl208	7.35E+04	0.00E+00	0.00E+00	0.00E+00	0.00E+00	0.00E+00	1.83E+02
Ir185	7.27E+04	6.92E+04	2.34E+04	1.77E+01	0.00E+00	0.00E+00	5.00E+04
Hg193m	7.19E+04	6.78E+04	1.76E+04	3.74E+00	0.00E+00	0.00E+00	4.25E+04
Tl192m	7.13E+04	1.52E+03	0.00E+00	0.00E+00	0.00E+00	0.00E+00	6.48E+02
Tl193m	6.97E+04	0.00E+00	0.00E+00	0.00E+00	0.00E+00	0.00E+00	1.27E+02
Os185	6.78E+04	6.77E+04	6.76E+04	6.48E+04	5.19E+04	4.60E+03	8.10E+06
Pb193m	6.75E+04	5.19E+01	0.00E+00	0.00E+00	0.00E+00	0.00E+00	3.48E+02
Au185	6.15E+04	3.46E+00	0.00E+00	0.00E+00	0.00E+00	0.00E+00	2.55E+02
Tl194m	6.03E+04	1.70E+04	0.00E+00	0.00E+00	0.00E+00	0.00E+00	1.97E+03
Tl190	5.90E+04	0.00E+00	0.00E+00	0.00E+00	0.00E+00	0.00E+00	1.56E+02
Hg205	5.35E+04	1.80E+01	0.00E+00	0.00E+00	0.00E+00	0.00E+00	3.12E+02
Pb190	4.95E+04	0.00E+00	0.00E+00	0.00E+00	0.00E+00	0.00E+00	7.10E+01
H3	4.95E+04	4.95E+04	4.95E+04	4.94E+04	4.92E+04	4.68E+04	3.89E+08
Total	**5.78E+07**	**3.37E+07**	**1.53E+07**	**4.00E+06**	**1.07E+06**	**3.94E+05**	

6.1.2. Closed shutter – H1.1

The dosimetry situation of the shutter pit in the closed state is demonstrated in the following figures. Figure 21 and Figure 22 show neutron and photon spectra averaged over the beam in area of 5 × 11 cm^2 inside the tunnel just behind the bunker wall. For 2D dose maps of the shutter body and the shutter pit, see Figure 23 and Figure 24. The worst fast neutron dose rate in the shutter pit is 17 mSv/h, this value is at the location of beam entrance and is averaged over the beam area. Figure 25 and Figure 26 show 2D neutron and photon doses maps in the whole shutter pit. These figures correspond to calculation with source emitting particles preferably forward. This source was compiled, based on the analysis of bunker model calculations.

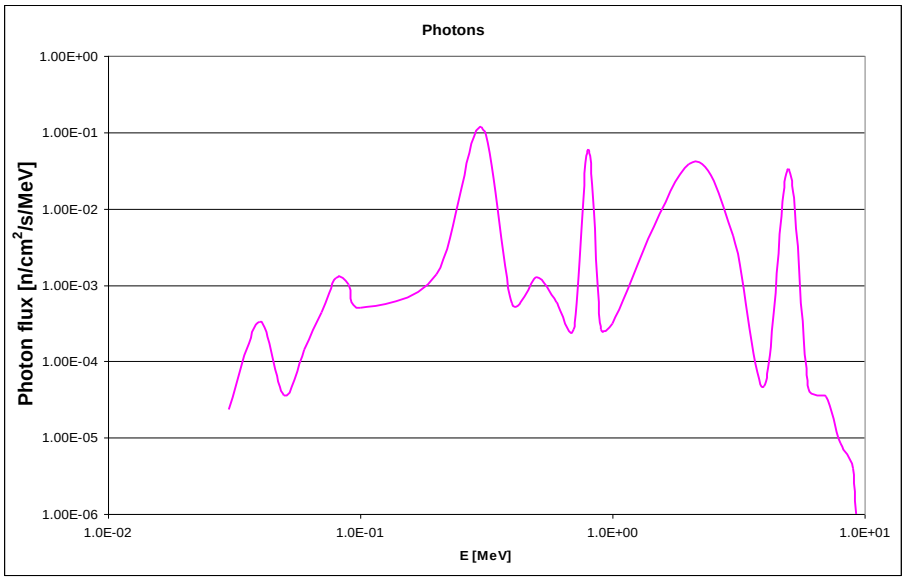

Figure 21: Photon spectrum behind the shutter pit wall.

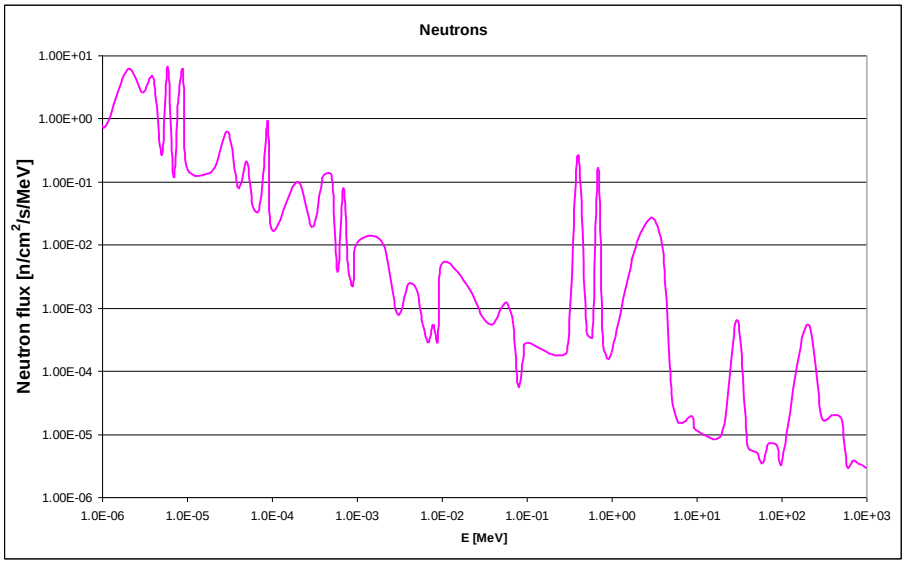

Figure 22: Neutron spectrum behind the shutter pit wall.

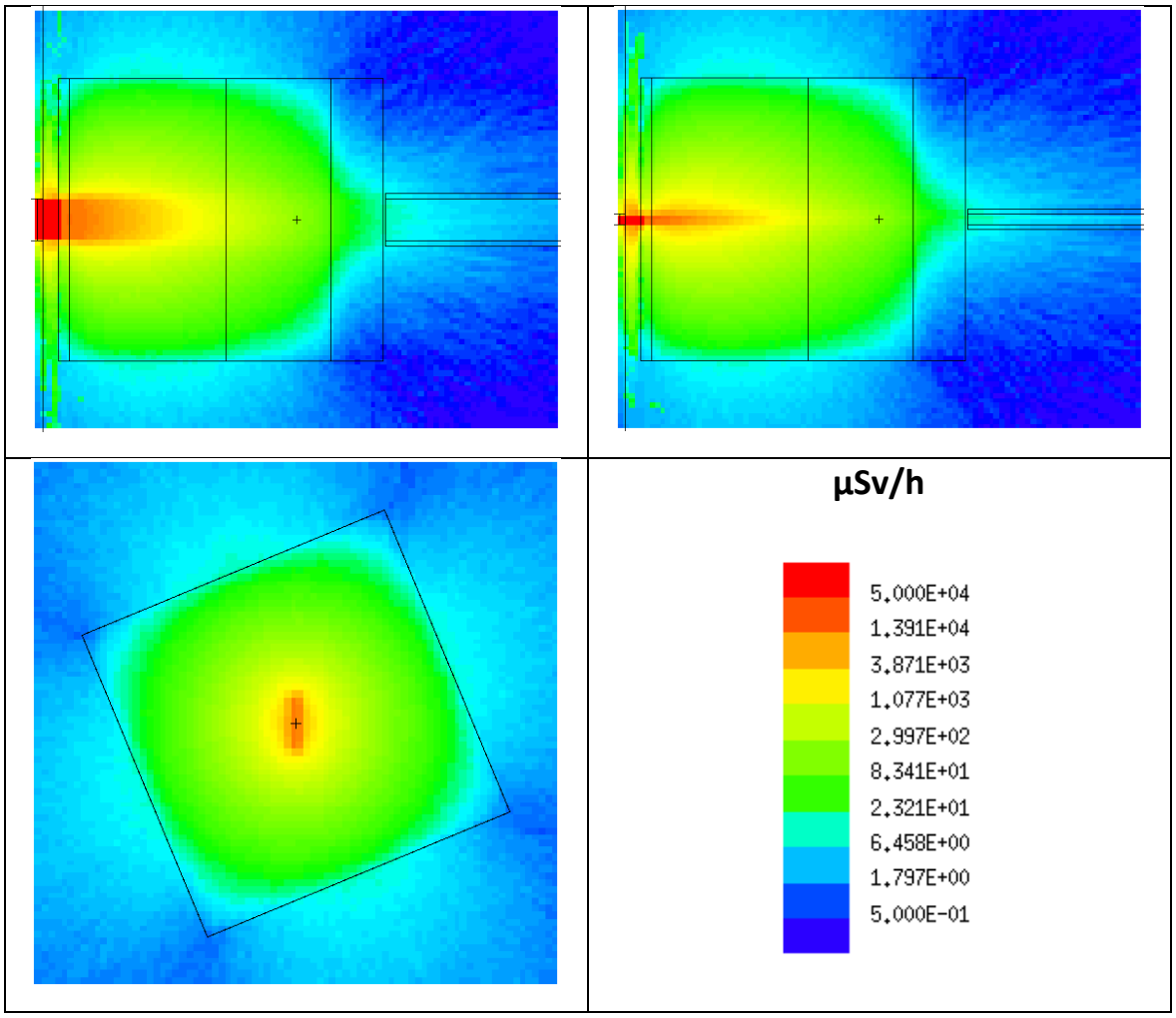

Figure 23: Neutron doses rates in and around the shutter.

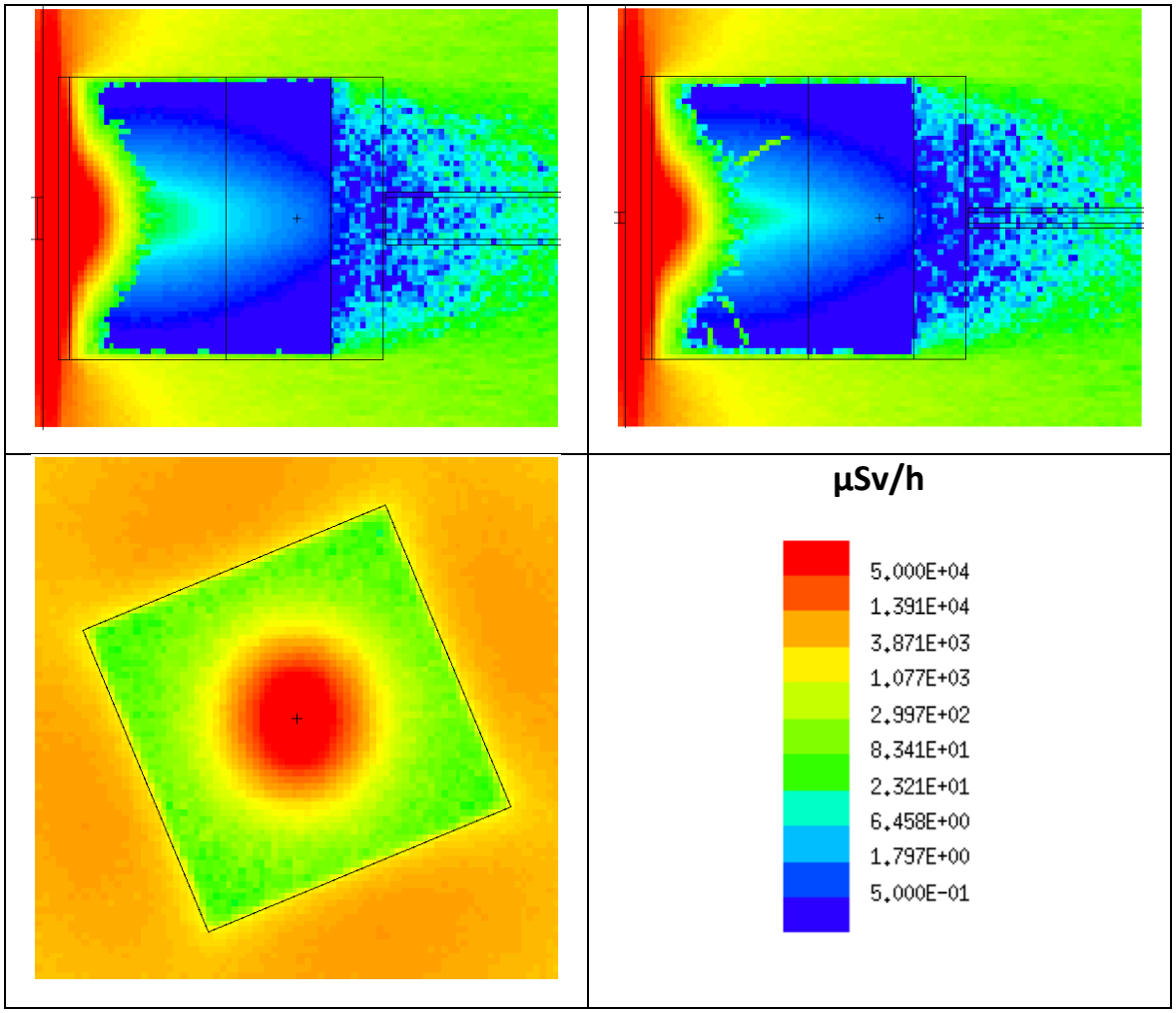

Figure 24: Photon doses rates in and around the shutter.

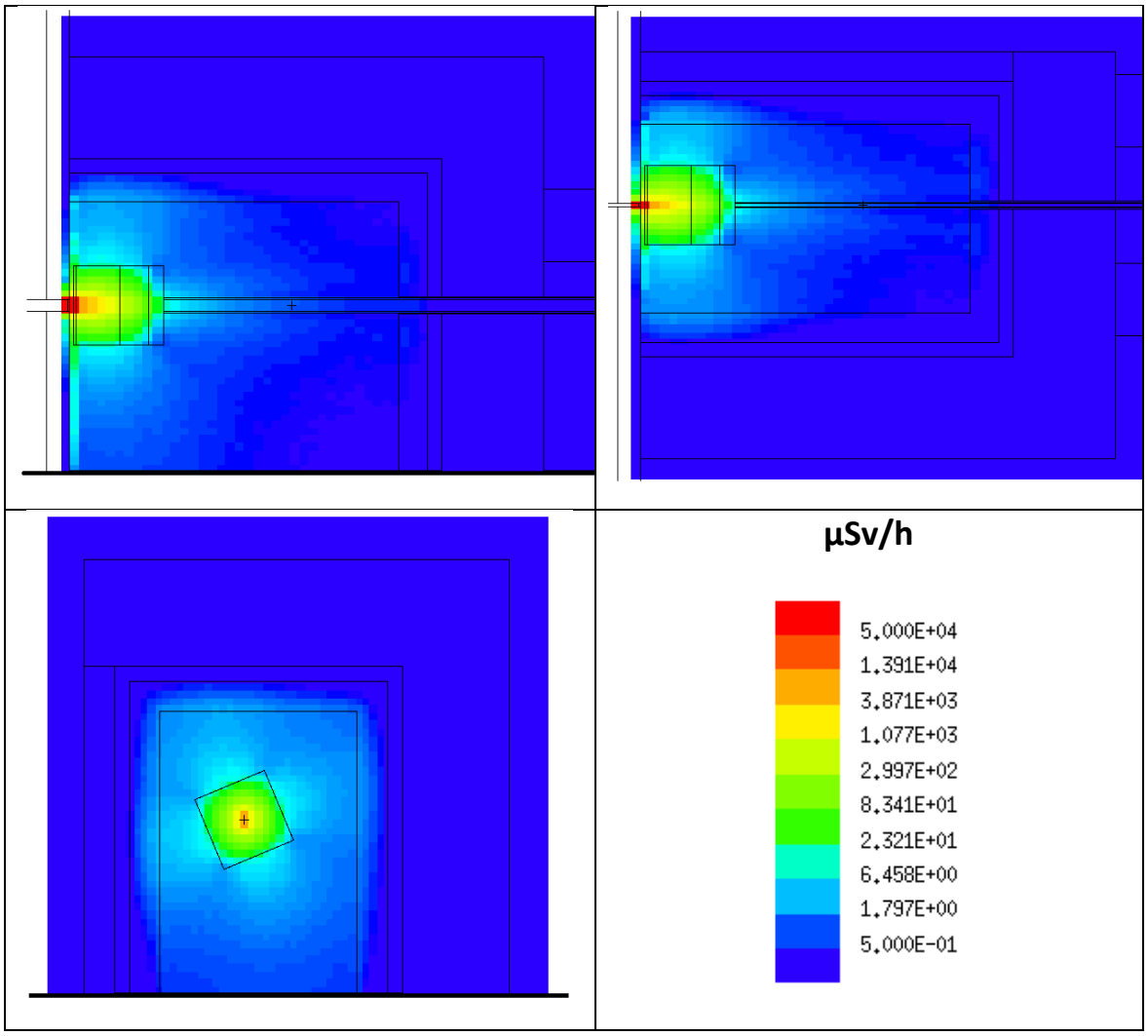

Figure 25: Neutron dose rates in the shutter pit in the closed state.

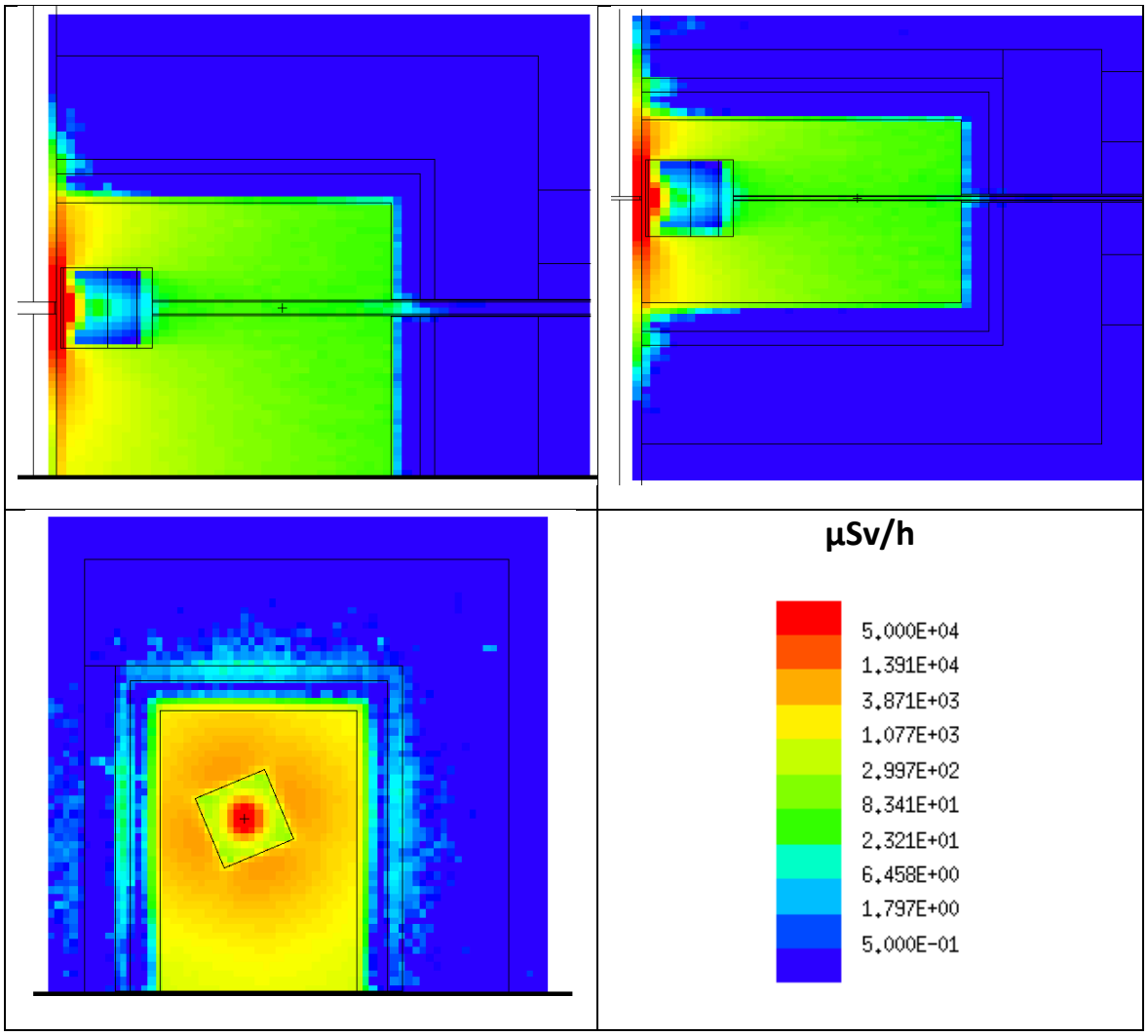

Figure 26: Photon dose rates in the shutter pit in the closed state.

6.1.3. Opened shutter – H1.2

The state of the radiation doses in the shutter pit and surroundings in the opened state describes Figure 27. The doses in the problematic places which were found using mesh tally were calculated by means of f4 tally. In the current shutter pit design, the cumulative (neutrons and γ) dose rates in all of the most exposed locations do not exceed 0.5 µSv/h.

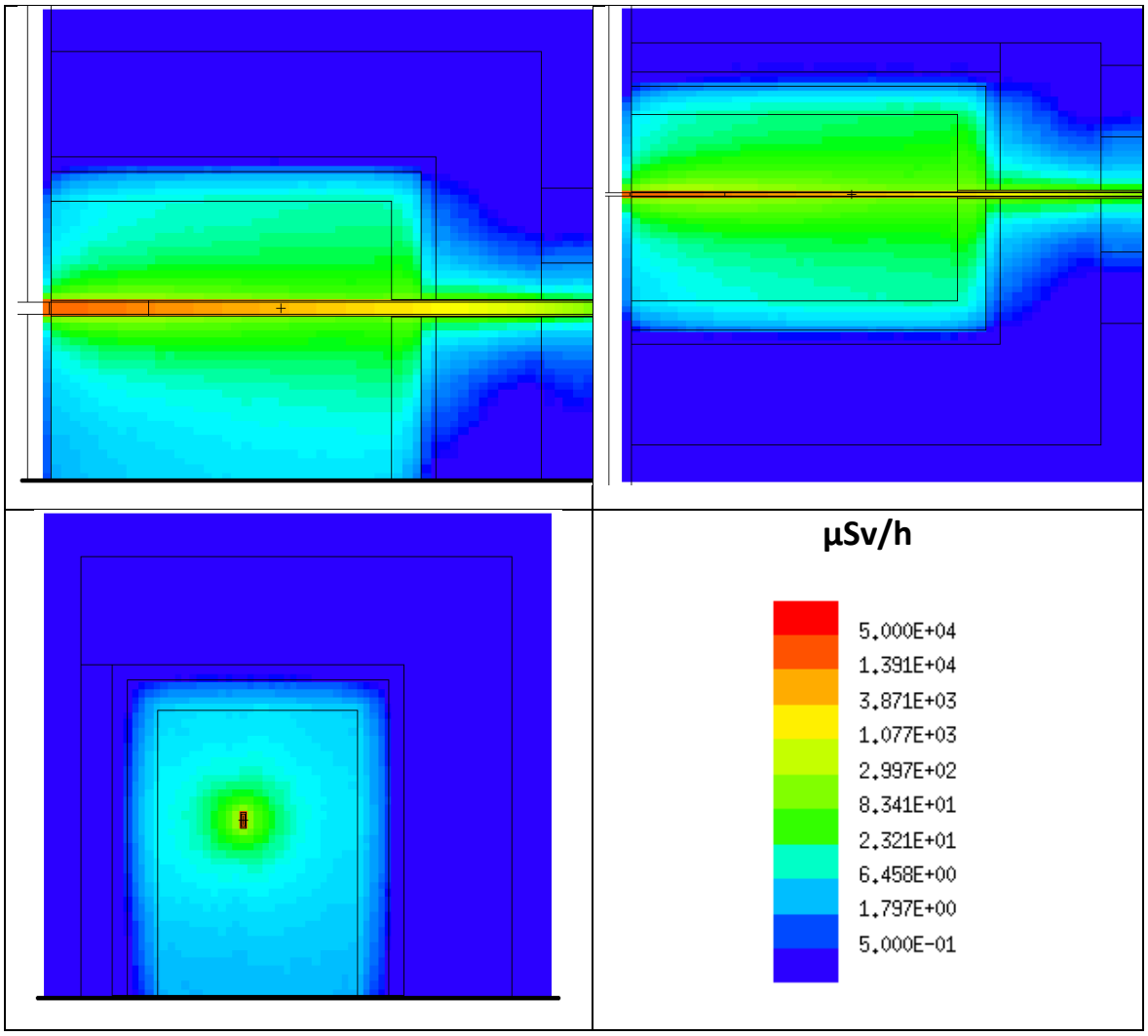

Figure 27: Fast neutron dose rates in the shutter pit in the opened state.

6.1.4. Behind shutter put when the shutter is open – H1.3

Figure 28 (coarse mesh) and Figure 29 (fine mesh) show the radiation situation in the tunnel behind the shutter pit wall. The figure takes into the account only radiation caused by the fast neutrons in the case of the open shutter. The lower limit of simulated 1.5 µSv/h is safely achieved in the distance of 110 cm behind the wall of the shutter pit (440 cm behind the bunker wall). Precise dose numbers were estimated using f4 tallies due to statistical checks. It was found that all segments of the following tunnel are sufficient to be designed for the thermal neutrons only, see Figure 28 and Figure 29, respectively.

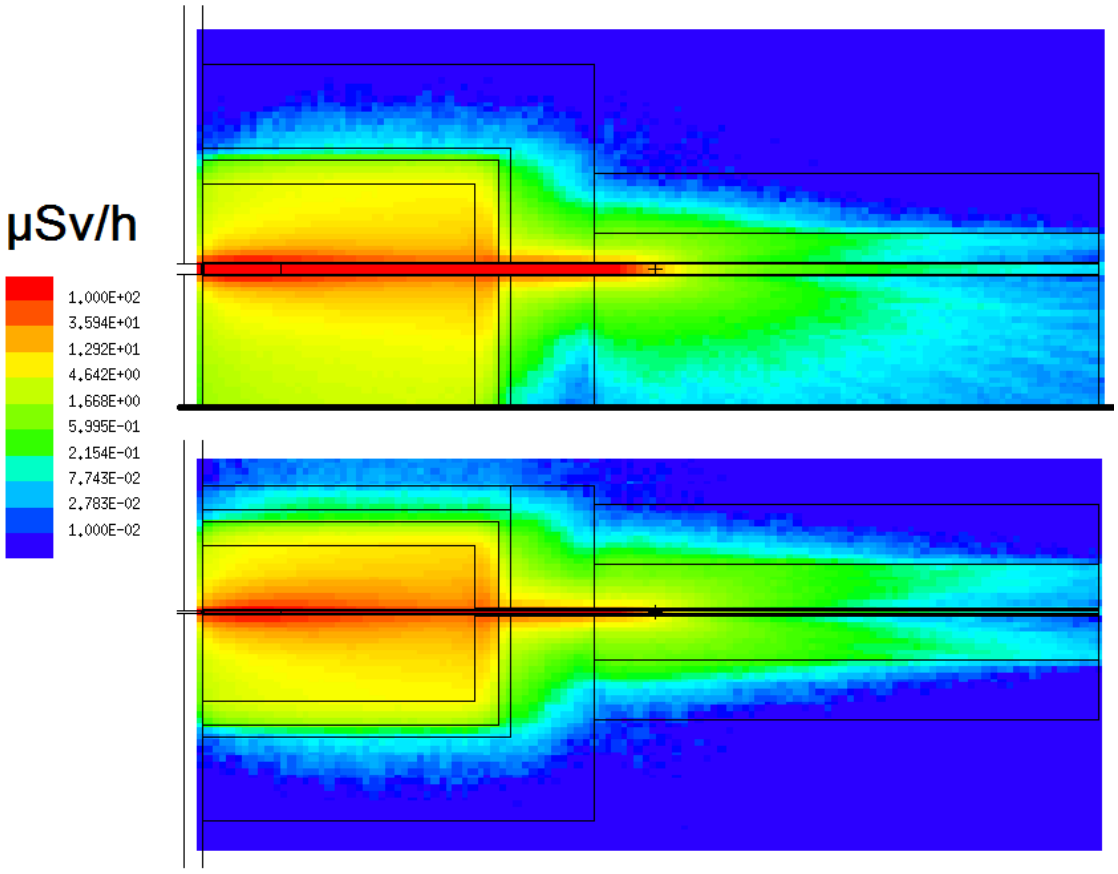

Figure 28: Fast neutron doses behind the bunker wall on the first 8 meters.

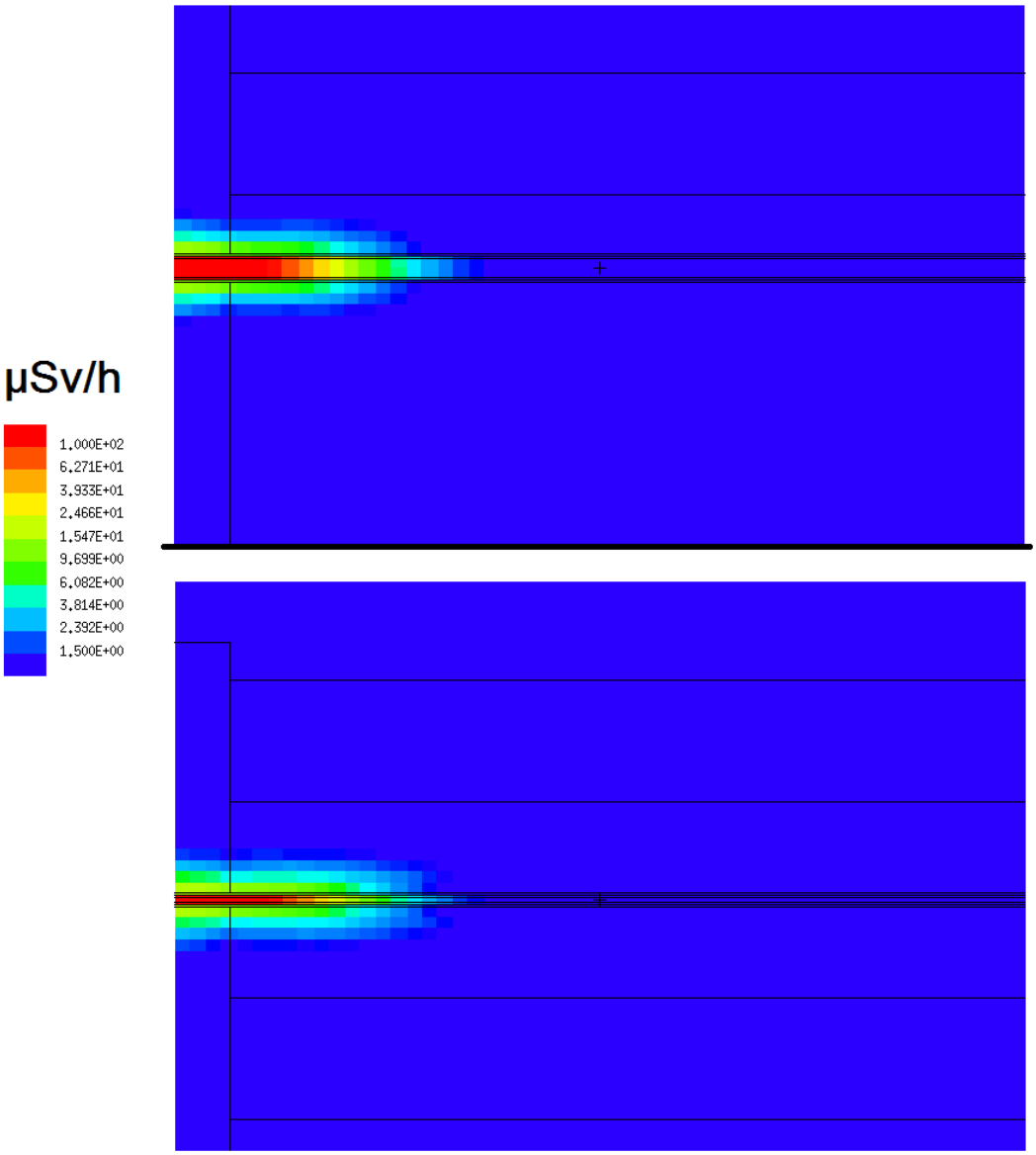

Figure 29: Fast neutron and photon doses behind the shutter pit on the first 3 meters.

6.2. Full beam within the chopper pit – H1.5

Detailed calculations of the dose maps reveal that 70 cm concrete will be sufficient to shield γ photons generated from boron, see Figure 30 and Figure 31 when all neutrons are isotropically scattered, and Figure 32 and Figure 33 in the case of boron carbide block placed in the beam with dimensions 5 cm x 5 cm x 0.2 cm (thickness), the dose rates in the most exposed point are kept bellow 0.5 µSv/h.

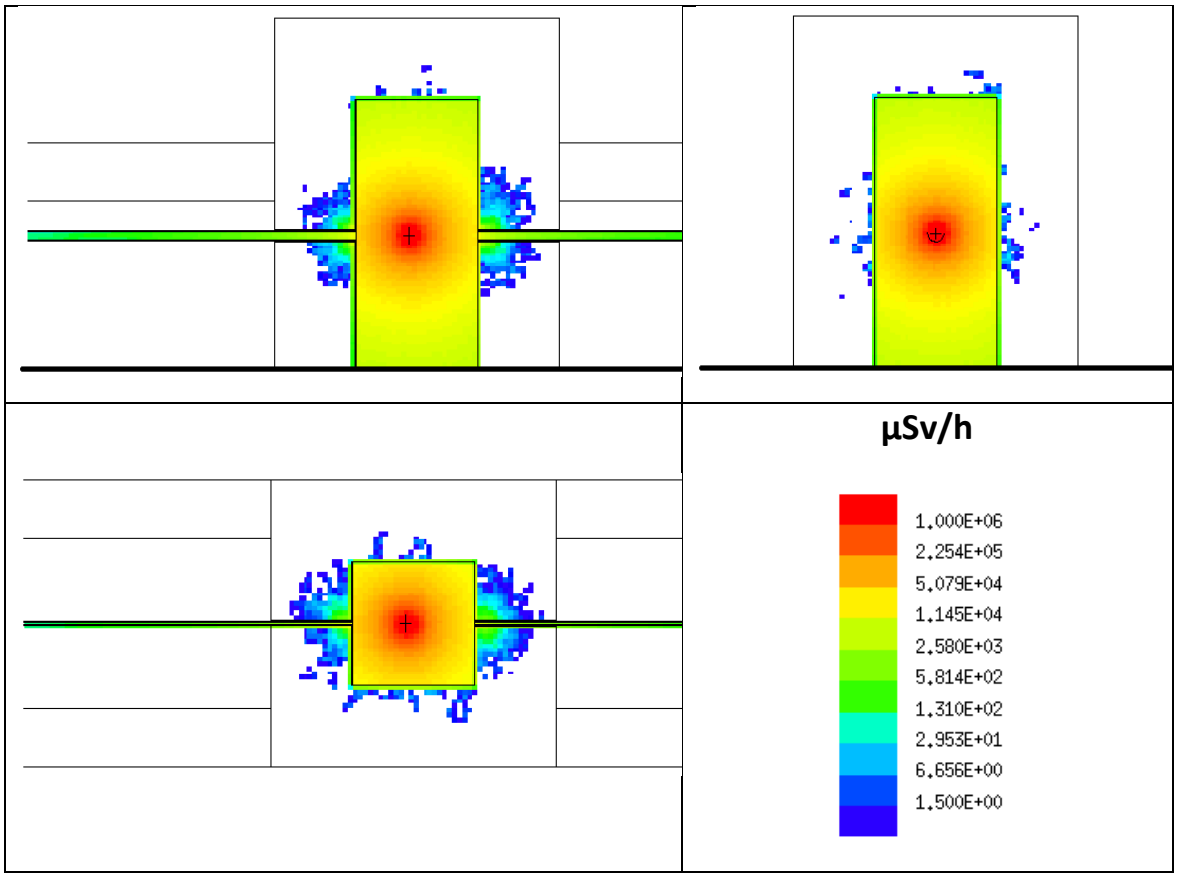

Figure 30: Neutron dose rates in the chopper pit in the case where all the neutrons are isotopically scattered.

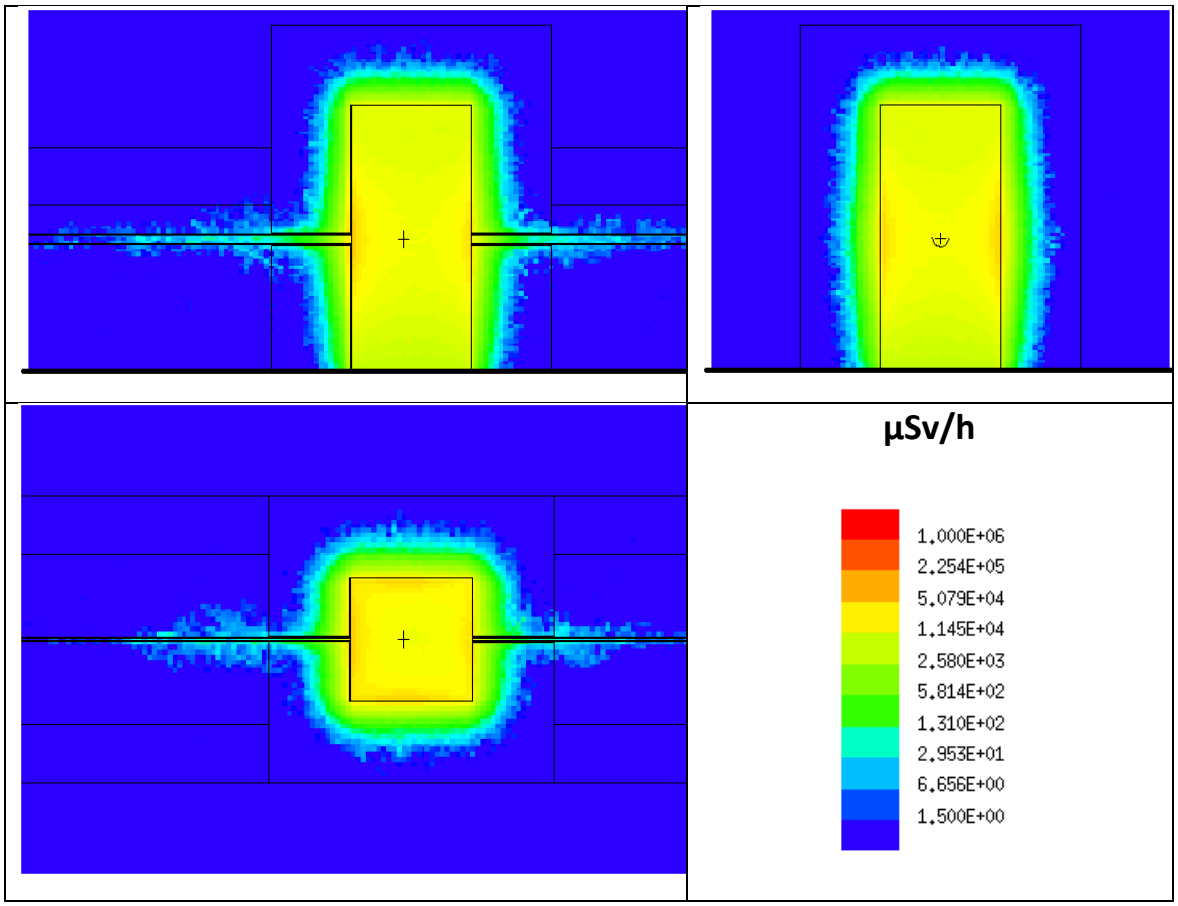

Figure 31: Photon dose rates in the chopper pit in the case where all the neutrons are isotopically scattered.

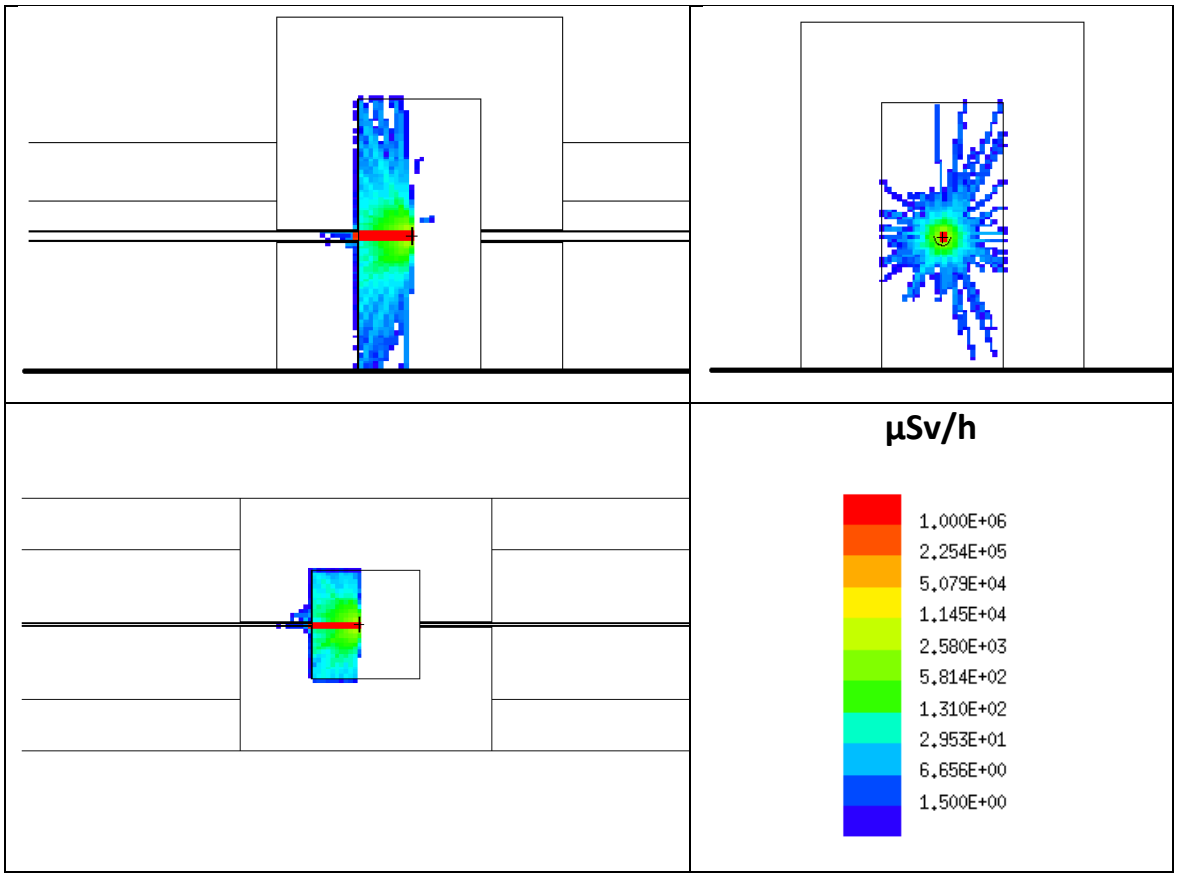

Figure 32: Neutron doses in the chopper pit in the case where all the neutrons absorbed by a B_4C plate.

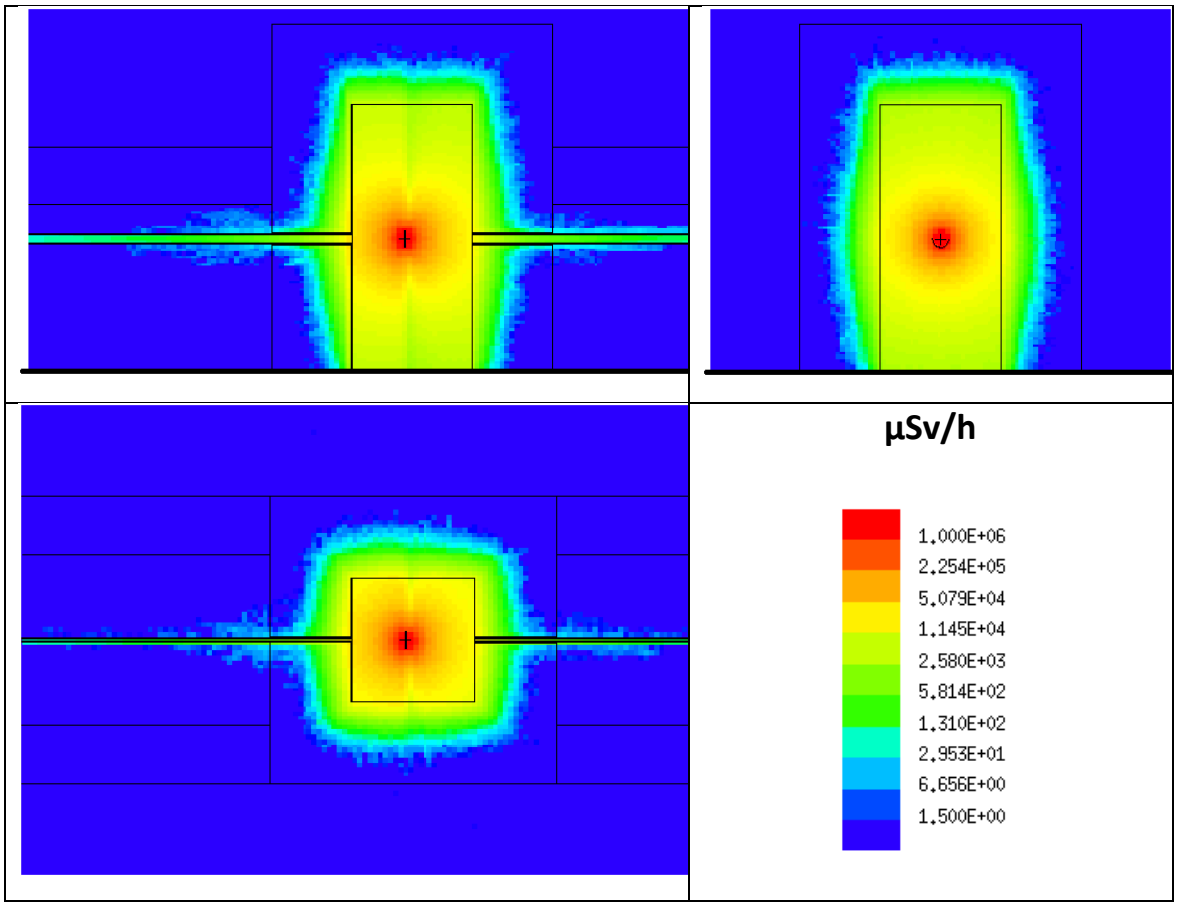

Figure 33: Photon doses in the chopper pit in the case where all the neutrons absorbed by a B_4C plate.

6.3. Neutron Guide

6.3.1. Thermal neutron shielding – H1.4

Figure 34 shows the γ dose rates around the wide section of the neutron guide shielding, where thermal neutrons represent the main limiting factor. Detailed calculations have shown that the average dose rate at the top part of the shielding (ca losest point on the shielding surface to the neutron guide) reaches 1.20 µSv/h for both sections of the neutron guide (wide and narrow). Hence the shielding thickness of 50 cm proves sufficient for the shielding tunnel, except the first 5 m just after the shutter pit. There, the simulated neutron capture rates increase up to 5E7 n/s/m, and hence a reinforcement of the shielding by additional 5 cm of a regular concrete equivalent may be required.

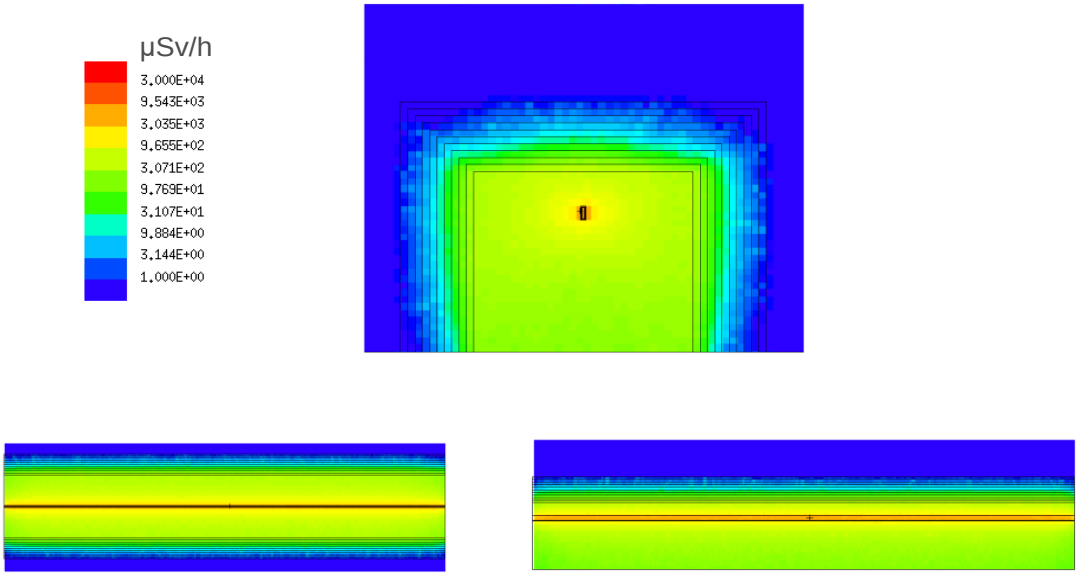

Figure 34: γ dose rates generated by thermal neutron interactions with the supermirror coating. Dose rates map around the wide section of the neutron guide shielding.

6.3.2. Focusing guide and slits system – H1.6

Separate simulations have been realized for the final 3 meters of the neutron guide around the distance of 152 m (from the target), where due to the presence of B_4C slits, the possibility of full thermal beam capture the tunnel thickness was increased to 60 cm.

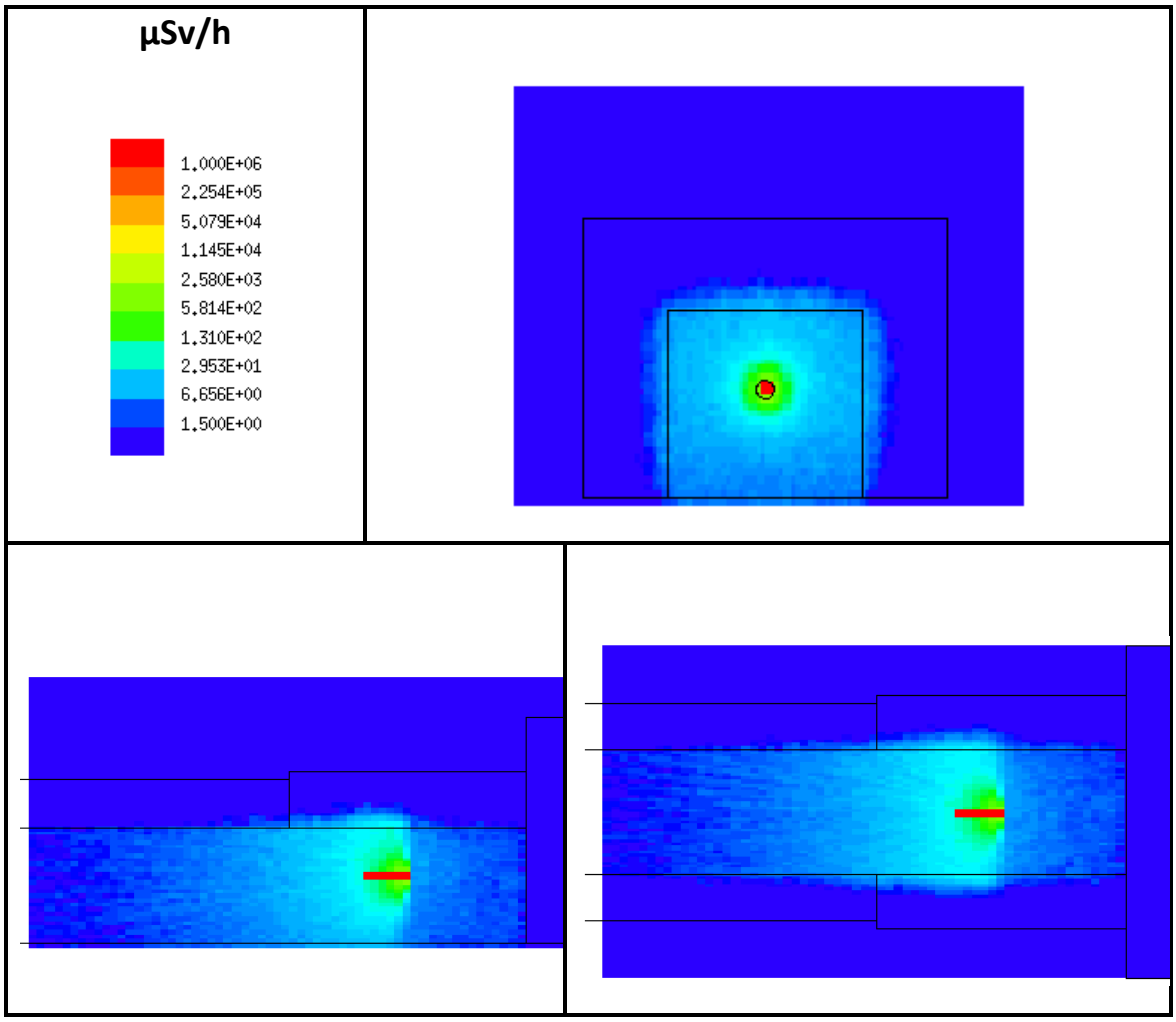

Figure 35: Neutron dose rates in the final 3 m of the guide tunnel around the B_4C slits before cave entering.

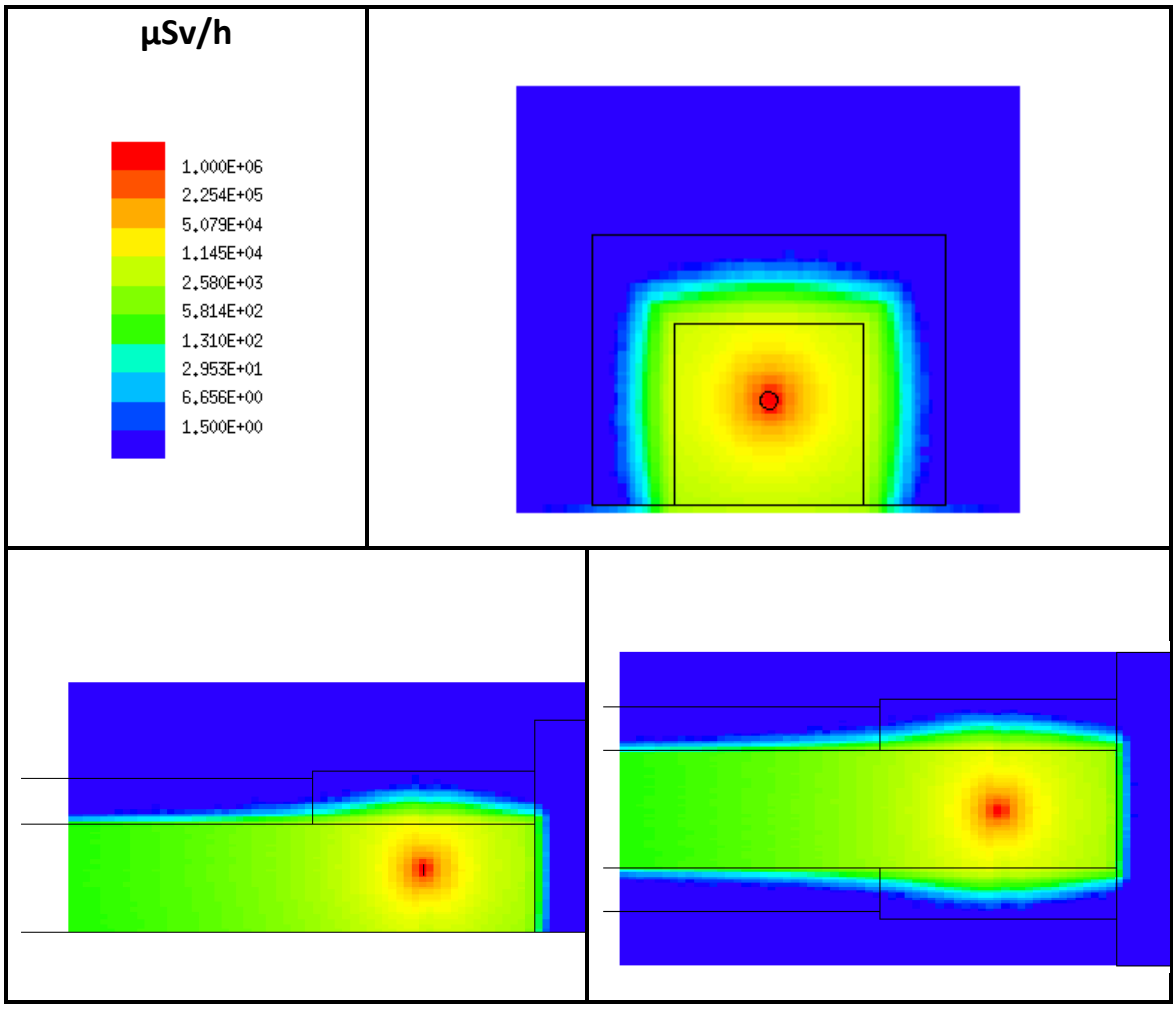

Figure 36: γ dose rates in the final 3 m of the guide tunnel around the B_4C slits before cave entering.

6.4. Instrument cave

The dose rate values in the instrument cave presented in this report are shown in the planar cuts as identified in Figure 37. The limits were successfully achieved for all considered scenarios, see Figure 37-Figure 45. All results are summarized in the next section.

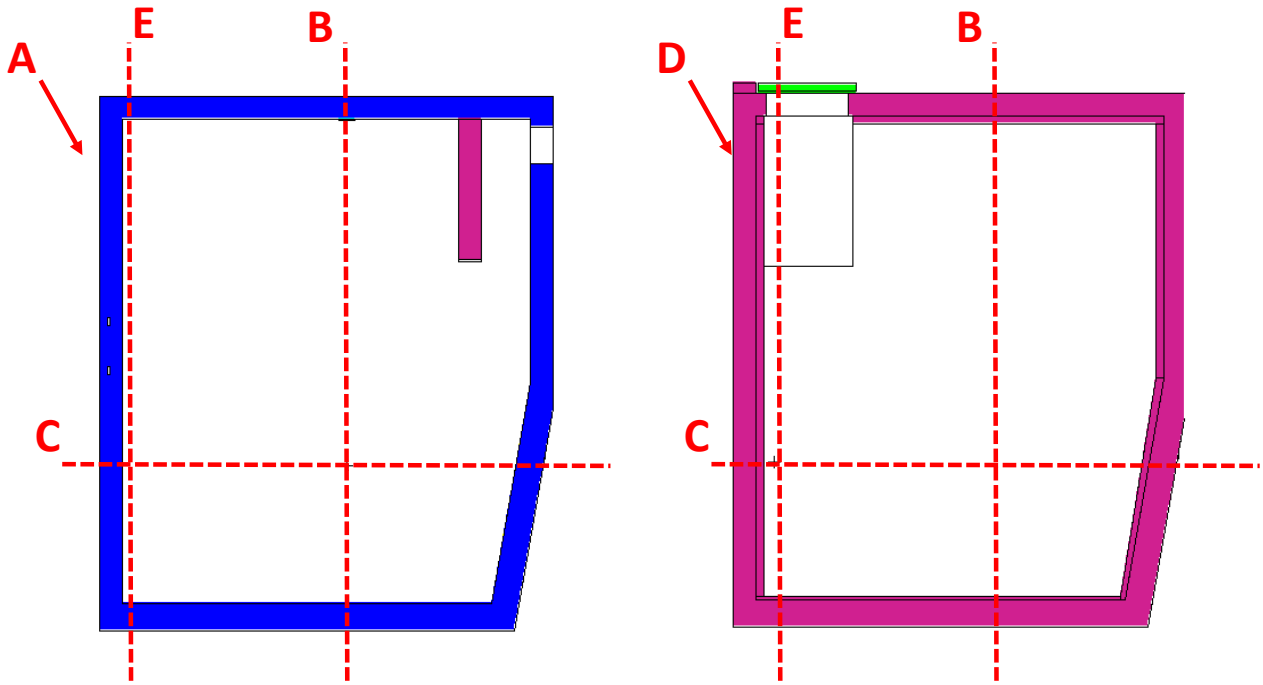

Figure 37: Instrument cave model with the identification of the planar sections where the dose rates are shown.

6.4.1. AFM beam scattered from the sample location – H2.1

This case assumes the thermal neutrons are isotropically scattered at the sample position simulated through a point source with the spectrum and intensity of the **AFM** beam – H2.1. Figure 38 and Figure 39 show γ and neutron doses in the experimental cave, respectively.

H2.1 scenario is likely accident event with probability more than once a year. It can occur during the change of the operation mode, misalignment of the sample environment (SE) or by a misfortune opening of the slit systems. The shielding design is expected to handle this scenario **passively**. This expectation is **fulfilled**. This scenario supersedes H1.8.

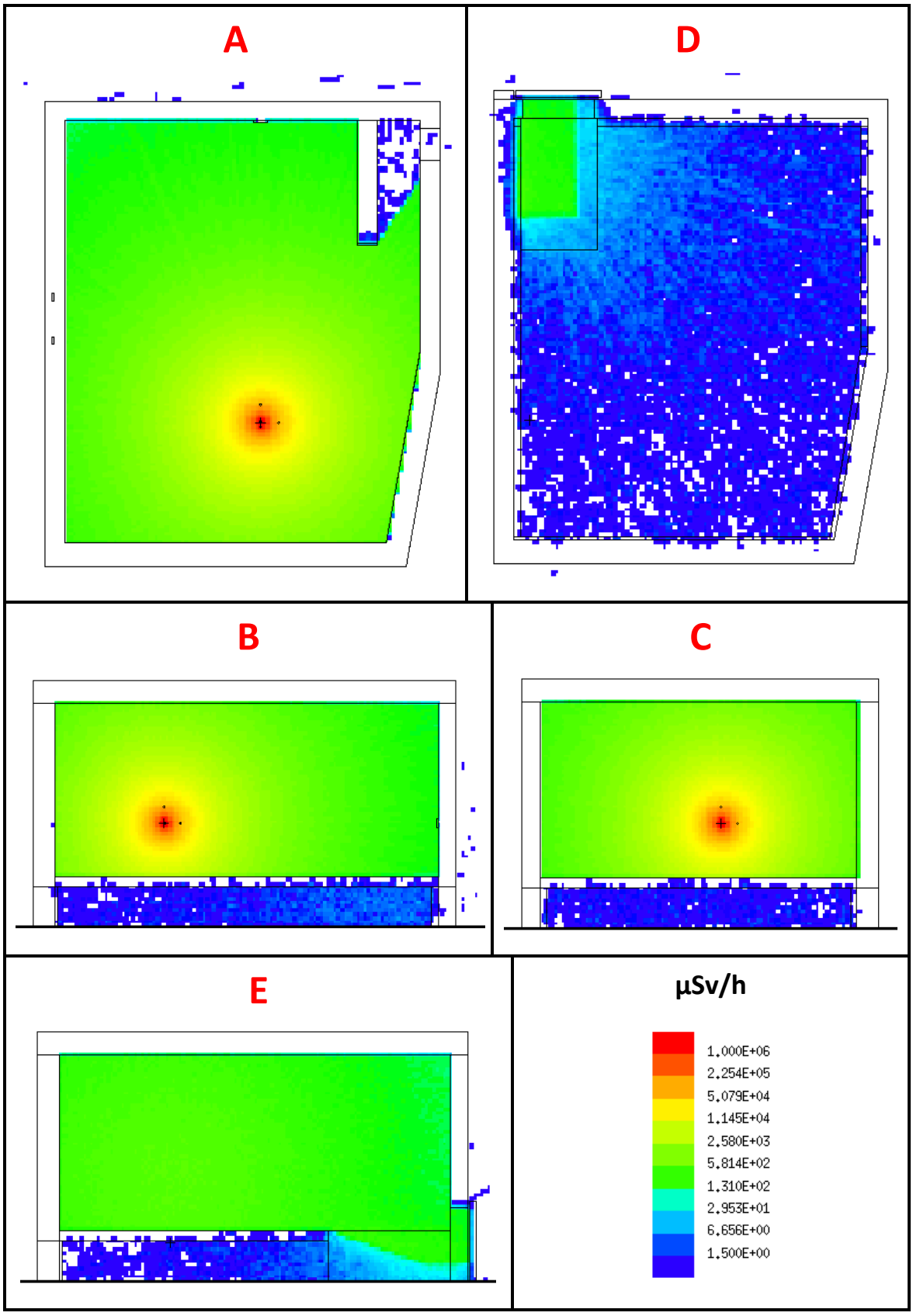

Figure 38: Spatial neutron dose rate distribution in the instrument cave for the H2.1 scenario– isotropically scattering sample.

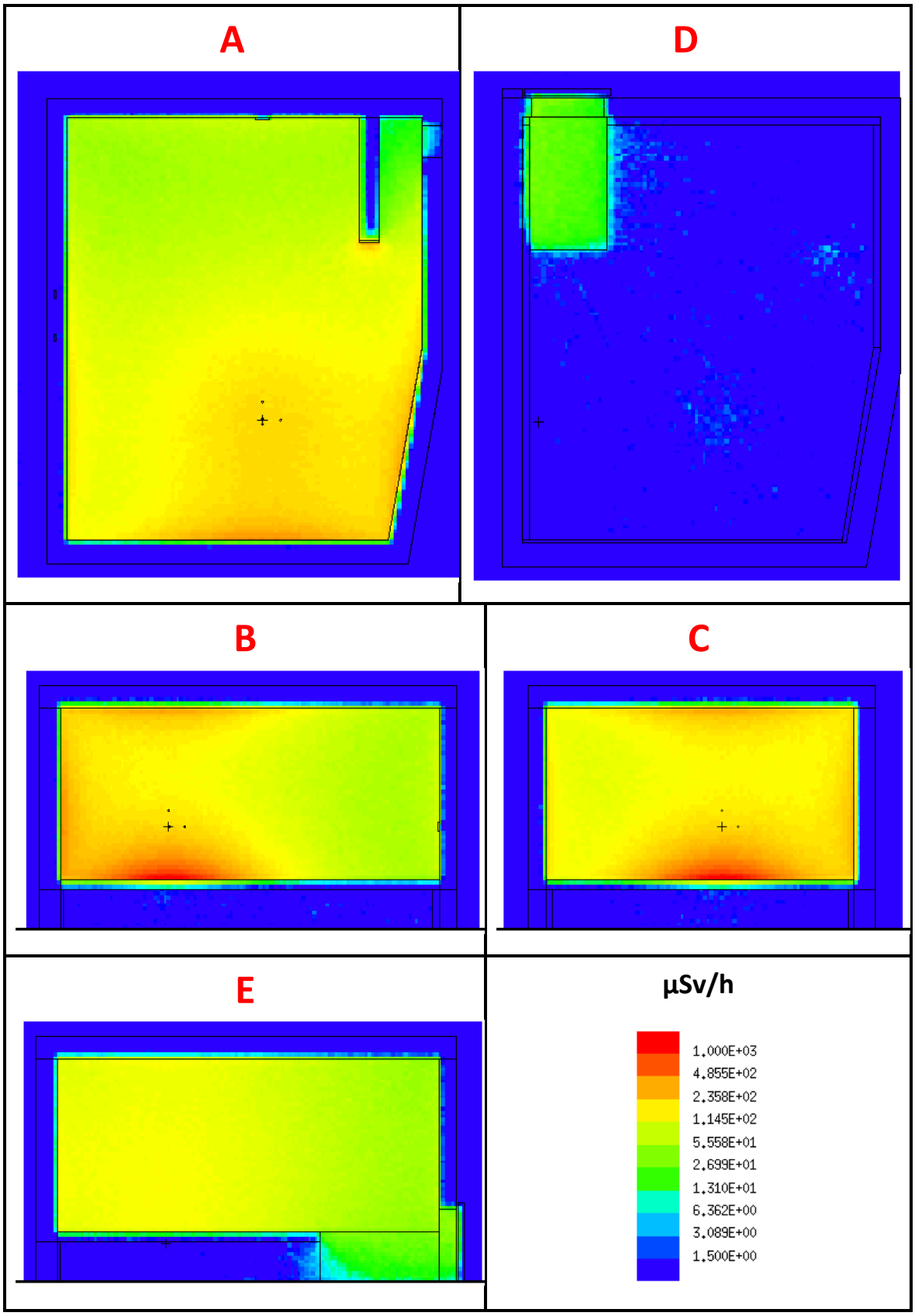

Figure 39: Spatial γ dose rate distribution in the instrument cave for the H2.1 scenario – isotropically scattering sample.

6.4.2. Nickel sample in AFM beam – H2.2

This scenario assumes γ radiation generated by thermal neutrons capture in a Ni sample (w×h×thickness=4.4×4.4×1.5 cm^3) placed in the sample position perpendicularly to the **AFM** beam – H2.2. Figure 40 and Figure 41 show γ and neutron doses in the experimental cave, respectively.

H2.2 scenario is likely accident event with probability more than once a year. It can occur during the change of the operation mode, misalignment of the sample environment (SE) or by a misfortune opening of the slit systems. The shielding design is expected to handle this scenario **passively**. This expectation is **fulfilled**. This scenario supersedes H1.9.

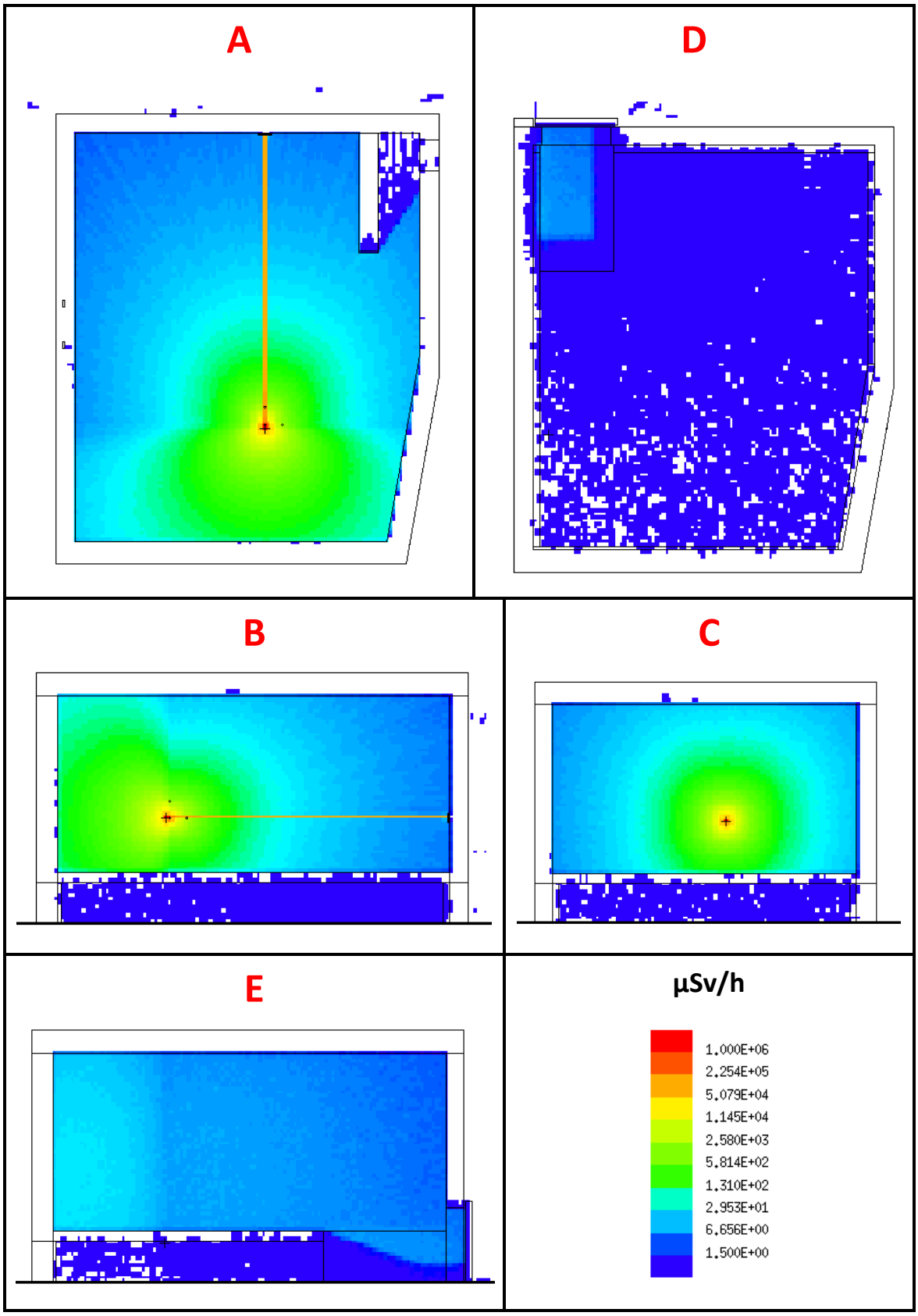

Figure 40: Spatial neutron dose rate distribution in the instrument cave for the nickel sample placed in the AFM beam – H2.2.

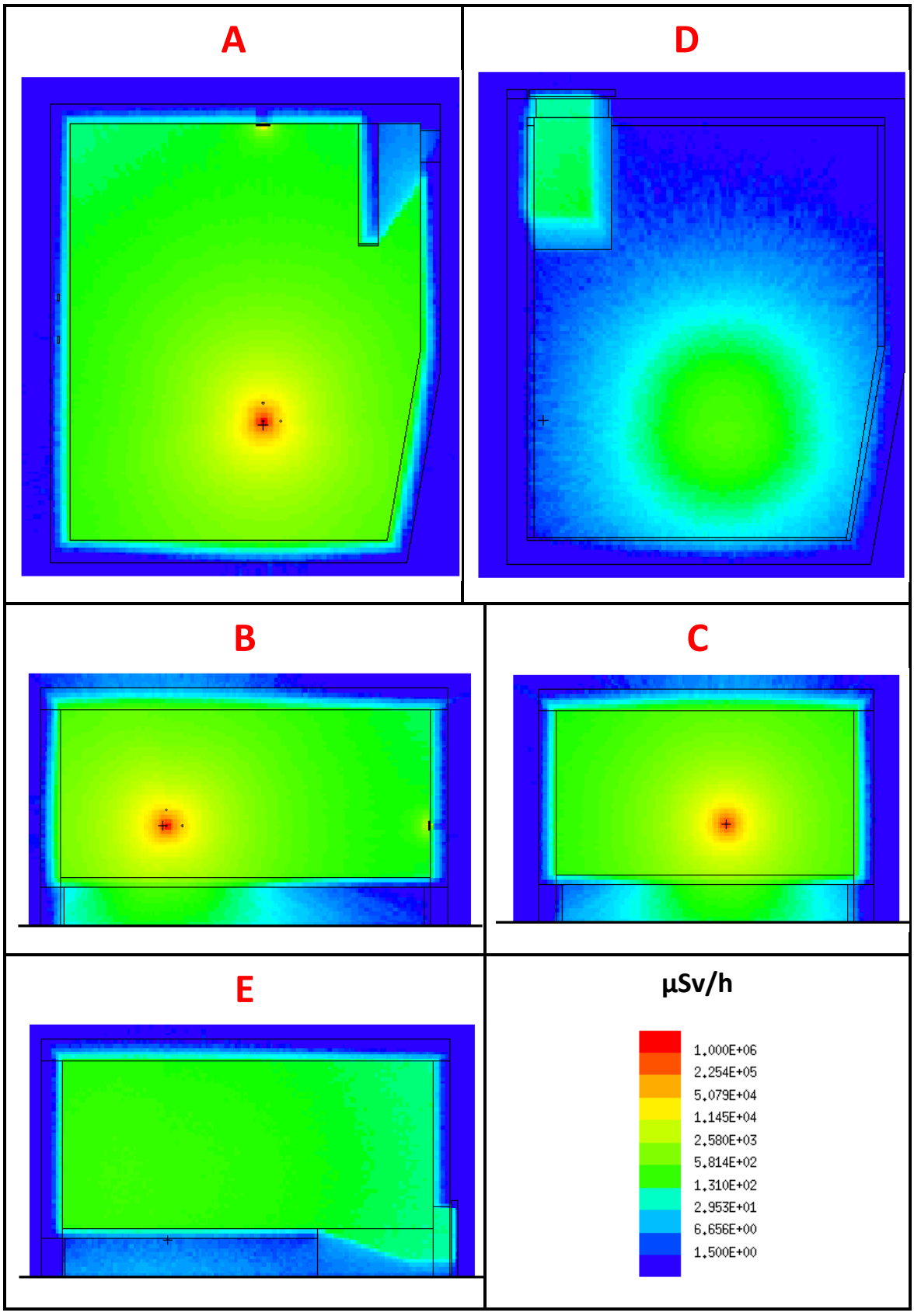

Figure 41: Spatial γ dose rate distribution in the instrument cave for the nickel sample placed in the AFM beam – H2.2.

6.4.3. Nickel Sample in MWB beam – H2.5

The severe accident scenario assumes γ generated by thermal neutrons capture in an identical Ni sample like in the 6.4.2 scenario placed into the **MWB** beam. Figure 42 and Figure 43 show neutron and photon doses in the experimental cave, respectively.

H2.5 scenario is severe accident event with low probability. It occurs when everything fails – all choppers stopped open, all slits system fully open. The shielding design is **not** expected to handle this scenario **passively**. But the **dose rates are kept as low as possible** to have enough time to detect this event and take actions before the dose limit of 1 mSv for H2 event is fulfilled.

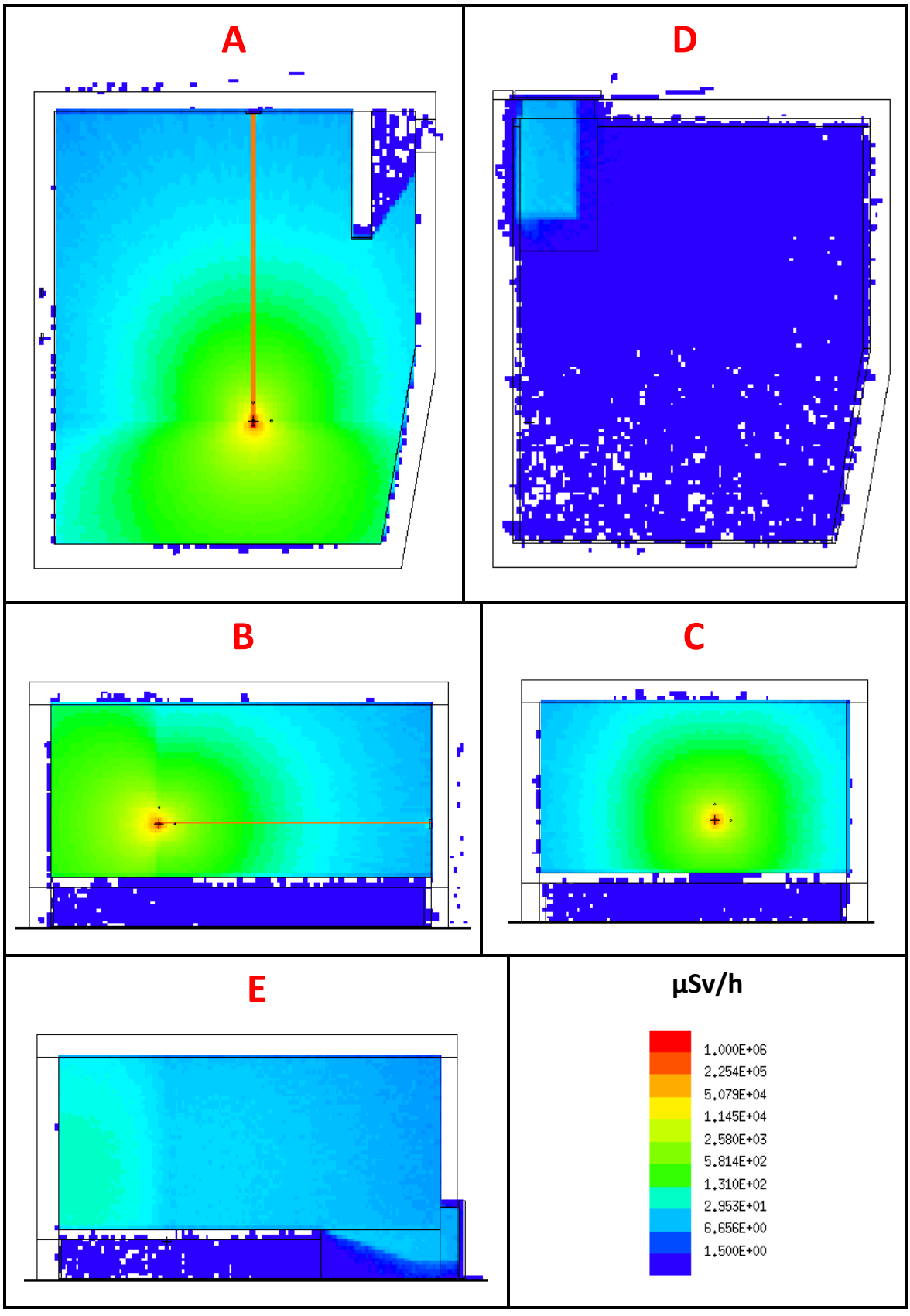

Figure 42: Spatial neutron dose rate distribution in the instrument cave for the nickel sample placed in the MWB beam – H2.5.

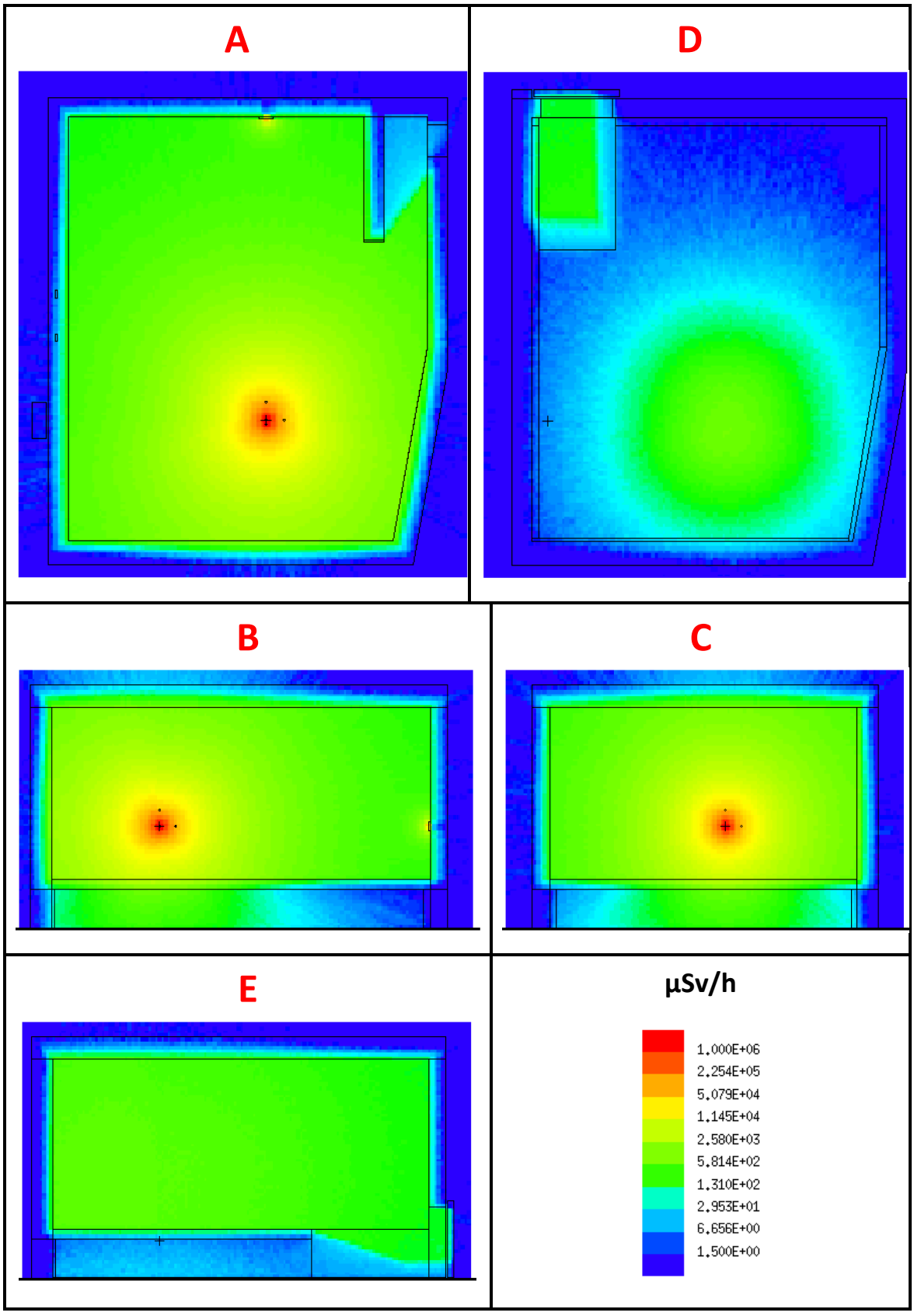

Figure 43: Spatial γ dose rate distribution in the instrument cave for the nickel sample placed in the MWB beam – H2.5.

6.4.4. Cadmium plate in MWB beam – H2.6

The severe accident scenario assumes γ generated by thermal neutrons capture in a 1 mm thick cadmium plate placed into the MWB beam, covering the whole beam area while the plate is rotated by 45° in every direction. Figure 44 and Figure 45 show neutron and photon doses in the experimental cave, respectively.

H2.6 scenario is severe accident event with low probability. It occurs when everything fails – all choppers stopped open, all slits system fully open. The shielding design is **not** expected to handle this scenario **passively**. But the **dose rates are kept as low as possible** to have enough time to detect this event and take actions before the dose limit of 1 mSv for H2 event is fulfilled.

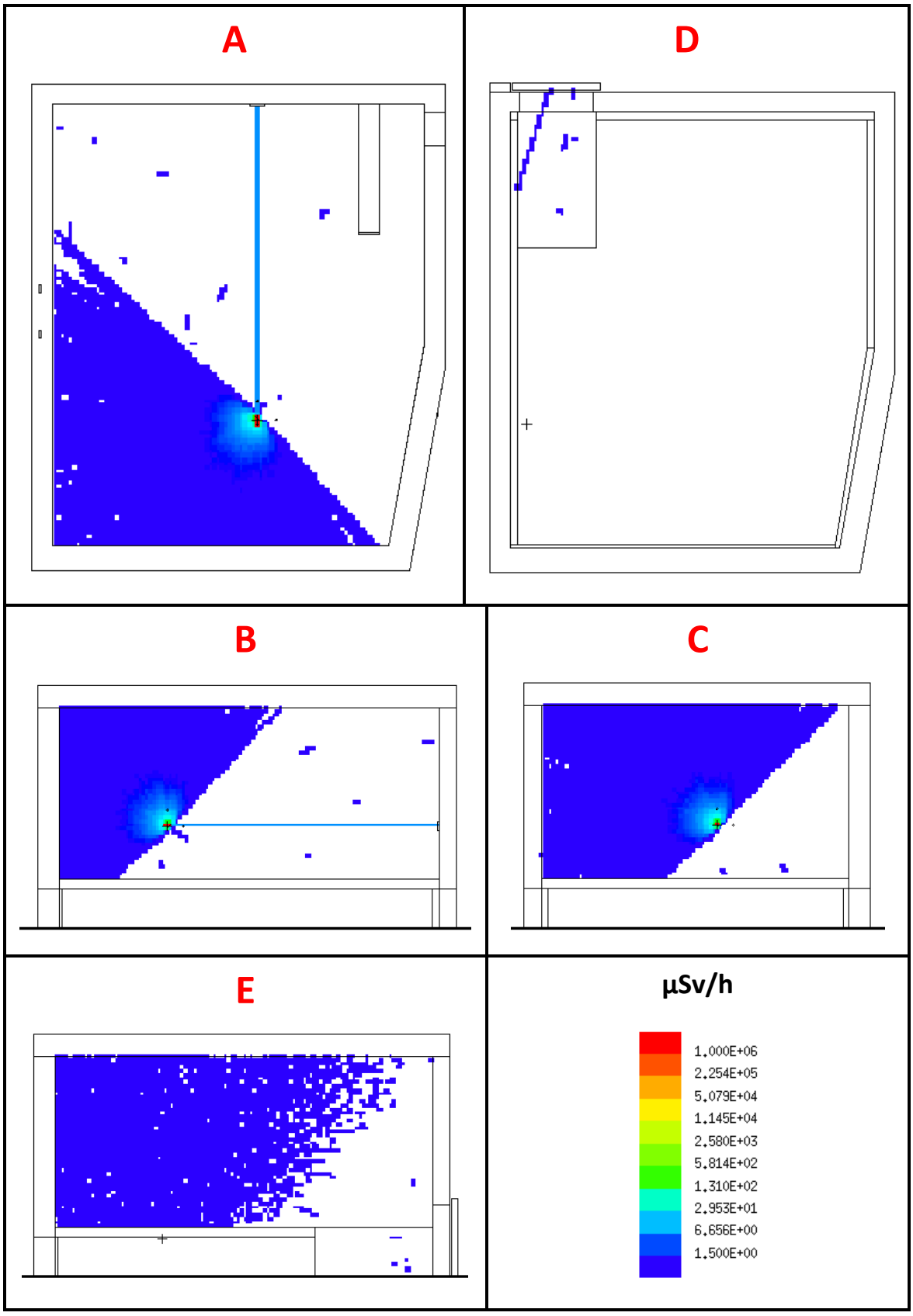

Figure 44: Spatial neutron dose rate distribution in the instrument cave for the cadmium plate in the MWB scenario – H2.6.

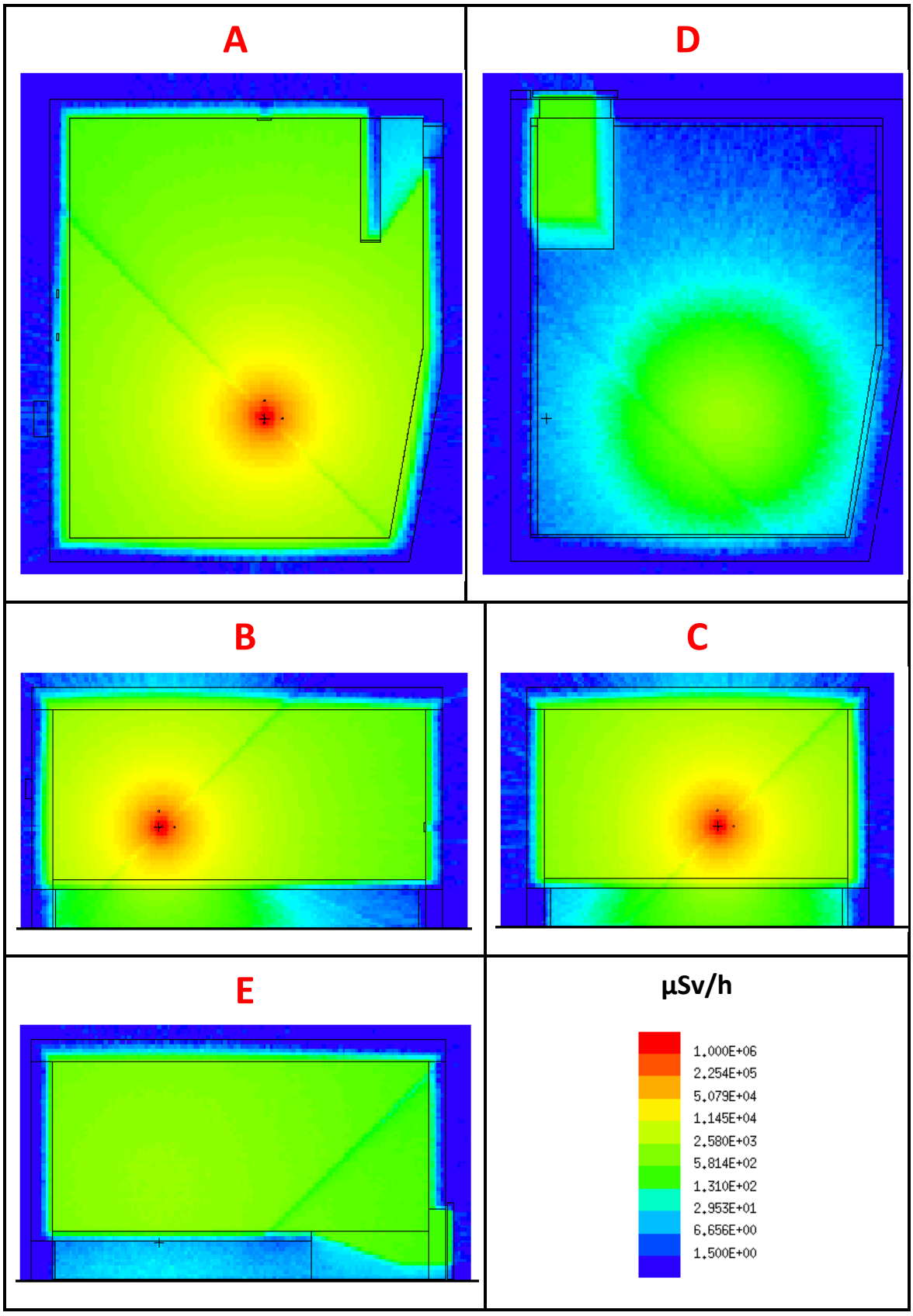

Figure 45: Spatial γ dose rate distribution in the instrument cave for the cadmium plate in the MWB scenario – H2.6.

6.4.5. Full beam hitting the beam-stop – H2.7

The beam-stop, with its proposed dimensions of 40×25 cm^2, was tested in the limiting beam configuration (MWB beam). The neutron spatial distribution and the capability of the beam to absorb the thermal neutrons from the beam is demonstrated in Figure 46. The neutron and γ dose rates occurring while the MWB beam is hitting the beam stop is shown in Figure 47 and Figure 48.

H2.7 scenario is severe accident event with low probability. It occurs when everything fails – all choppers stopped open, all slits system fully open. The shielding design is not expected to handle this scenario passively. But simulations show that the current shielding and beam-stop design can shield this accident scenario **passively**. This scenario supersedes H2.3 and H1.10.

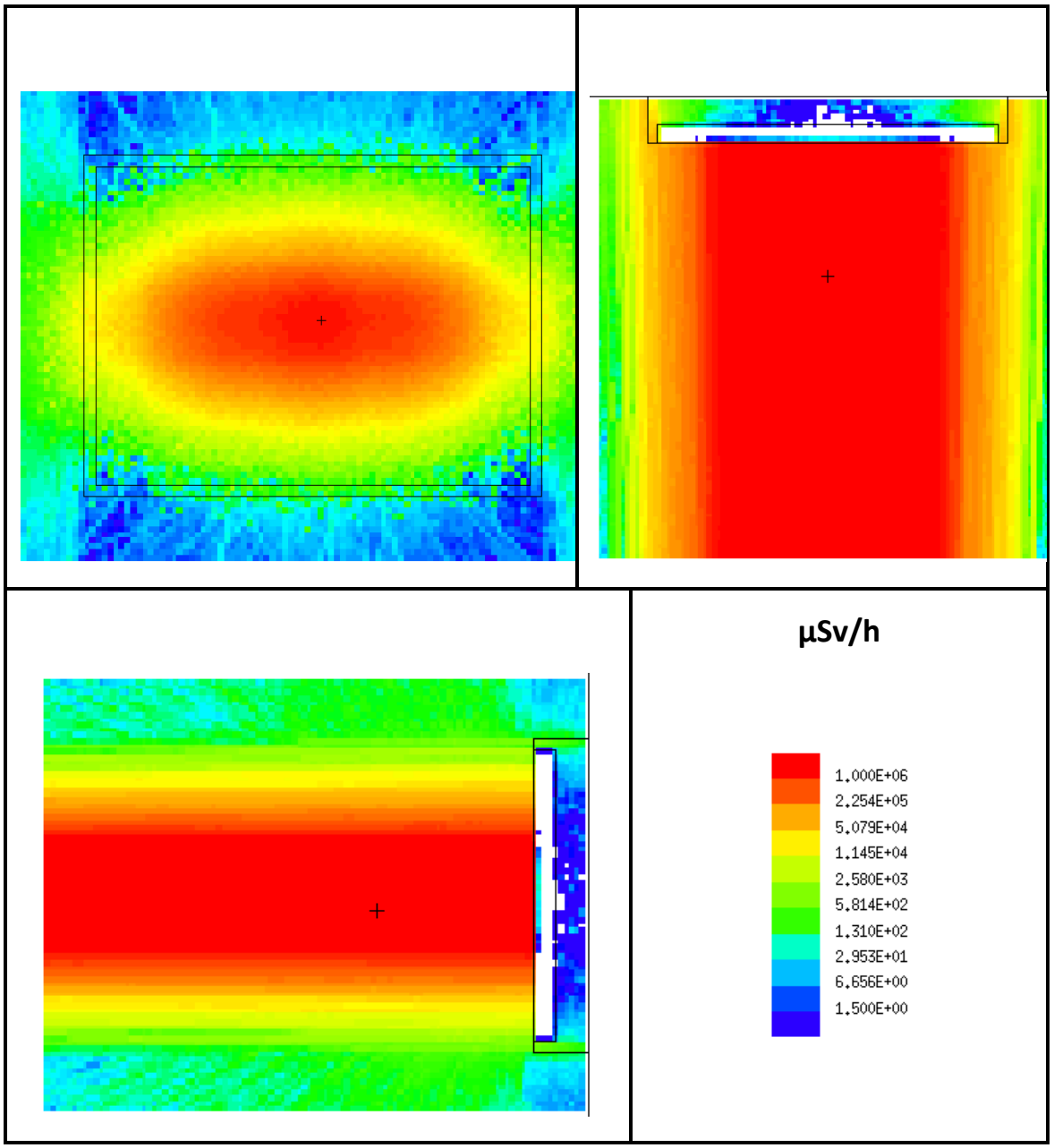

Figure 46: Neutron dose rate profiles at the entry point of the beam-stop.

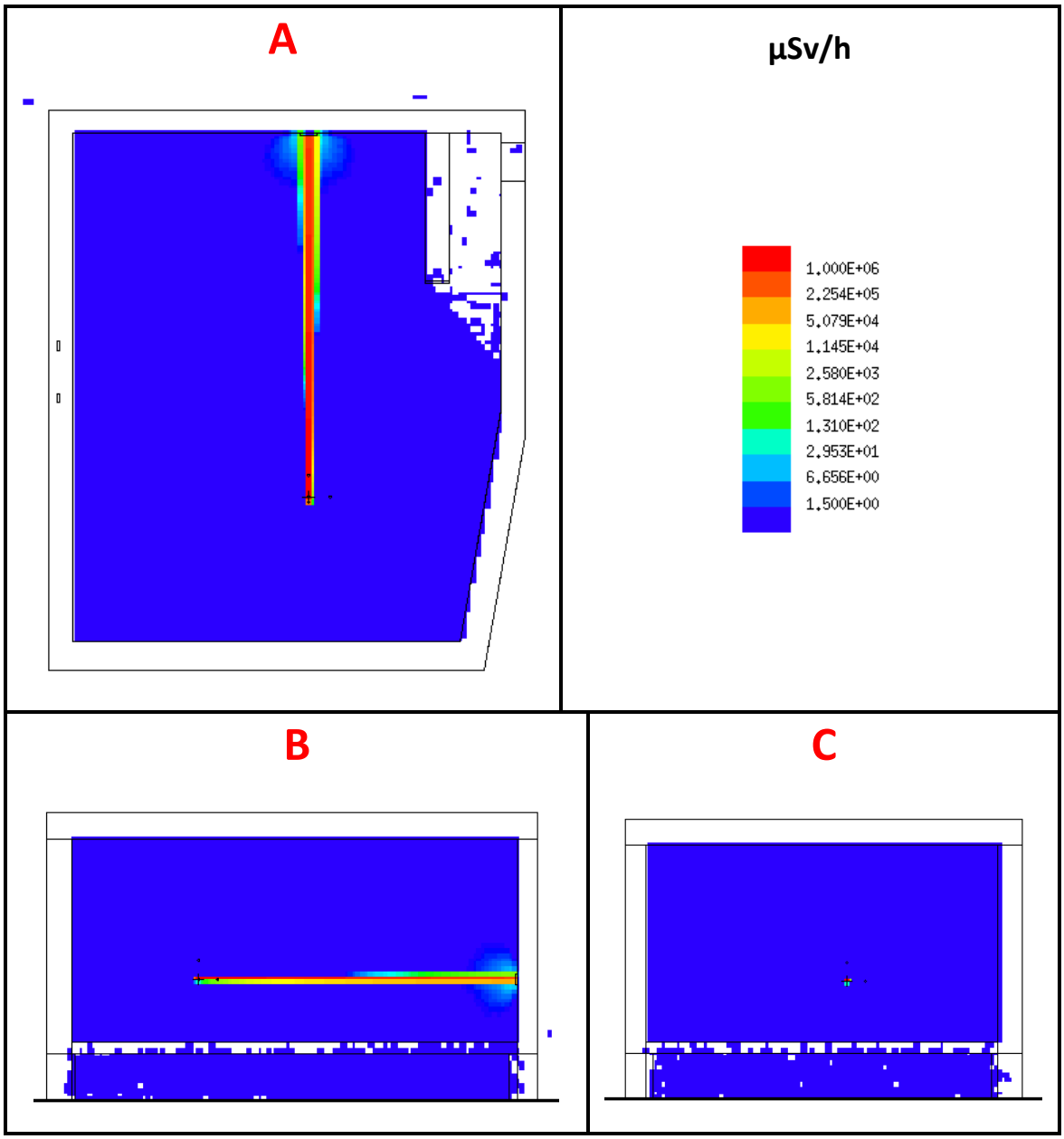

Figure 47: Spatial neutron dose rate distribution in the instrument cave for MWB beam hitting the beam-stop.

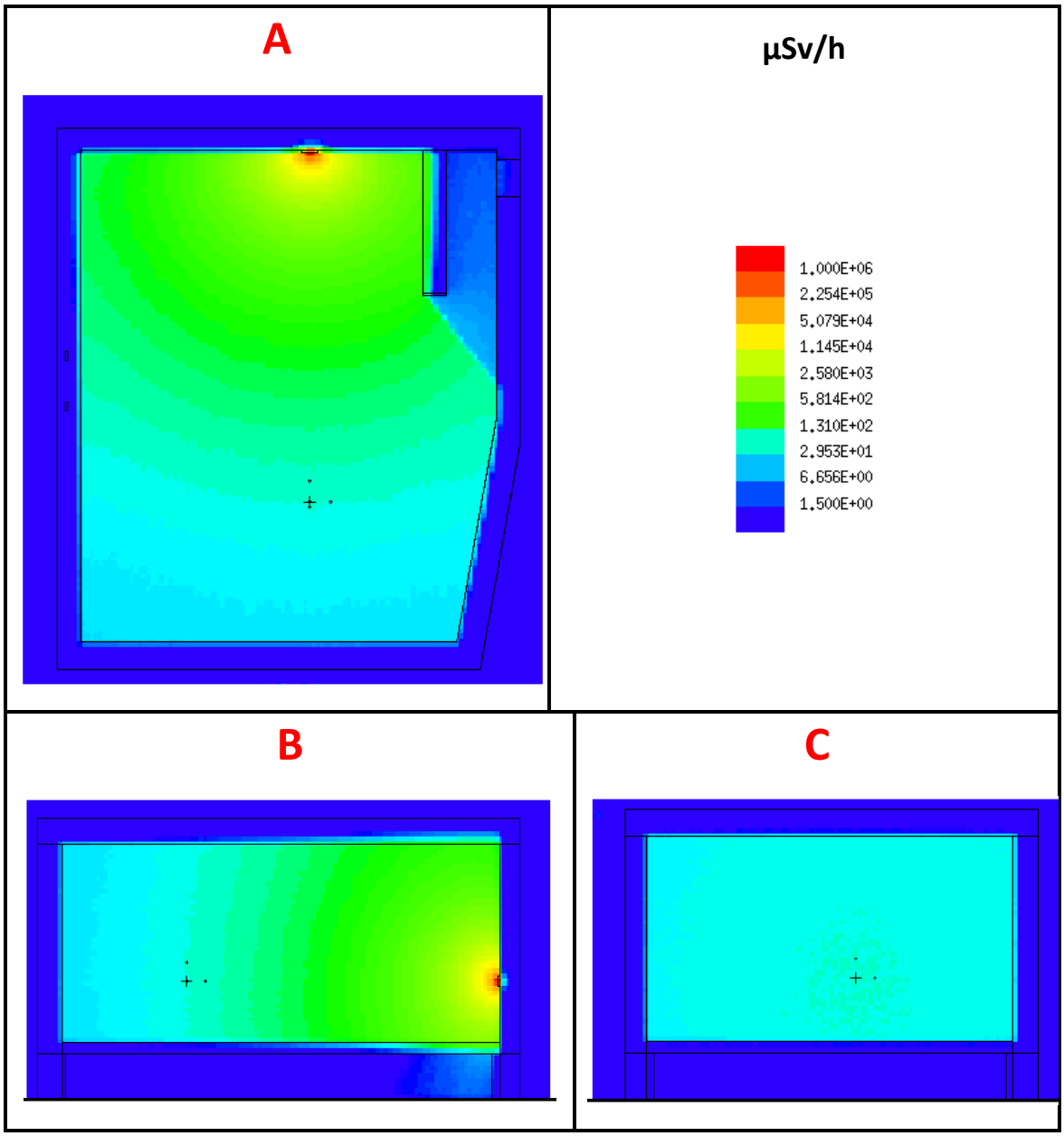

Figure 48: Spatial γ dose rate distribution in the instrument cave for MWB beam hitting the beam stop.

6.4.6. General cave shielding summary

For each of the examined cases, a detailed dose rate calculation was realized in certain points where the highest expositions were expected (Figure 49– P1, P4, P5, P6, P11 are located near the beam height, 163.7 cm above the cave floor). The prompt-γ and neutron dose rates at these points for wall thickness, according to Figure 19 are listed in Table 22. The **neutron doses** at the **outer wall surface are negligible** due to the application of the **B_4C** layer on the inner walls and the capability of the beam stop to absorb the primary beam neutrons. It represents **sufficient shielding** for scenarios of the neutron scattering sample or the beam-stop hit by the MWB (**H2.4** and **H2.7**). The 3D dose rate distributions have also shown the **successful application** of the **heavy sliding door** and the **wall chicane** around the personal entry. Nor cable trays in the design represent a problem according to the dose rate calculations. In case of the severe accident scenarios **H2.5** and **H2.6**, where the **MWB** hits Cd plate or the limiting Ni sample, the predicted

dose rates **exceed** the limit of 1.5 µSv/h (in the supervised areas) or 12.5 µSv/h (in the controlled areas - cave roof) for **simulated** dose rates by a **factor of up to 2.1** in some points. These values are at the limit of the actual measured dose rates limits. If these limits are exceeded, an active radiation monitoring and safety system will be applied to close the shutter automatically or manually in a case of accidental conditions.

The samples of **Fe**, **V**, **Cr**, **Cu** and **B_4C** of similar dimensions as Ni sample and **Al** block of 10×10×10 cm^3 were also tested, and they **fully satisfy** the limits.

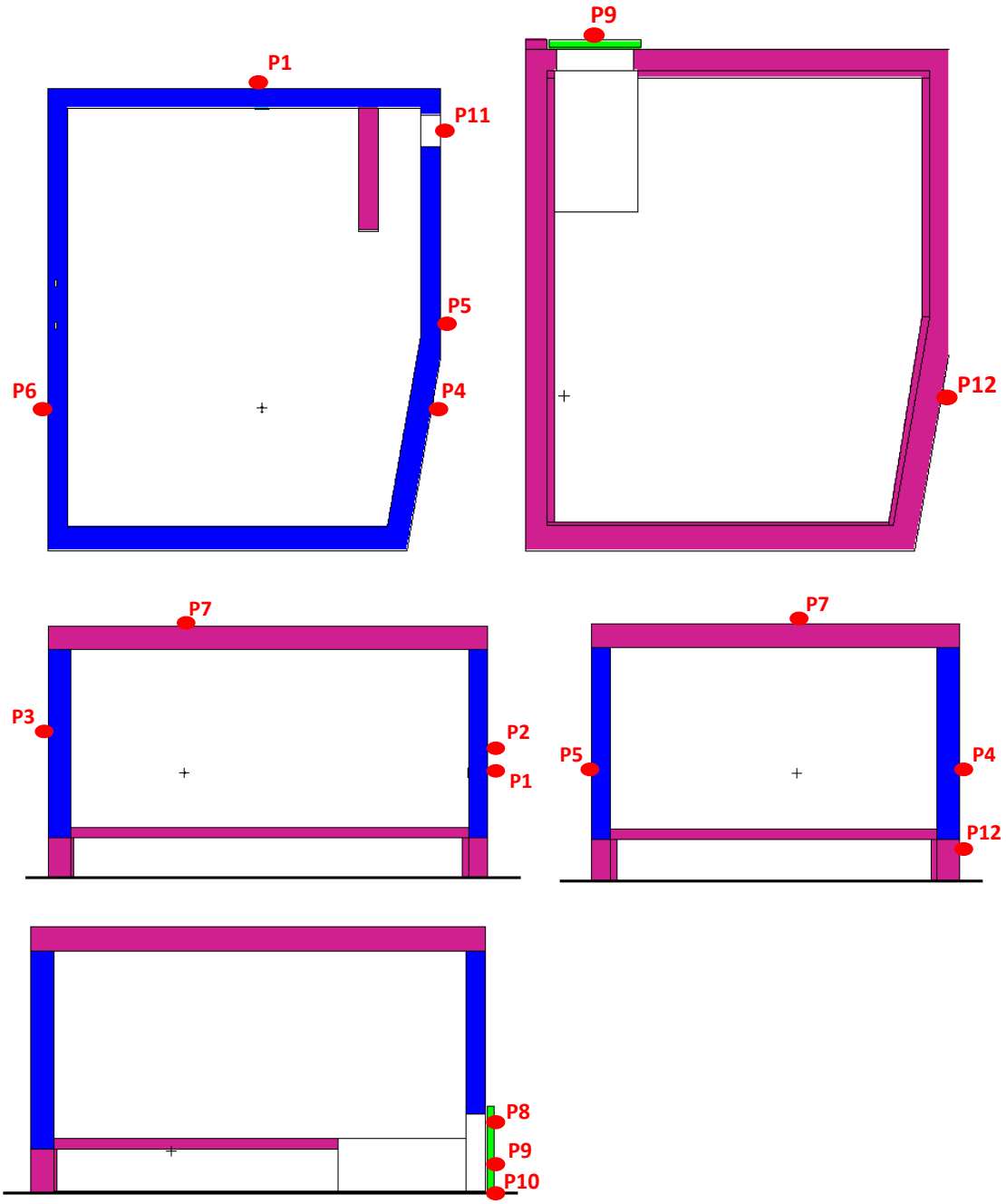

Figure 49: Dose rate hotspot identification for detailed calculations.

Table 22: Calculated sums of γ and neutron dose rates in the defined hotspot points.

Dose rate (µSv/h)				
Sample	Beam scattered	4.4x4.4x1.5 cm^3 Ni	4.4x4.4x1.5 cm^3 Ni	1 mm Cd plate rotated by 45°
Scenario	**H2.1**	**H2.2**	**H2.5**	**H2.6**
Beam	**AFB**	**AFB**	**MWB**	**MWB**
P1 (back wall)	0.01	0.53	0.91	1.15
P2 (back wall)	0.01	0.75	1.30	1.40
P3 (front wall above neutron-guide tunnel)	0.001	1.24	2.15	1.68
P4 (right wall leaning)	0.001	0.78	1.37	1.50
P5 (right wall straight)	0.001	0.73	1.28	1.57
P6 (left wall)	0.001	1.31	2.26	3.11
P7 (roof)	0.004	10.44	18.45	23.93
P8 (heavy door top)	0.004	1.01	1.75	2.82
P9 (heavy door bottom)	0.006	0.02	0.05	0.06
P10 (heavy door gap)	0.82	0.57	1.08	1.39
P11 (personal entry)	0.90	0.62	1.13	1.65
P12 (right wall leaning foundations)	0.001	0.24	0.41	0.36

6.4.7. B_4C layer activation

The application of the B_4C layer on the inner cave wall to minimize the thermal neutron impact on the cave's concrete wall is designed to be realized by wall tiles made of epoxy, B_4C powder and silica sand, with a content of 3 kg B_4C powder per 1 m^2 of the tiles (the equivalent of 1 mm B_4C layer). For the decommissioning purposes of the cave structure materials, the activation of the tiles was estimated in a conservative scenario by the FISPACT-II 4.0 code [12]. For this scenario, 1 kg of tile matter was simulated to be irradiated uninterrupted for 5 years by a total neutron flux of 1E+06 $n/cm^2/s$ of the same neutron spectra as at the sample position. After a one week of the cooling time the following long-life radioisotopes occur in the irradiated tiles:

H-3	3000	Bq/kg
Fe-55	180	Bq/kg
Fe-59	20	Bq/kg.

In the case that standardly occurring impurities in B_4C powders (mainly iron oxides) are taken in account the activation estimation is the following:

H-3	3000	Bq/kg

Fe-55	4000	Bq/kg
Fe-59	400	Bq/kg.

These values are far below the yearly intake limits set by the ICRP-61 document (Annuals Limits on Intake of Radionuclides by Workers Based on the 1990 Recommendations) and safe to work with while decommissioning. The ICRP-61 yearly values are listed in Table 23.

Table 23: ICRP-61 yearly intake limits.

H-3	1E+09 Bq		Zn-65	4E+06 Bq
C-14	4E+07 Bq		Se-75	9E+06 Bq
F-18	4E+08 Bq		Sr-90	6E+04 Bq
Na-22	7E+06 Bq		Tc-99m	1E+09 Bq
Na-24	5E+07 Bq		I-125	1E+06 Bq
P-32	5E+06 Bq		I-131	8E+05 Bq
P-33	3E+07 Bq		Cs-134	1E+06 Bq
S-35	3E+07 Bq		Cs-137	1E+06 Bq
Cl-36	3E+06 Bq		Pb-210	1E+04 Bq
Ca-45	1E+07 Bq		Ra-226	9E+03 Bq
Cr-51	2E+08 Bq		Th-232	9E+01 Bq
Fe-55	3E+07 Bq		U-238	6E+02 Bq
Fe-59	5E+06 Bq		Pu-239	3E+02 Bq
Co-60	4E+05 Bq		Am-241	3E+02 Bq
Ni-63	1E+07 Bq			

6.5. Conclusions

Based on the presented series of calculations, it can be concluded that the design of the BEER instrument can be realized according to the stated specifications summarized in Table 24. The calculations prove that dose rate limits (**passive shielding**) are met for **all H1** scenarios and also for **H2.1**, **H2.2**, **H2.3**, **H2.4** (likely accidents) and even **H2.7**. It needs to be noted that this is true, in the case of experimental cave, only for vertical walls. The **roof** is required to meet the limits for the **blue-control-zone** [4]. These limits are satisfied in the above-mentioned scenarios. For all other H2 events (**H2.5** and **H2.6**), the dose rates limits are **exceeded** only by a **factor 2.1 or less**.

The **area-averaged dose rates** were calculated (see Table 25) for all vertical surfaces based on the request in the *Dose budget allocations for instrument shielding design* [13]. In the case of the cave, two scenarios were considered. One conservative scenario of the like accident scenario H2.2 and the second one more realistic of H1.2 mixed with H2.2 (80:20). **All surfaces satisfy** the denoted dose rate budget of **0.5 µSv/h** for the BEER instrument as a contribution to the white zones.

Table 24: Radiological simulations summary

Component	Dimensions and materials
Experimental cave	Heavy concrete walls, 65 cm thickness (front and nearest side wall) or 55 cm (other walls), 70 cm thickness of standard concrete for the roof to meet the controlled area limit, heavy door 20 cm thickness of steel, all walls, roof and floor, chicane outer walls, heavy door inner side covered by a 1mm B_4C layer equivalent.
Shutter pit	20 cm thick iron walls, followed by 10 cm plastic with 5% of B_4C content (or equivalent) finished by 70 cm thick concrete walls or 20 cm steel wall towards the NMX instrument
Shutter	1 cm Mirrobor part, followed by 50 cm of cooper finished by 10 cm of plastic (polyethylene) containing boron
Chopper pit	70 cm thick concrete walls covered by a B4C containing layer
Neutron guide	50 cm thick concrete through the whole distance from the shutter pit to the experimental cave; expect the final 3 meters where a strengthening to 60 cm is required due to the presence of the boron slits.

Table 25: Area-averaged dose rates

Component	Dose rate
Experimental cave	0.46 µSv/h (100 % H2.2) 0.17 µSv/h (20 % H2.2; 80 % H1.2)
Neutron guide shielding in D03	0.33 µSv/h
Neutron guide shielding in E02	0.23 µSv/h

7. GLOSSARY

Term	Definition
ESS	European Spallation Source
MCNP	Monte Carlo N-Particle
MCPL	Monte Carlo Particle Lists
NMX	Macromolecular Diffractometer
NPI	Nuclear Physics Institute
PE	Polyethylene
SE	Sample Environment
AFB	Accidentally Full Beam
MWB	Maximum White Beam

8. REFERENCES

[1] ESS-0019931- ESS Procedure for designing shielding for safety
[2] ESS-0052625 - NOSG phase 2 guidelines for designing instrument shielding for radiation safety
[3] ESS-0039408 - Neutron Optics and Shielding Guidelines, Requirements and Standards
[4] ESS-0001786 - Definition of Supervised and Controlled Radiation Areas
[5] BEER - H1 and H2 scenarios for radiation shielding (ESS-1407242)
[6] Optics Report for the BEER Instrument (ESS-0238217)
[7] T. Goorley *et al.,* "Initial MCNP6 Release Overview", Nuclear Technology, 180, pp 298-315 (Dec 2012).
[8] M. B. Chadwick *et al.,* ENDF/B-VII.1: next generation evaluated nuclear data library for nuclear science and technology. Nuclear Data Sheets 112, 2887, (2011).
[9] MCPL tool, available from https://github.com/mctools/mcpl
[10] V Santoro, DD DiJulio, S Ansell, N Cherkashyna, G Muhrer, PM Bentley, IOP Conf. Series: Journal of Physics: Conf. Series 1046 (2018) 012010 doi :10.1088/1742-6596/1046/1/012010
[11] R. Kolevatov, Ch. Schanzer and P. Böni, Nucl. Instr. Meth. A 992 (2019) 98-107. https://doi.org/10.1016/j.nima.2018.12.069
[12] M. Fleming, T. Stainer and M. Gilbert, editors. The FISPACT-II User Manual, Jan. 2018, UKAEA-R(18)001. Available from fispact.ukaea.uk
[13] Dose budget allocations for instrument shielding design (ESS-1108220)

DOCUMENT REVISION HISTORY

Revision	Reason for and description of change	Author	Date
1	First issue	Jaroslav Soltes	2018-11-07
2	Second issue – redesign after IDR	Jaroslav Soltes	2019-07-26
3	Second edition – changes in tunnel shielding calculation inputs and methodology	Jaroslav Soltes	2020-04-07